A smart grid ready building energy management system based on a hierarchical model predictive control.

Antoine Lefort

2014-10-TH

THESE DE DOCTORAT

DOMAINE : S.T.I.C.

SPECIALITE : AUTOMATIQUE

Ecole doctorale "Mathématiques, Télécommunications, Informatique, Signal, Systèmes Electroniques"

Présentée par :

Antoine LEFORT

A smart grid ready building energy management system based on hierarchical model predictive control

Date de soutenance : 2 Avril 2014

Jury :

M. Guillaume ANSANAY-ALEX	CSTB - Direction Energie Environnement	Co-Encadrant de thèse
M. Romain BOURDAIS	Supélec, IETR	Co-Encadrant de thèse
M. Stéphane GRIEU	Université de Perpignan VD, PROMES	Rapporteur
M. Hervé GUEGUEN	Supélec, IETR	Directeur de thèse
M. Yacine LAMOUDI	Schneider Electric	Examinateur
M. Bernard MULTON	ENS Rennes - SATIE	Examinateur
M. Stéphane PLOIX	Université de Grenoble, G-SCOP	Rapporteur

Contents

List of Figures . . . 2
List of Tables . . . 5
0.1 Problématique . . . 7
0.2 Objectif . . . 7
0.3 Gestionnaire d'énergie (GE) . . . 8
0.3.1 Formalisation du problème . . . 8
0.3.2 Méthode de résolution . . . 10
0.3.3 La structure du GE . . . 10
0.3.4 Méthode de distribution . . . 11
0.4 Applications . . . 11
0.5 Conclusions et Perspectives . . . 12

1 Introduction **13**
1.1 Background . . . 13
1.1.1 World energy context . . . 13
1.1.2 Impact and role of buildings . . . 14
1.2 Problematic . . . 16
1.3 Contributions of the thesis . . . 16
1.4 Manuscript plan . . . 16

2 BEMS problematic **19**
2.1 Building and systems characteristics . . . 19
2.1.1 Buildings . . . 20
2.1.2 Systems . . . 22
2.2 Building Energy Management System (BEMS) . . . 23
2.2.1 Existing control . . . 23
2.2.2 Advanced control . . . 24
2.3 Conclusion . . . 31

3 BEMS development **33**
3.1 Generic MPC definition . . . 34
3.1.1 Systemic view . . . 34
3.1.1.1 System model . . . 34
3.1.1.2 Global system view . . . 38

3.1.2 MPC formalization . . . 41
3.1.2.1 Operators . . . 42
3.1.2.2 Problem definition . . . 43
3.2 MPC controllers . . . 45
3.2.1 MPC configurations studies . . . 48
3.2.1.1 Centralized Open Loop (C-OL) . . . 48
3.2.1.2 Centralized Closed Loop (C-CL) . . . 51
3.2.1.3 C-CL with varying sampling time (C-VCL) . . . 53
3.2.1.4 Varying horizon and horizon size impact . . . 55
3.2.1.5 Conclusion . . . 56
3.2.2 The Multi-layers BEMS architecture . . . 56
3.2.2.1 Hierarchical Architecture Principle . . . 57
3.2.2.2 Hierarchical Tracking mode (H-Track) . . . 60
3.2.2.3 Hierarchical Commitment mode (H-Cmt) . . . 64
3.2.3 Conclusion . . . 65
3.3 Distributed control . . . 66
3.3.1 Block matrix problem formulation . . . 66
3.3.2 Dantzig-Wolfe Decomposition . . . 69
3.3.3 Resolution principle . . . 70
3.3.3.1 BEMS Modularity . . . 71
3.3.4 Algorithm behaviour . . . 72
3.4 Conclusion . . . 74

4 Applications **77**
4.1 Buildings description . . . 78
4.1.1 Home A: Low Energy . . . 78
4.1.2 Home B: All-Electric . . . 83
4.2 BEMS performance . . . 85
4.2.1 Simulations conditions . . . 86
4.2.2 Indicators . . . 89
4.2.3 Conventional control . . . 90
4.2.4 Qualitative results . . . 91
4.2.5 Building strategies . . . 93
4.2.6 BEMS improvement . . . 101
4.2.7 Conclusion . . . 102
4.3 Building Smart grid ready . . . 103
4.3.1 Scenario . . . 103
4.3.2 Indicator . . . 104
4.3.3 Varying cost strategy . . . 104
4.3.4 Building commitment . . . 110
4.4 Conclusions . . . 112

5 Conclusions and perspectives **115**

List of Figures

1 Structure de contrôle prédictive, hiérarchisée et distribuée. . . 8
2 Vision systémique générique d'une installation. 9
3 Représentation fonctionnelle de la vision système indépendante des installations reliées à un coordinateur 11

2.1 Basic MPC scheme. 25
2.2 Basic MPC scheme. 26
2.3 Conceptual framework for assessing the performance of MPC from [1] 26

3.1 System scheme. 34
3.2 Electrical equivalent air thermal dynamic building model. The capacities C_w and C_a are associated to mass and air dynamics. R_i are the thermal resistances and u_i are the loads imposed on the different temperature nodes. 35
3.3 Coulped systems scheme 41
3.4 Distubances profiles 46
3.5 $w_{buy}(t)$ profile of the illustrative case. $w_{sell}(t)$ *is set equal to* $w_{buy}(t)/2$. 46
3.6 Resolving computing time function of N_{opti}. *The* N_{opti} *values is displayed in the bottom axis and the* Δ_L *constant sampling time on the top axis.* 49
3.7 Benchmark indoor temperature trajectory 50
3.8 Prediction disturbance of the simulation example 50
3.9 Indoor temperature trajectory with disturbance 50
3.10 Indoor temperature trajectory without unpredicted disturbance 52
3.11 Indoor temperature trajectory with unpredicted disturbance (C-CL) 52
3.12 Scheme of the C-VCL sampling time distributions 53
3.13 Temperature regulation with unpredicted disturbances in function of Δ_f. 54
3.14 Computing time function N_{opti} (Δ_f). *The* N_{opti} *values is displayed in the bottom axis and the* Δ_f *finer sampling time on the top axis.* 55

3.15 Impact of the horizon on the objective cost value 56
3.16 Hierarical BEMS scheme 57
3.17 Scheme of the piloting energy stage time 60
3.18 Scheme of piloting information update with $\Delta_S = 5.\delta_f$. 62
3.19 Principle of the Hierarchical Tracking mode 62
3.20 Temperature regulation for H-Track configuration - Simulation Disturbed -. 63
3.21 Temperature regulation for H-Track configuration - Simulation Informed -. 64
3.22 Principle of the Hierarchical Commitment mode 65
3.23 Diagram of the global BEMS with 5 systems 67
3.24 Diagram of independent systems linked to the Dantzig-Wolfe coordinator with five systems 69
3.25 Algorithm resolution iterative principle 70
3.26 Dantzig Wolfe algorithm criterion convergence to optimale values 0 . *Value 0 has been changed in 1 on order to use logarithmic scale.* 73
3.27 Dantzig Wolfe algorithm iteration number in function of N_{opti} . 73
3.28 Scheme of the BEMS 74

4.1 *Low Energy* house **A** thermal step response 79
4.2 *All electrical* house **B** thermal step response 84
4.3 Simulation scheme 86
4.4 Difference for a winter week data between the predicted and the real disturbances profiles. 87
4.5 Difference for summer week data between the predicted and the real disturbances profiles. 88
4.6 Difference for spring week data between the predicted and the real disturbances profiles. 89
4.7 Hourly electricity tariff with low price (LP) period (6.14 c€.kWh^{-1}) and a high price (HP) (9.91 c€.kWh^{-1}). 90
4.8 Winter heat pump energy efficiency factor *(COP)* 92
4.9 House A behavior in winter day 94
4.10 House A behavior in summer day 95
4.11 House A behavior in spring day 96
4.12 House B behavior in winter day 97
4.13 House B behavior in summer day 98
4.14 House B behavior in spring day 99
4.15 Internal temperature comparisons between the house A and B strategies for a winter day. 101
4.16 Hourly electricity tariff with low price (LP) period (6.14 c€.kWh^{-1}), high price (HP) (9.91 c€.kWh^{-1}) and critical-peak price (CPP) period (19.82 c€.kWh^{-1}) 104

4.17 House B hourly energy consumption in a winter day. CPP between 5 to 7 pm. 106
4.18 House B hourly energy consumption in a winter day. CPP between 6 to 8 pm. 107
4.19 House B hourly energy consumption in a winter day. CPP between 7 to 9 pm. 107
4.20 Effect of the information time h_d on the house B consumptions and operating cost 109
4.21 Results of the commitment simulations over a day period . . 111

Resumé

0.1 Problématique

De nos jours, la société fait face à un nouvel enjeu énergétique. La gestion du réseau d'énergie est un problème de plus en plus complexe, que ce soit au niveau de la production, où il faut gérer les fluctuations liées à la part croissante des énergies renouvelables, comme au niveau de la consommation, où les demandes de puissance se sont encore accrues. La grande difficulté est d'arriver à faire coïncider la production avec la consommation. Pour se rapprocher de l'équilibre, les réseaux de fourniture sont amenés à proposer des tarifications et des puissances disponibles variables au cours de la journée, entraînant une grande variabilité de la disponibilité de l'énergie pour le consommateur.
Dans ce contexte, la maîtrise des consommations énergétiques des bâtiments, responsables du tiers de la consommation énergétique globale, devient primordiale dans la facture énergétique. Parallèlement, l'évolution de l'interface entre le bâtiment et le réseau de distribution, avec l'arrivée progressive des compteurs communicants, permet de développer de nouvelles stratégies de contrôle. Une piste possible est le développement de Gestionnaires Energétiques (GE) dans l'habitat.

0.2 Objectif

L'objectif de ce travail de recherche est de concevoir des stratégies de pilotages des installations d'un bâtiment résidentiel, en proposant une méthodologie pour la synthèse d'un controleur qui :

- Assure le confort des occupants efficacement, ce pourquoi le bâtiment est conçu.
- Soit indépendante des technologies utilisées afin de s'adapter à tout type de bâtiment et de respecter les contraintes des systèmes.
- Soit modulaire pour pouvoir évoluer de façon simple durant l'intégralité de la vie du bâtiment.
- Tire avantage de son environnement afin d'optimiser la gestion des

consommations.
- Permette une interaction avec le réseau pour prendre en compte de nouvelles contraintes et demandes afin de jouer un rôle dans le management global de l'énergie.

0.3 Gestionnaire d'énergie (GE)

Pour répondre à la problématique posée, nous avons mis en place une commande prédictive, hiérarchisée et distribuée (HD-MPC) (cf. Figure 1) .
- L'anticipation a pour objectif de minimiser la facture énergétique et de satisfaire les besoins de l'habitat. Le principe est d'utiliser des modèles dynamiques des systèmes afin de prédire leur comportement et ainsi de pouvoir : anticiper et satisfaire les besoins des occupants ; utiliser les systèmes de stockage pour décaler les consommations dans les périodes tarifaires basses.
- La hiérarchisation permet d'une part, de pallier la grande complexité de résolution en travaillant sur deux échelles de temps et d'autre part de développer une structure permettant de communiquer avec le réseau.
- La distribution assure la modularité de la méthode afin de s'adapter à tous les types de bâtiments.

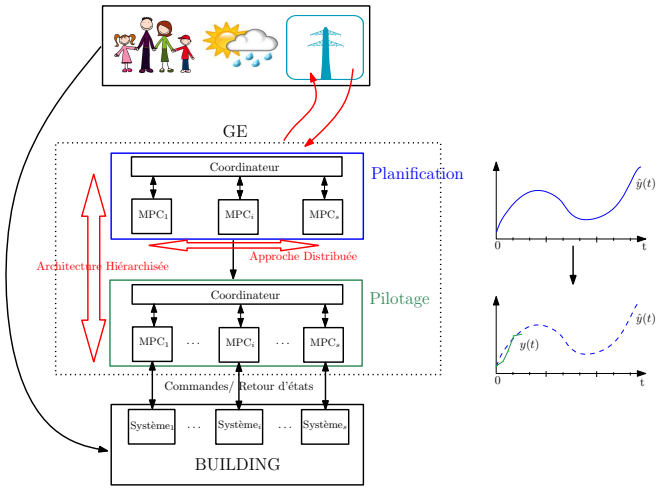

FIGURE 1 – Structure de contrôle prédictive, hiérarchisée et distribuée.

0.3.1 Formalisation du problème

Afin d'utiliser la commande prédictive, il est nécessaire dans un premier temps de formaliser le problème d'optimisation. Dans notre démarche, nous

avons utilisé une vision systémique des installations de l'habitat schématisé sur la Figure 2. On note :

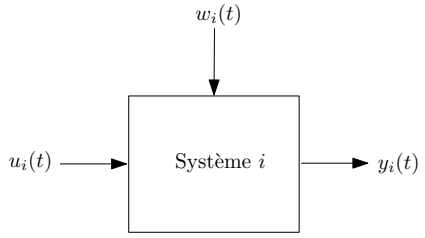

FIGURE 2 – Vision systémique générique d'une installation.

- $u_i(t) \in \mathbb{R}^{m_i}$ le vecteur d'entrée du système i,
- $x_i(t) \in \mathbb{R}^{n_i}$ le vecteur d'état,
- $w_i(t) \in \mathbb{R}^{l_i}$ le vecteur de perturbation.

Ainsi pour chaque système i, on décrit la dynamique par une fonction différentielle :

$$\dot{x}_i(t) = f_i(x_i(t), u_i(t), w_i(t)), \tag{1}$$

et les contraintes sont définies par la fonction :

$$g_i(x_i(t), u_i(t), w_i(t), t) \leq 0, \tag{2}$$

A ceci s'associe le vecteur de sortie $y_i(t)$, défini par :

$$y_i(t) = h_i(x_i(t), u_i(t), w_i(t)) \tag{3}$$

Dans cette représentation générique, chaque système est modélisé de façon indépendante avec des contraintes locales et un objectif local. Les couplages entre les systèmes sont pris en compte par l'intermédiaire de la variable de perturbation w_i. Tandis que les contraintes globales de l'habitat sont décrites par une contrainte globale :

$$C(\mathbf{u}, \mathbf{w}, x) = 0 \ , \ C \in \mathbb{R}^{n_g} \tag{4}$$

Où $\mathbf{u}$ et $\mathbf{w}$ sont les vecteurs d'entrées et de perturbations du système global.

La dernière étape de la formalisation du problème est la définition de la fonction objectif. Dans cette thèse, nous nous sommes intéressés à minimiser la facture énergétique de l'habitat. Nous considérons que la tarification de l'électricité est variable et qu'il est possible d'acheter et de vendre de l'électricité sur le réseau au prix $w_{achat}(t)$ et $w_{vente}(t)$. Notant P_{grid} la puissance électrique échangée entre le réseau et le bâtiment, on définit la fonction coût :

$$J_{glo} = \int_0^\infty \begin{cases} w_{achat}(\tau).P_{grid}(\tau)d\tau & \text{si } P_{grid}(\tau) > 0 \\ w_{vente}(\tau).P_{grid}(\tau)d\tau & \text{si } P_{grid}(\tau) < 0 \end{cases} \tag{5}$$

0.3.2 Méthode de résolution

Pour tendre vers la solution du problème, nous utilisons la commande prédictive qui est une méthode de contrôle avancée. La commande prédictive consiste à résoudre le problème initial sur un horizon glissant H. Pour ce faire, le problème est discrétisé. L'objectif est alors de définir la fonction optimale $\tilde{u}$, continue par morceaux, qui minimise la fonction objectif J'_{glo} tout en respectant les contraintes aux instants de discrétisation eq. (1), (2) et (4).
Dans le cas de la gestion de l'énergie du bâtiment, nous sommes confrontés à un problème de grande taille du fait de la disparité des dynamiques des systèmes qui nécessitent un grand horizon d'anticipation et un pas de temps fin de contrôle. Cette complexité de résolution entraîne un temps de calcul important avec une méthode de discrétisation classique. Pour pallier ce problème, une méthode de discrétisation à pas de temps variables a été utilisée. Cette méthode permet de prendre en compte les dynamiques rapides, avec un pas de temps fin sur les premières heures, ainsi que les dynamiques lentes, avec un pas de temps plus gros sur le reste de l'horizon. Cependant, cette méthode de planification dynamique n'est pas approprié à l'interfacage avec le réseau. C'est pourquoi, nous proposons de structurer le gestionnaire.

0.3.3 La structure du GE

Dans l'optique de proposer un GE pouvant communiquer avec le réseau électrique, nous avons mis en place une structure de contrôle hiérarchisée, composée de deux niveaux prédictifs :

- Au niveau haut, le GE reçoit les profils tarifaires de la part du réseau. L'objectif de planification alors posé est d'ordonnancer les flux de consommations d'énergies sur un horizon long H_S. Ce niveau prend en considération uniquement les dynamiques lentes, obtenant ainsi des tendances qui doivent être respectées afin de minimiser la facture énergétique. Ceci doit être fait en respectant l'ensemble des contraintes.
- Au niveau bas, il ne s'agit plus d'optimiser la facture énergétique, mais d'essayer de suivre les trajectoires fournies par le niveau haut, en respectant au mieux les contraintes énergétiques associées. Cette double contrainte est introduite via un objectif multi-critère. L'horizon d'optimisation est plus court et le pas de temps est plus fin.

Dans le cas non-idéal, la pondération au niveau bas entre le respect des trajectoires et le respect des contraintes énergétiques associées amène à effectuer un compromis. En fonction de celui-ci, deux modes de contrôle sont définis. Un premier mode priorise le suivi de trajectoire et donc le confort des occu-

pants. Et un second mode priorise le respect des contraintes énergétiques, ceci afin de pouvoir s'engager auprès du réseau quant à sa consommation.

0.3.4 Méthode de distribution

Grâce à la structuration systémique du problème, il est possible d'en décomposer la résolution. Il en resulte une structure de contrôle distribuée répondant à la problématique posée. Dans notre approche linéaire, la distribution de la résolution est apportée à chaque niveau par la méthode de décomposition de Dantzig-Wolfe. Le principe est d'introduire un coordinateur (c.f. Figure 3) qui, via une méthode itérative, converge vers la solution optimale du problème centralisé en respectant les contraintes globales. Le principe est de pondérer les variables de chaque sous système indépendant afin de trouver la meilleure séquence de contrôle global. Avec une formalisation plus complexe, d'autres techniques de distribution peuvent être utilisées.

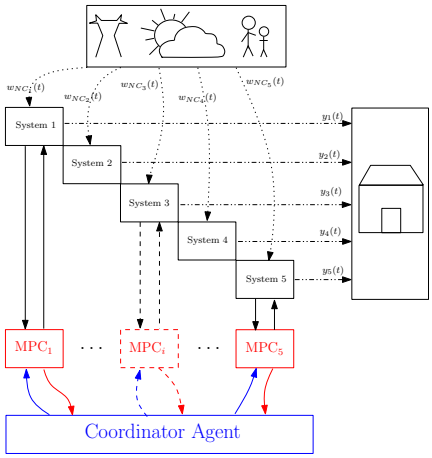

FIGURE 3 – Représentation fonctionnelle de la vision système indépendante des installations reliées à un coordinateur

0.4 Applications

Le gestionnaire du bâtiment et ces deux modes sont testés en simulation sur deux bâtiments d'étude. Les simulations ont été effectuées sous MATALB/Simulink en utilisant les modèles de la bibliothèque SIMBAD dans le processus et des modèles de prédiction simple dans le contrôleur.
La comparaison avec des contrôles conventionnels montre les bonnes performances du GE en hiver comme en été. On remarque qu'en fonction du bâtiment les stratégies des GE sont différentes. On constate une stratégie de lissage pour un bâtiment à forte inertie composée de systèmes à faibles puissances, tandis qu'une stratégie plus dynamique est constatée avec un

bâtiment moins isolé composé de systèmes plus puissants et réactifs. L'implementation du GE sur ces deux bâtiments différents met en avant son adaptabilité.
Du point de vue du réseau, les études montrent qu'une tarification variable entraîne un décalage de la consommation du bâtiment. Cependant, on montre que pour un bâtiment muni d'un GE, une politique d'échange tarifaire ne permet pas l'effacement rapide de la consommation à moins d'augmenter très fortement le prix de l'électricité.
Une dernière étude met en avant la capacité du bâtiment à s'engager sur sa courbe de consommation sur un certain horizon. Les résultats montrent la complexité d'un tel engagement au vue de la grande incertitude sur les consommations non contrôlables liées aux occupants. Ceci étant, l'utilisation de profils d'engagement assouplis avec une marge d'erreur donnée permettrait de satisfaire le confort des occupants tout en respectant leurs engagements.

0.5 Conclusions et Perspectives

Dans cette thèse nous proposons un gestionnaire énergétique du bâtiment résidentiel. Le gestionnaire a pour avantages de proposer un formalisme générique doté d'une grande modularité et adaptabilité répondant ainsi à la problématique de l'habitat. L'architecture hiérarchisée sur deux niveaux permet d'assurer la robustesse et la réactivité du contrôle. Les apports de ce GE ont été illustrés par différentes simulations, en comparaison avec des contrôles plus conventionnels et pour différentes stratégies réseaux. Le GE permet de mettre en avant le rôle important que peut jouer le bâtiment dans le contexte énergétique actuel.

Les perspectives pour ces travaux sont :
- d'intégrer des systèmes plus complexes dans le GE.
- de s'orienter vers un management d'un ensemble d'habitats.
- de prendre en compte le comportement et les réactions des usagers.
- d'effectuer une analyse de sensibilité de l'approche vis-à-vis des modèles et données de prédiction.

Chapter 1

Introduction

Contents

1.1 Background 13
1.1.1 World energy context 13
1.1.2 Impact and role of buildings 14
1.2 Problematic 16
1.3 Contributions of the thesis 16
1.4 Manuscript plan 16

This chapter is devoted to analyse the energy management context. In this world energy transitional phase, this analysis aims at extracting the future needs for the building control in order to present the work objective.

1.1 Background

1.1.1 World energy context

Nowadays, due to the energy consumption increase and to the consumers' demand, linked to the demographic growth, the recent energy market liberalization and the increasing part of local renewable production units, the electricity network is exposed to important issues, which threaten the balance between production and consumption. Added to this, the depletion of fossil energies leads to increase the electricity price. Moreover, the international agreement for climate protection involves to reduce and manage the energy more efficiently. In agreement with that, the worldwide challenges of all the nations have focused on, firstly, the reduction of the energy consumption, secondly on the development of "smart" electricity grid ("smart grid"). The energy consumption reduction target and the smartgrid rollout present fundamental changes in the energy control approaches. It highlights the emergency to develop new energy management strategies in order to reduce the peak consumption and match the supply and demand.

The smart grid aims at improving monitoring and operating the high-voltage transmission grid and it also enables system operators to control energy electricity which is generated, delivered, consumed and priced. Many research programs and tests are already developing it. This is principally because the peak consumption cost is extremely expensive. It requires to start expensive energy power plants (fuel or gas) and it requires new transmission and distribution network lines which is a huge investment, especially as it occurs less than 1% of the time during the whole year [2]. Among the scenarios, those which seem the most advanced are:

- Tariff-Of-Use (TOU) program or Real-Time Pricing (RTP) program. It consists in establishing time varying electricity tariff according to the real energy production cost. The final aim is to encourage the customer to modify his electricity consumption behaviour. This divides the day into number of periods with different rates. The price within each period is known in advance and can be reset or not, depending on the program. This program has been defined as the best program for residential house peak reduction in [3]. It is already used in different places in the world, e.g. Illinois [4].
- Demand Response (DR) program or Demand-Side management. It consists in transmitting specified set of requirements to a consumption installation. Then, local controllers will monitor and manage the operation according to the information. Depending on the installation, it provides load shifting and shedding with already some emerging open standards, e.g. OpenADR, which is a protocol "for letting smart grids and smart building talk to each others" [5].
- Direct Control (DC) program. It consists in stopping a device during a specific period of time. This period depends on the device characteristics. It could be a renewable production plant or consumption devices (e.g. building heating system or public streetlight). Already developed in some countries, DC has the advantage to reduce instantaneously the load consumption. However, overshoot could occur when the local controller restarts. Moreover, there is no comfort guarantee during the load shifting, as a consequence users could start the device manually.

These programs can be performed on every load consumptions systems. Nowadays there are mostly implemented on electric load as the quarry plant, however these methods are not reduced to the industry but each load is called to help and make contribution efforts. Amongst these, a new load type is becoming the target: buildings.

1.1.2 Impact and role of buildings

According to the International Energy Agency (IEA), ordinary houses are the main electricity consumer, with about a third of the global energy

consumption. This, combined with its characteristics, makes it the biggest energy reduction potential. To decrease its part on the global energy consumption, the priority consists in reducing their energy loss in order to improve its energy efficiencies. This can be done by building restoration which is, for example in France, encouraged by political programs.
However, it is not the only potential. The ones which interest us are its flexibility capacities and its possible future energetic autonomy covered by renewable sources. Thanks to the development of the information and communication technologies (ICT), it is possible to develop and implement building energy management system (BEMS). The BEMS, which appeared first in 1970 [6], aims to integrate intelligence control in the building in order to manage the building energy flux and systems consumptions.

With the new electricity challenges, the BEMS is going to be an integral part of the smart grid that can potentially enable DR or TOU programs. The approach "from the smart grid to the smart homes" aims to develop algorithm or specific control for building appliances to decrease its consumption and reduce its impact on the grid or again provides load information to it. The BEMS lever arms are the building flexibilities, principally composed of the local power plants, the storages abilities and the degrees of freedom offered by the users, enabling to shift or shed the energy consumption. This aspect will be even more important as the building will integrate multi sources and be composed of more specific and controllable equipments.

In the development of these new technologies, two important things have to be kept in mind. First, occupants live in the building, and so, for their acceptability, the primary home installation functions need to be ensured, providing their comfort. Secondly, the electric network is the biggest system of the world and, as a consequence, the most complex one. It results that the reliability and robustness of the information are essential.

Among the different energies, let's note that the greatest importance is given to electricity supply. This reason is due to the electricity worldwide context but also because electricity is found in most physical transformation processes carried out by energy devices. It can also act as a control system or control mainly in the management of the other energetic flows, e.g. hot water, air, valves, pumps and fans. Moreover, the last building consumption queries show that, due to the reduction of the energetic equipments (providing heating, ventilation, lighting services), the part of specific users devices (tv, computer, etc) begin to be an important part of the building global consumption, up to 30% in the new residential buildings.

1.2 Problematic

The necessity to reduce and manage more efficiently our building consumption is a major problem for the society. To resolve this challenge, the development of intelligent electricity network called smartgrid and the development of smart buildings is coming.
In this context, a part of the solution is to introduce advanced building energy management systems (BEMS) which have to deal with different aspects:

- ensuring the occupant's comfort with reactivity. Because it has to keep its primal functionality,
- enabling to easily integrate new systems due to the ongoing evolution of building installation and usage,
- taking advantage of its environment and systems to optimize the energy management,
- communicating with the grid to deal with global energy constraints and playing a role in the global energy context.

The work objective is to analyse and develop a BEMS in order to prove that it is possible to manage efficiently building energy consumption. The main idea is to implement an advanced control algorithm and use communication technologies and installations capacities to optimize building loads. We will show as well that buildings are able to support advanced grid services to be an important actor in the global electricity network management problem.

1.3 Contributions of the thesis

In this thesis, the contributions are:

1. **Method** In this thesis, a structuring BEMS based on Model Predictive Control (MPC) method is presented. This advanced approach, with two time scale optimization layers and with modularity, responds to the building energy context.
2. **Application** The hierarchical BEMS developed is implemented on two virtual buildings. In order to quantify the potential of the building energy management, different simulation scenarios are carried out which can be real in the presented "building consum'actor" context.

1.4 Manuscript plan

The dissertation content is organized as follows:

The chapter 2 gives a brief history of the building energy management before introducing the new controllers class and the literature researches. In the first part, we will give a non exhaustive list of the existing building control systems by presenting their advantages and limits. Then, we will focus on advanced controllers and more particularly on the predictive controllers and their configurations in order to extract the work problematic.

The chapter 3 contains the major contributions of the manuscript. In this part, the BEMS problem is formalized thanks to a systemic model view of the building installations. Doing so, it will give a generic method to define it. Then the anticipative, reactive and modular methods of the control are described. The anticipation is provided by a control based on Model Predictive Control while the reactive one is given by the two level control architecture; as for the modularity, it is given by a distributed resolution program. These three aspects are analysed to propose a BEMS with the most adapted configuration resolution methods.

In chapter 4, the BEMS is implemented on two building cases. In the first part, the buildings facilities and their models are established. Then, the developed BEMS is implemented and simulations are performed to analyse their behavior and efficiencies. These simulations scenarios validate the modularity of the BEMS and highlight the building potential as an actor of the grid.

The last chapter concludes on the presented work in this manuscript, and offers several perspectives for future developments.

Chapter 2

Building energy management problematic and existing approaches

Contents

2.1 Building and systems characteristics 19
2.1.1 Buildings 20
2.1.2 Systems 22
2.2 Building Energy Management System (BEMS) 23
2.2.1 Existing control 23
2.2.2 Advanced control 24
2.3 Conclusion 31

In this chapter, we will firstly present the different characteristics of buildings and its devices in order to summarize the control complexity that they involve. In addition, in the aim to develop an anticipative efficient control we will give some solution aspects (already developed in the literature) to treat them.

Then, after a brief enumeration of existing controllers, we will list the several different BEMS control research with a focus on MPC and its various forms. We will do this in order to define the presented MPC BEMS particularities. Let's note that much research is related to the BEMS development, reflecting then its interest.

2.1 Building and systems characteristics

For building control, or any system control approach, it is important to understand the entire system before developing and controlling it. This as-

pect is especially important in our case because, contrary to many systems, the buildings have the particularity to be unique.

Remark In the manuscript, the system usually denotes building installations and devices and also the whole building facilities.

The uniqueness of the building system includes many points. There are the building envelope, the environment, the orientation and the systems. And even if we take two identical buildings located at the same place, the control will remain different depending on their use (users' needs and behaviours).

In order to give an overview, we will detail buildings and systems characteristics. The variabilities of both are enumerated separately in the following paragraphs but are completely coupled in their usages. These paragraphs will try to make a comprehensive view of their characteristics but also of their use and their constraints.

2.1.1 Buildings

Buildings are the principal construction sites in the world. They are identified as a property and are part of our daily life. There have been built for ages and are in constant development. That is why, their sizes and characteristics are so diversified. They must fit in different environments and space and are built by technical building construction bounded to history, geographical place or regulation laws.
These differences lead to various thermal performances between each others due, among others, to the thermal conductivity and inertia types. The thermal conductivity is mainly performed by covering walls, windows and roof and defines the thermal resistance of the building to outside impacts. The thermal inertia is performed by the walls material layers. It results in a slow thermal building dynamic behavior which is included into a large range from 2 to 12 hours for an average house.

In this thesis, we will focus on the control aspect. Buildings are built to satisfy the occupant's comfort, more precisely a thermal temperature comfort. Considering the long time constant characteristics and the power limit of the controllable system, thermal regulation requires anticipated control. However, in order to efficiently determine the thermal building energy demand, or more accurately, its internal temperature, many effects have to be taken into account. The internal temperature or the building energy needs cannot be easily estimated. The building thermal model is very complex, involving air humidity, solar gain, internal gain, convective and radiative

aspects, building orientation and shades, air pressure ...

A method to define the building energy load is to use predicted models. Much research concerns the modeling of the thermal building dynamics. We can cite the heuristic approach of [7] based on ARX regression method to predict 1h ahead the thermal building behavior, validated on four building models. Or we may cite the stochastic approaches of [8],[9] and [10] which, respectively use kalman filter, statistical or genetic algorithm identification methods. These studies show that, to modelize and predict the thermal building behavior, the most difficult points are the abilities:

- to correctly excite the temperature points values and to measure the real buildings via instrumentation in order to obtain a correct model,
- to predict the influences data, as the solar flux or the external temperature, and also the users' behaviors which have important impact to good predictions,

A list of the significant factors in modeling residential buildings is given in [11].

In support of this, among the studies made on the various disturbances with a significant effect, in [12] and [13], authors highlight the importance of the occupant's behavior on building controls and their impact on consumptions. In [14], it is shown that the weather, one of the most important influence data on building thermal performance, behaves in a stochastical manner. Depending on the building, the predicted data has not the same impact on the behavior or loads estimation predictions but still are very hard to predict.

Ultimately, the research shows that it is unrealistic to expect to be able to predict building thermal performances with total accuracy, especially knowing that each building is different. That is why, simplified models are more adapted. A state of art of simplified models and a brief history of building behavior modeling is done in [15].
The literature simplified model developed in [16], [17] or [18] seems to be a good compromise and is often used in building control works.

To sum up, buildings can be seen as a complex system subject with many disturbances and with the objective to ensure an internal temperature comfort. To do this, we will look at the type of systems (heating, cooling, refreshing, ...) which it disposes. Doing so, we will describe the numerous other systems which are used to provide the ever-growing users' needs.

2.1.2 Systems

Buildings are nowadays filled with many systems to ensure occupants' needs; these systems correspond to several functions. They can be divided into the following categories:

- The Main function category, matching 80 % of the current global building consumption, used for the occupants' needs: heating and cooling the air temperature, heating the domestic water, renewing the internal air and lighting.
- The Auxiliary function category associated to the appliance systems and users' systems like the food heating, the washing machine, refrigerator, the TV or the computer.

The installations previously enumerated include a wide range of systems. They include chillers boilers, air handling units (AHUs), fan coil units (FCUs), heat pump units (HPUs) and variable air volume boxes (VAVs). Here is a non exhaustive list of their properties:

- These systems can be simple and without interactions, e.g. the electrical radiator or the single-flow ventilation unit.
- They can integrate storage capacities like a thermal inertia radiator or a hot water tank.
- They can be coupled with other systems, e.g. a solar hot water exchanger, a water/air heat pump unit, or a condensing boiler.
- The systems can strongly interact with the environment (e.g. solar protection) and between each other in order to save energy and reduce investment costs.
- They can also be integrated in the building architecture, e.g. cooling tower and refresh wall.

The presented list is constantly evolving. Also due to the political commitments and incentives, the building becomes more and more self sufficient, and so new systems appear, the local energy producers and local storages devices, i.e. PV panel and urban wind and battery and cogeneration units and hybrid solar panels combined.

In addition to the system properties which characterize their dynamics and interactions, the control must take into account their numerous specific constraints so as to control all the building complex devices. Systems have limited power and capacity, they involve minimum operating time, internal regulation and consumption for specific components or limited discharge and charge power.

To sum up, we have many complex systems which are used for many functions. They can be in interaction between each other, they have common or local objectives and are controlled independently. This set of systems is specific for each building.

To summarize, the global system is very complex. It is composed of large scale dynamics, it is strongly affected by the environmental conditions, it is unique and regularly evolves. It is composed of various systems (renewable production, storages, users' devices ...). Globally, it can be seen as a set of specific systems in interaction, with their own constraints, local objectives and dynamics and with a common global objective.

In order to develop a BEMS, taking into account all these aspects, we will look to the already existing ones and the advanced controls methods.

2.2 Building Energy Management System (BEMS)

The systems (for heating, cooling ...) used in the building are already much controlled. However, if in the past, the simplicities of the systems and the energy context enabled to implement basic control laws, nowadays the building energy management has changed. This wide range of building and systems leads to a high level management complexity which needs advanced control. In this part, we will briefly trace the evolution history of the building control, and then focus on advanced controls and more precisely on the predictive controls.

2.2.1 Existing control

The system control devices have much improved since the 1970s. After being mechanical (pneumatic, electrotechnical), the control devices became popular with the development of the analog electronic in the 1980s providing faster response and higher precision. This innovation has allowed to implement more regulation components like the processing unit or the thermostat which are the most common ones in the house. Since most of the current buildings were built during this decade, and due to its implementation simplicity, we find nowadays many regulations of the different installations (e.g. heating and cooling air, heating hot water, start and stop ventilation) based on closed loop control originating from the analog electronic development. The most common ones are:

- The command law type "on-off-control" modular or not modular. The control command signal takes the value start or stop according to $e(k) = y_{ref}(k) - y_{mes}(k)$ and the commutation frequency is defined to ensure the actuator and long-lived system, and the magnitude of oscillation.
- The continuous control, composed by proportional (P), proportional-integral and also derivative (PI or PID) techniques. The discrete time controllers performance depends on the parameter P,I and D. However

the tuning required to adjust is not trivial. In addition they have to be re-adjusted correctly with the building evolution. In reality, the setting-up procedure occurs more often when the building is unoccupied and unfurnished and so is not proper.

– Rule-based Control: a current control practice for room automation and system. It determines all control inputs based on a series of rules of the form "if condition, then action". The conditions and actions are usually associated with numerical parameters (e.g. threshold values) that need to be chosen. The good performance depends on a good choice of rules and associated parameters.
  This kind of controller is inflexible and also cannot be generalized and follows the changes in building use.

In the 1990s digital control devices (DDC) came on the scene. That enabled to develop more precise advanced functions like the optimal start-up control which allows to start the devices ahead in order to reach the order on time. However, as there were no established standards for this digital communication, various manufacturers created their own (proprietary) communication methods. This led to uncoupled control without interoperability and without sharing information which vainly multiply the sensors. For building equipped with DDC devices, it results in a set of complex systems controlled individually and by specific controls which could be cancelled each other out (heating the air and renewing the air at the same time) and are difficult or impossible to make evolve or change.

2.2.2 Advanced control

By the late 1990s and especially during the 2000s, the "intelligent" control techniques appear. This control type is based on artificial intelligent brought by various approaches. It is the study of many researchers and a new generation of control is flourishing. This new type of control aims to adapt to the significant complex changes of the energy management. Most of them are listed in [19]. Among the advanced controls, we find the fuzzy logic rules controls which are an improvement of the rule-based control. This control research is used to establish strategies according to different variables in relation to the work developed. For example, the works, published in [20], apply a fuzzy logic control to manage a Supermarket provided with a battery and a PV. It gives the possibility to make load shedding while minimizing the energy bill. It uses electricity bill to determine the fuzzy rules. Strategies are established separately according to the price period modes (off-peak - shoulder -peak).
This kind of control is often used to decrease the computational time or ease the implementation, but not only. We find advanced fuzzy control in [21] or [22], where the authors elaborate an adaptive PID-type fuzzy logic to

control HVAC system and an adaptive hybrid PID-fuzzy control scheme for heat sources without process models. These methods seek to be adaptive and the fuzzy control is added to the existing PID controller in order to be a solution for the already existing devices.
An advantage of this approach is its particularity to work on real-time and its ability to integrate priority laws to satisfy occupants' demand or specific system as shown in [23].
Even if the fuzzy logic rules can be determined by heuristic methods (see [19]), its major inconvenient is its need to elaborate specific laws for each equipment and building.

To go further in the building efficiency in the search of the optimality, another approach already used in another area seems to be well adapted to the building regulation, the Model Predictive Control. The following part presents these approaches which will be used throughout the manuscript.

Predictive Control

Predictive control belongs to the optimal control branch. This control theory deals with designing controls for dynamical systems by minimizing a performance index function of the systems variables. The basic structure of a MPC control loop is illustrated in figure 2.1. Process model, predictive data and an objective function are required. The model predictive control approach refers to a class of control algorithms that compute a sequence of control moves based on an explicit prediction of outputs within a future horizon. It consists in solving an optimal control problem, on finite time horizon knowing the system dynamic models and constraints on states and control variables. Figure 2.2 summarize the MPC control principle.

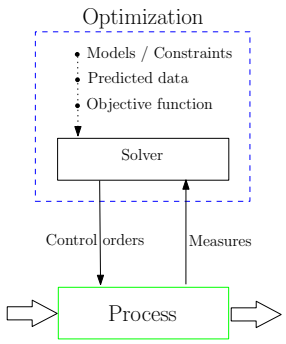

Figure 2.1: Basic MPC scheme.

MPC is identified as being one of the best candidates for providing an optimal solution of building control due to its advantages over the other control algorithms. It can integrate multiple aspects in the optimization criteria (e.g. comfort, energy, bill), able to use forecast (e.g. occupancy schedule, price profile, load profile). Numerous research and implementations have proved that the MPC have potential for energy building management. Its theoretical and realistic potential is schematized in Figure 2.3. The realistic potential corresponds to the transition from perfect models and predictive

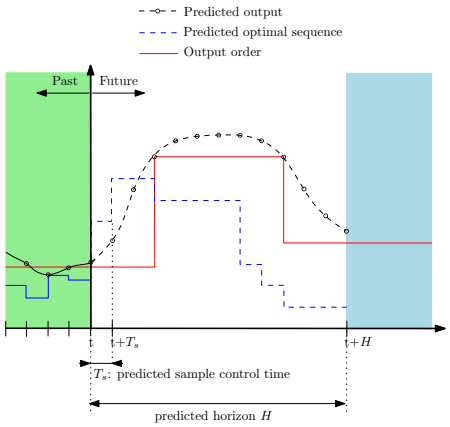

Figure 2.2: Basic MPC scheme.

data to real world.

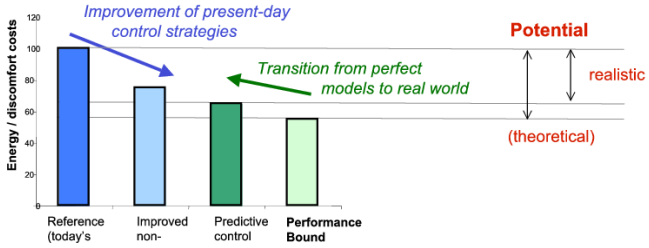

Figure 2.3: Conceptual framework for assessing the performance of MPC from [1]

For BEMS works based on MPC, there are three major things that differentiate them:

1. their formalization type,
2. their program architecture,
3. and their implementation methods.

In the next paragraphs, we will detail the 3 MPC aspects and define our choices.

2.2.2.0.1 Problem formulation The problem formulation for MPC consists in modeling the systems behaviors, defining the possible constraints and expliciting the cost function.

Let's note that the MPC prediction precision is strongly dependent on the controlled models accuracy. That is why, in many applications where dynamical system models are used to describe the behavior of the real world system, stochastic components and random noises are included in the model to capture uncertainties in the operating environment and the system structure of the physical process being studied.
In [24] a comparison between Stochastic MPC and current control practice shows that SMPC is a promising approach but varies with the quality of the model and available input data. This is also pointed out in the receding SMPC approach [25], where authors take into account the prediction incertitude thanks to Bellman function. One particularity of this work is that it integrates the fatal power consumption which is becoming to be an important part of the total building electrical consumption and is hard to predict.

A stochastic approach aims to bring more robustness to the control as it is used for NLP receding MPC problem in [26], where the formalization is done thanks to a trapezium discretization method while the optimization use Tailored Seq Quad Prog and primal dual interior points methods. Its objective is to minimize the energy consumption of a HVAC system combined with a variable air volume system (VAV) while respecting the internal building temperature constraints. However, even if the result shows an average energy gain of 30 % compared to a base line building control, the stochastic approaches appear to be very complex and its performances strongly depend on the stochastic laws which describe the non-linear model. In the case where a stochastic approach is used to compensate a linearization, it is easier to determine the stochastic model law, but if the knowledge of the model or the perturbation is not well known, the performance can be very degraded. The validity of the stochastic laws developed is a major aspect of this type of control. For this reason, a majority of stochastic control approaches use strong probabilist methods, e.g. Monte carlos, which need high computational capacities and, depending on the stochastic type, are very hard to solve. However, these technics can be very useful to define the prediction load consumption profiles ([27] , [28]).

The choice to use a stochastic or a deterministic MPC is not guided by the control performance but rather by the problem aspect and knowledge. That is why, many deterministic MPC BEMS controls can be found in literature. This kind of control can offer the advantages to be easier to implement, less costly in computing and as proved in the MILP approach [29] to perform quite well, for building management, compared to stochastic approach.
Among the deterministic BEMS MPC works, a large range of them are concerning the temperature regulation. This is due to the historical high

consumption of the heating system. However, like in our work, the tendency is to focus on the energy optimization see [30]. In this work, followed by [31] and [32], authors use a Mixed Integer method to formalize the problem. It is principally because they consider that all the devices are communicant and controllable, and like many of them are controlled by logic controllers, integer variables are used. This kind of formalization needs a heavy modelization work in order to integrate the whole devices control aspects, e.g. flexibility, consumption profile, satisfaction criterion etc.

Due to the high problem complexity, many other formalizations are studied. We can find in [33],[26] and [34] non linear MPC. Their works present two different resolving methods to treat the problem efficiently. In [33] an optimization method used relaxed linear problem algorithm while in [26] a quadratic Tailor sequence is used to linearise the equation. The literature proposes also to solve the high complex energy management problem with Particle Swarm Optimization [35] or Neural Network [28] algorithm or Genetic Algorithm [36] or adaptive control which are heuristic method with their own advantages and inconvenient. In [37], an adaptive multiple model-based predictive control approach is proposed. Its principle is to proceed to optimizations in advance thanks to multiple local models and control policies for the current conditions.

We can cite other methods which consider linear formalization as in [38] or in [39]. The linear approaches, which could suffer from poorly realism, provide good performances compared to others. The main argument is that the linearization approximations create weak errors if we consider all the errors sources for BEMS, i.e. data prediction, model uncertainties, occupants' behaviors, etc. Moreover, local compensations can be set in order to adjust the control, like in [38] or in [2], where authors use linear problem forms to control inside temperature via a HVAC system. After computing the output optimal sequence, taking into account the real time electricity prices and the user's thermal discomfort tolerance index, the controller employs nonlinear specific equations plant model and specific local processes to re-build the optimal trajectories in order to adjust the linear approximations.

As in these works, in the present work we chose to use a linear formalization approach which is detailed in the next part.

2.2.2.0.2 Control architecture In the cited articles and the other literature works, we remark that BEMS are face to computing time issues, whether for minimizing building energy consumption from a customer point of view, or for reducing peak consumption from a smart grid point of view

(see [40], [41],[42]). As detailled in the buildings description, this is due to the various ranges of systems' dynamics. For instance, BEMS have to manage a slow thermal house system (6 to 12 hours) while controlling an electrical battery with a fast dynamics (5min). Thus, the common difficulties of these enumerated works, whatever the formulation method, are to treat a large time scale problem.
In order to combine MPC optimality control and offer robustness, most of the implemented BEMS based on MPC use receding horizon as in [43]. Nevertheless, the receding sampling time is often the same as the problem discretization sampling, corresponding to period chosen to reduce the computational burden and result in a suboptimal real-time control.

In this paragraph, we will be interested in the control solutions to reduce the computing time and optimize the control.
However as noted in [44] the horizon has an important impact on the control efficiency and so must be chosen carefully.

In order to add robustness and compensate the prediction error due to the optimization sampling time, in [45], where mixed integer program is used so as to optimize the integration of a solar panel in residential house, the author introduces a rescheduling function which causes a new optimization each time the error between the real trajectories and the predicted trajectories is too big. Even if this proposed solution increases the control robustness, it is not an optimal solution for the large scale time problem.

Another approach, which can be found in [46] consists in using variable horizon MPC to improve the control efficiency. The idea is that the horizon is fixed according to the states and information provided instead of work with a fixed horizon always the optimal one. In this case, the horizon is defined in order to match with the end of each charge and discharge cycles of an ice tank. This "varying" horizon idea can also be used for the sampling time step. In [47] the author uses a varying time step to decrease the number of variable while anticipating on a long horizon. The varying time step is often used in the hybrid system field.

Another approach commonly used and which has received a significant attention during the last decade is hierarchical MPC architectures, a list of them can be found in [48]. The interest was not only motivated by the difficulty to control the large-scale systems with centralized control structures, but also because an important number of systems are multi-scale dynamics systems clearly separable and so are equipped with multi-scale local controllers. The hierarchical structure is then used to coordinate the local controllers while having a global overview, e.g. for power plant [49] or chemical process [50] or micro-grid [51].

For BEMS, the hierarchical approach mainly includes two MPC layers with different time scales [52]. Usually, the high layer, noted the scheduling layer, works on a long horizon and takes into account the slow dynamic in order to define tendencies trajectories and energy consumptions. Whereas the low layer, noted the piloting layer, works on short time horizon and takes into account the fast dynamics. The two layer mechanisms, their exchanged information and their range of computing sampling time are very important aspects of the program.
In the literature, we find in [53] methodology for the design of the two MPC layers. This synthesis method ensures convergence and robustness properties for the overall system with switching on/off actuator policies. As previously said, the basic principle is to use the high level result as a reference for the low level. The high level works is a fixed horizon with a constant time step.

To sum up, it exists many control architectures and configurations for the BEMS MPC. In this work, we will investigate the numerous configurations between hierarchical approach, receding, variable horizon and fixed or variable time step in order to define the most adapted one to our BEMS problem.

However, to match with the BEMS constraints, a last point needs to be discussed: the implementation method.

2.2.2.0.3 Implementation methods Nowadays, a majority of the MPC are centralized. Meaning that the problem is solved by a unique solver. This motivation comes from the fact that the computing capacities enable to solve large-scale problems and that this architecture corresponds to many existing control designs. However, they suffer from many drawbacks such as the increase computing time or the lack of modularity and the problem of defect mode or also the communications complexities. That is why, there is a new interest for decentralized method which also lies in the search of easier implementations and bigger interoperability capacities, expandability capacities and a simplified maintenance.

The decentralized methods refer to the decomposition class methods which consist in dividing the global problem into several local subproblems. Among these, we have the noncooperative, the cooperative and the hierarchical approaches. Hence, we are interested in the MPC control methods where subproblems are independently treated while ensuring a global efficiency, corresponding to the noncooperative and the cooperative methods.

The noncooperative method consists in splitting the global problem into

subproblems without taking into account the interactions [48]. Their performances can be high but have the particularity to steeply decline when the subsystems have strong coupling. In this last case, the neglected interactions can lead to instability and worse global objective values compared to centralize methods. It exists some methods ensuring stability [54], but they lead to robust control and so reduce the performances. Among them, in [55], an almost noncooperative method based on Lyuapunov approach is proposed for coupled nonlinear systems. However, this method needs to find complex Lyapunov functions for each subsystem, only depending on their own subsystem states, and the global convergence is ensured if each local controller is allowed to use the states of the neighboring systems for feedback.

In our case, we preferred to focus on cooperative method. These simple methods consist in introducing a coordinator controller in order to exchange information between subsystems. These methods have similarities with the emerging multi-agent class used in [31] and [32]. However, the drawback of this class is that a majority of them doesn't provide control optimality. They are based on informatic theories in which negotiations procedure using expert rules are established.
In [57] a cooperative MPCs control is proposed for nonlinear hybrid electric powertrain. This study shows good performance compared to centralized method, where the MPCs are coupled by their objectives function to ensure the global performance. Among the recent papers, we find the linear cooperative method [58] for generator load frequency control or the one described in [59] ensuring some robustness and convergence when the inputs are not coupled. Closer to our work, a distributed model predictive control is used for building temperature regulation in [60] or to manage a power plant porfolio in [61]. This last work uses the mathematic Benders' decomposition approach based on the duality decomposition [62].

2.3 Conclusion

In this chapter, we have detailed the building control complexity and cited advanced control work for the BEMS. We have focused on model predictive control that seems the most adapted to the building energy management problem. It offers a large range of formalization possibilities, an anticipative aspect much needed for the new energy context and it gives the possibility to be structured by hierarchical and distributed methods. The hierarchy can bring an answer to the problem of computing time, while the distributed aspect brings modularity and adaptability. In this work, in order to respond to our problematic, we will propose a hierarchical distributed MPC BEMS which is detailed in the next chapter.

Chapter 3

Energy Management Control development

Contents

3.1 Generic MPC definition 34
3.1.1 Systemic view 34
3.1.2 MPC formalization 41
3.2 MPC controllers 45
3.2.1 MPC configurations studies 48
3.2.2 The Multi-layers BEMS architecture 56
3.2.3 Conclusion 65
3.3 Distributed control 66
3.3.1 Block matrix problem formulation 66
3.3.2 Dantzig-Wolfe Decomposition 69
3.3.3 Resolution principle 70
3.3.4 Algorithm behaviour 72
3.4 Conclusion 74

In this chapter, we will formalize the Building Energy Management System (BEMS) problem and define control modes based on model predictive control methods. Our approach is developed with a systemic point of view of the home installation in order to be as generic as possible. The proposed BEMS aims to manage the whole controllable energy flows and deals with integrating the new smartgrid information and demands.
From the following part, an optimal Hierarchical and Distributed control architecture based on Model Predictive Control is developed. These advanced building controls have two control configurations: the tracking and the commitment modes. The tracking mode aims to optimize building objectives while the commitment mode implies more electrical network constraints.

3.1 Generic MPC definition

As explained in chapter 1, building control and electricity grid evolution lead to integrate more and more intelligence in building in order to control its consumption while ensuring the grid stability. Firstly, for a building, the objective is to enable to plan its energy flows while ensuring occupants' comfort and fulfilling systems constraints. To do so, and in order to develop an adaptable BEMS, we will present the systemic view used in this work. Then the scheduling problem will be formalized.

3.1.1 Systemic view

Historically, the building common controllable systems cover five categories: the ventilation systems, the air cooling and heating systems, the water heating systems, the producing systems and the storage systems. However, nowadays, many other consumption systems are found in the building and are controllable. In addition, thanks to communication technologies the controllability is extended to all systems. The problem formulation is established to take into account the new system integrations.

3.1.1.1 System model

In this work, we will describe all the systems by a unique system representation. This generic systemic view will enable to easily integrate and modify energy management system. To do so, all the considered models are supposed time-invariant. The constraints defined as follows may be simple upper or lower bounds or more complicated expressions. The following description refers to the Fig 3.1.

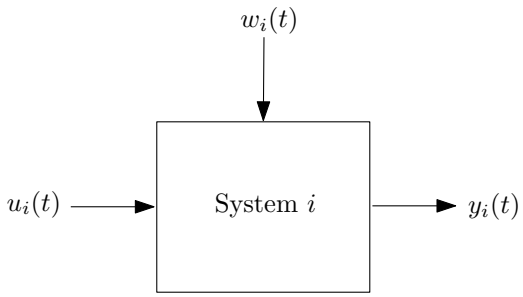

Figure 3.1: System scheme.

We note $u_i(t) \in \mathbb{R}^{m_i}$ the input state vector of system i, $x_i(t) \in \mathbb{R}^{n_i}$ the system state vector and $w_i(t) \in \mathbb{R}^{l_i}$ the system disturbance vector. Thus,

the system i is described as :

$$\dot{x}_i(t) = f_i(x_i(t), u_i(t), w_i(t)), \tag{3.1}$$

s.t.

$$g_i(x_i(t), u_i(t), w_i(t), t) \leq 0, \tag{3.2}$$

With $f_i : \mathbb{R}^{n_i} \times \mathbb{R}^{m_i} \times \mathbb{R}^{l_i} \to \mathbb{R}^{n_i}$ dynamics behaviour function of rank n_i and $g_i : \mathbb{R}^{n_i} \times \mathbb{R}^{m_i} \times \mathbb{R}^{l_i} \times \mathbb{R} \to \mathbb{R}^{n_{c_i}}$ the n_{c_i} system constraints which are time dependent, for instance, the temperature bounds can vary depending on the occupancy.

The system output is denoted $y_i(t)$ ($y_i \in \mathbb{R}^{p_i}$) by:

$$y_i(t) = h_i(x_i(t), u_i(t), w_i(t)) \tag{3.3}$$

To clarify the description, let us detail two basic system models.

3.1.1.1.1 Example 1: Heating system model Let's take an installation, noted system 1, composed of a room equipped with an electric heater. We suppose that the indoor dynamic temperature T_a can be modelized by a two order model with the two dynamic constant times, corresponding to the air and mass inertia. The indoor temperature dynamic behaviour is linearly influenced by the outdoor temperature T_{ext} and the solar flow I_{sr}. The electric heater power has a direct bounded power control command u_r.

The thermal air dynamic can be described by a simple air thermal model based on the one in [18]. It is composed of five thermal conductances and 2 capacities. The electric analogy of this thermal model is shown in figure 3.2.

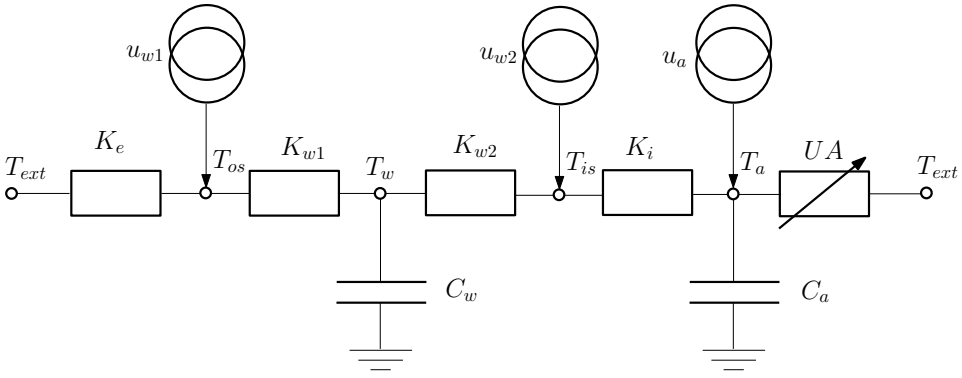

Figure 3.2: Electrical equivalent air thermal dynamic building model. The capacities C_w and C_a are associated to mass and air dynamics. R_i are the thermal resistances and u_i are the loads imposed on the different temperature nodes.

C_i et C_w are the internal and mass capacities ($J.K^{-1}$). T_a is the interior air temperature, T_w is the temperature of the thermal mass, T_{is} is the inside wall temperature and T_{os} is the outside wall temperature(°C). K_e, K_{w1}, K_{w2}, K_i and UA are respectively the thermal conductances between external air and outside wall surface, between outside wall surface and the mass, between mass and internal surface, between internal surface and indoor air and between indoor air and the external air through windows and ventilation ($W.K^{-1}$). u_a, u_{w1} and u_{w2} are the thermal loads on air and mass nodes (J) which combine heating, occupants, solar and weather loads.

In this example, a simple electric heater is used. Its thermal convective and radiative parts $u_{r,conv}$ and $u_{r,rad}$ are defined by:

$$\begin{bmatrix} u_{r,conv} \\ u_{r,rad} \end{bmatrix} = \begin{bmatrix} \eta_{conv} \\ (1 - \eta_{conv}) \end{bmatrix} u_r \tag{3.4}$$

where, η_{conv} is the convective factor and u_r is the electric radiator control.

For this system, the objective is to regulate the indoor temperature T_a. The available controllable variable is the radiator power u_r while the uncontrollable variables are the external temperature T_{ext} , the solar gain I_{sr} and the occupancy period O_{cc} which modify the temperature order bounds.

Using the system view described, this system can be formalized as:
The state vector:

$$x_1(t) = \begin{bmatrix} T_a(t) \\ T_w(t) \end{bmatrix} \tag{3.5}$$

with $T_a(t)$ the indoor air temperature of the controlled area and $T_w(t)$ the wall temperature.
The input vector:

$$u_1(t) = [u_r(t)], \tag{3.6}$$

with $u_r(t)$ corresponding to the radiator input control.
The disturbance vector:

$$w_1(t) = \begin{bmatrix} T_{ext}(t) & I_{sr,in}(t) & I_{sr,out}(t) & O_{cc}(t) \end{bmatrix}^T \tag{3.7}$$

Here we distinguish the solar gain through the windows $I_{sr,in}(t)$ and the solar gain on the external walls $I_{sr,out}(t)$. The output vector considered for the heating system:

$$y_1(t) = \begin{bmatrix} T_a(t) \end{bmatrix} \tag{3.8}$$

The link between the thermal loads and the system vectors are:

$$u_a(t) = \alpha_{conv}.I_{sr,in}(t) + \eta_{conv}.u_r \tag{3.9}$$

$$u_{w1}(t) = \alpha_{conv}.I_{sr,in}(t) + (1 - \eta_{conv}.u_r \tag{3.10}$$

$$u_{w2}(t) = I_{sr,out} \tag{3.11}$$

From the model equation, we find the dynamics input state function such as $\forall t \in [0; +\infty[$:

$$\dot{x}_1(t) = A_1.x_1(t) + B_1.u_1(t) + D_1.w_1(t) \tag{3.12}$$

where

$$A_1 = \begin{bmatrix} \frac{1}{C_a}.\frac{-K_i.K_{w2}}{K_{w2}+K_i} - UA & \frac{1}{C_a}.\frac{K_{w2}.K_i}{K_{w2}+K_i} \\ \frac{1}{C_w}.\frac{K_{w2}.K_i}{K_{w2}+K_i} & \frac{1}{C_w}.\frac{K_{w2}.K_i}{K_w2+K_i} \end{bmatrix} \tag{3.13}$$

$$B_1 = \begin{bmatrix} \frac{1}{C_a}.\eta_{conv}.\frac{K_i}{K_i+K_{w2}} \\ \frac{1}{C_w}.(1-\eta_{conv}).\frac{K_{w2}}{K_i+K_{w2}} \end{bmatrix} \tag{3.14}$$

$$D_1 = \begin{bmatrix} \frac{1}{C_a}.UA & \frac{\alpha_{conv}}{C_a} & \frac{1}{C_a}.(\frac{K_i}{K_{w2}+K_i}) & 0 \\ \frac{1}{C_w}.\frac{K_{w1}.K_e}{K_{w1}+K_e} & \frac{1}{C_w}.(\frac{K_{w1}.\alpha_{rad}}{K_{w1}+K_e}) & \frac{1}{C_w}.(\frac{K_{w2}}{K_{w2}+Ki}) & 0 \end{bmatrix} \tag{3.15}$$

Then the constraints are defined. It is considered that the radiator power is limited such as:

$$0 \leq u_r(t) \leq \overline{u}_c \tag{3.16}$$

and that the indoor temperature bounds depend on the occupancy time:

$$T^{[down]}(t) \leq T_a(t) \leq T^{[up]}(t) \tag{3.17}$$

where $\overline{u}_c$ is the maximal radiator power, $T^{[down]}(t)$ and $T^{[up]}(t)$ the varying bounds of the temperature such as:

$$T^{[down]}(t) = \begin{cases} 15°\text{C} & \text{if } Occ(t) = 0 \\ 20°\text{C} & \text{if } Occ(t) = 1 \end{cases} \tag{3.18}$$

and

$$T^{[up]}(t) = \begin{cases} 30°\text{C} & \text{if } Occ(t) = 0 \\ 23°\text{C} & \text{if } Occ(t) = 1 \end{cases} \tag{3.19}$$

3.1.1.1.2 Example 2: Battery model Let's take another example with an electrical battery, noted system 2. SOC is the energy battery storage capacity or state of charge, which is constrained by the bounds $SOC^{[down]}$ and $SOC^{[up]}$, corresponding to 20% and 80% of its maximal capacity. The charge and discharge powers are bounded and associated to specific dynamics. To consider the fast dynamics of a battery, a simple RC model is used. In the dynamical model of the energy stored in the battery (SOC), the efficiency (η_{batt}) factor depends on the charge or discharge state whereas the loss factor ($\eta_{ch,loss}$) is constant:

$$\frac{dSOC(t)}{dt} = -\eta_{loss,batt}.SOC(t) + \eta_{batt}(u_{batt}(t)).u_{batt}(t) \tag{3.20}$$

From the systemic view, this system can be formalized as:
The state vector:

$$x_2(t) = [SOC(t)], \tag{3.21}$$

The input vector:

$$u_2(t) = \left[u_{batt}(t)\right] \tag{3.22}$$

The output vector:

$$y_2(t) = \left[SOC(t)\right] \tag{3.23}$$

The system dynamics equations are derived from the equation (3.20) such as $\forall t \in [0; +\infty[$:

$$\dot{x}_2(t) = -\eta_{loss,batt}.x_2(t) + \eta_{batt}(u_2(t)).u_2(t) \tag{3.24}$$

where

$$\eta_{batt}(u_2(t)) = \begin{cases} \eta_{ch,batt} & \text{if } u_2(t) \geq 0 \\ \eta_{dis,batt} & \text{if } u_2(t) < 0 \end{cases}, \tag{3.25}$$

The constraints define the charge and discharge powers bounds:

$$P_{batt}^{[down]} \leq u_{batt}(t) \leq P_{batt}^{[up]} \tag{3.26}$$

and the battery state of charge bounds:

$$SOC^{[down]} \leq SOC(t) \leq SOC^{[up]} \tag{3.27}$$

After having detailed the system view and having shown two examples, we will present the global system view.

3.1.1.2 Global system view

From a BEMS point of view, the global home system can be seen as a gathering of s system models that have to be controlled in order to satisfy each specific model constraint. In the rest of the manuscript and for the clarity of the notation, the time dependence of the variables will be omitted when it is not useful.

Let's consider s systems described by the dynamical eq. 3.1 and subject to 3.2. Then, let's denote the global output vector:

$$y = \begin{bmatrix} y_1 \\ \vdots \\ y_s \end{bmatrix}, \; y \in \mathbb{R}^p \text{ ,with } p = \sum_{i=1}^{s} p_i \tag{3.28}$$

the global input vector:

$$u = \begin{bmatrix} u_1 \\ \vdots \\ u_s \end{bmatrix}, \; u \in \mathbb{R}^m \text{ ,with } m = \sum_{i=1}^{s} m_i \tag{3.29}$$

the global state vector:

$$x = \begin{bmatrix} x_1 \\ \vdots \\ x_s \end{bmatrix} \text{ , } x \in \mathbb{R}^n \text{ ,with } n = \sum_{i=1}^{s} n_i \tag{3.30}$$

and the global disturbance vector:

$$w = \begin{bmatrix} w_1 \\ \vdots \\ w_s \end{bmatrix} \text{ , } w \in \mathbb{R}^l \text{ ,with } l \leq \sum_{i=1}^{s} l_i \tag{3.31}$$

Now, we will detail the global equations and firstly we will pay attention to dynamically independent systems.

3.1.1.2.1 Uncoupled systems First, we suppose that the systems are independent. This means that they have no interactions between each other.

To formalize the global system, we consider the dynamical equations:

$$\begin{bmatrix} \dot{x}_1 \\ \vdots \\ \dot{x}_N \end{bmatrix} = \begin{bmatrix} f_1(x_1, u_1, w_1) \\ \vdots \\ f_N(x_N, u_N, w_N) \end{bmatrix} \tag{3.32}$$

This can be compacted in:

$$\dot{x} = f(x, u, w) \tag{3.33}$$

with f global dynamics functions.
For the constraints, we formalize the independent constraints by:

$$\begin{bmatrix} g_1(x_1, u_1, w_1, t) \\ \vdots \\ g_N(x_N, u_N, w_N, t) \end{bmatrix} \leq 0 \tag{3.34}$$

which can be compacted in:

$$g(x, u, w, t) \leq 0 \tag{3.35}$$

with g the global specific system constraints function.

Even though the systems are dynamically independent, they can be linked by n_c global constraints which are denoted:

$$C(u, w) \leq 0 \tag{3.36}$$

with $C : \mathbb{R}^m \times \mathbb{R}^l \to \mathbb{R}^{n_g}$.

The common constraints (3.36) correspond to the global building constraints. For example, in the electricity power management case, it corresponds to the power electricity balance equation. If we take the two previous presented systems 1 and 2 and we note u_{grid}(t) the electricity power of the building at the coupling point with the electricity network, the constraint (3.36) is:

$$u_{grid}(t) = u_r(t) + u_{batt}(t) \tag{3.37}$$

For another example, we can consider the fatal power consumption of the installation w_{fatal} corresponding to the uncontrollable electric power. Then the equation (3.37) becomes:

$$u_{grid}(t) = u_r(t) + u_{batt}(t) + w_{fatal}(t) \tag{3.38}$$

Next, we will focus on the coupled system case, and show that the formalization remains the same.

3.1.1.2.2 Coupled systems Now, we suppose that systems can be coupled by the input and states variables. This may happen, for example, if we consider that the indoor temperature is affected by the heating system input and by the ventilation system temperature output, or also if the heat pump efficiency is affected by the indoor temperature (return temperature). The couplings are taken into account as described in Figure (3.3). The system formulation does not change, the coupling is taken into account thanks to the disturbances vectors and in the common constraint.

More precisely, let's denote with N_i the set of all systems j that act on system i with $j \neq i$.
These interactions will be considered in the disturbance vector w_i, which can be divided in two parts; w_{NC_i}, the uncontrollable part, and w_{C_i} the disturbance part that comes from other systems. The disturbance vector is also:

$$w_i = \begin{bmatrix} w_{NC_i} & w_{C_i} \end{bmatrix}^T \tag{3.39}$$

And we define the coupling vector w_{C_i} such as:

$$w_{C_i} = \varphi_i((x_j, u_j)_{j \in N_i}) \tag{3.40}$$

This leads to have the same global formalization as for uncoupled systems case. This enables the modularity of the formalization.
For instance, let's consider the previous system 1 impacted by the solar gain through a window $I_{sr,in}$. When the blind opening is not controlled, the solar gain is uncontrollable and as a consequence is included in w_{NC_1} such as:

$$w_1 = w_{NC_1} = \begin{bmatrix} T_{ext} & I_{sr,in} & I_{sr,out} & O_{cc} \end{bmatrix}^T \tag{3.41}$$

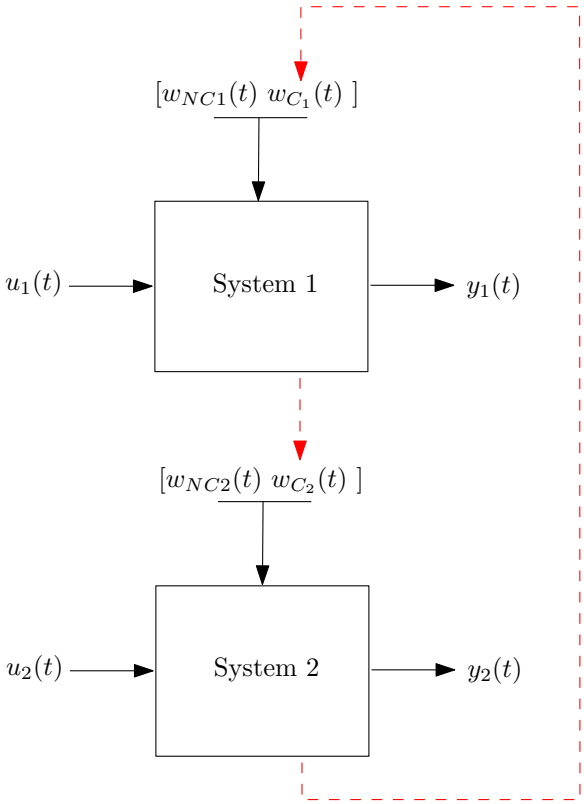

Figure 3.3: Coulped systems scheme

However, if the blind opening is controllable via another system, the solar gain through the windows will depend on the second system order u_2. Therefore, without modifying system 1, it will affect system 1 via w_{C_1} such as the vector equation (3.7) may be expressed as:

$$w_1 = \begin{bmatrix} w_{NC_1} & w_{C_1} \end{bmatrix}^T \tag{3.42}$$

with

$$w_{NC_1} = \begin{bmatrix} T_{ext} & I_{sr,out} & O_{cc} \end{bmatrix}^T \tag{3.43}$$

and

$$w_{C_1} = \varphi_1(u_2) \tag{3.44}$$

3.1.2 MPC formalization

In this thesis, we will focus on the optimization of an objective cost function J. This cost function will depend on the input vector. It can be defined by different ways depending on the researched goal (linear, nonlinear,

continuous, discrete, ...). Here, we note the MPC problem objective:

$$\min_u \int_0^\infty J(x(\tau), u(\tau), w(\tau))d\tau \tag{3.45}$$

To minimize this function and thus to optimize the control, we will use a Model Predictive Control method. This method consists in predicting the dynamics behaviours of the systems in order to define the optimal control. To do so, at each solving time chosen δ_j, instead of searching a continuous function solution under infinity, we transform the problem into a receding horizon problem on H such as the MPC problem objective becomes:

$$\min_u \int_{\delta_j}^{\delta_j+H} J(x(\tau), u(\tau), w(\tau))d\tau \tag{3.46}$$

To solve it, we will not have a continuous approach, but a discrete one: we will look for the best piecewise constant function u. More precisely, the prediction horizon will be divided into N intervals.

Let's consider the resolution sampling time vector $\Pi = \{t_k\}_N$, $k \in \{0, \ldots, N\}$ and $t_0 = \delta_j$ and such as:

$$t_{k+1} > t_k, \qquad k \in [0, N-1]$$

The sampling times noted t_k correspond to the instants to which the constraints have to be respected and to which the optimal control sequence is defined.
$S(\Pi)$ is the set of piecewise constant function over Π, i.e. $u(t) \in S(\Pi)$ implies that:

$$u(t) = \tilde{u}(t_k) \tag{3.47}$$

$$\text{for } t \in [t_k, t_{k+1}[\quad , k\{0, \ldots, N-1\} \tag{3.48}$$

In this work, the horizon is defined such as $H = t_N - \delta_j$. The optimal sequences are re-computed periodically (receding horizon). In our work, we will note the solving times δ_j with $j \in \mathbb{N} - \{0\}$ and such as $\forall j$:

$$\delta_{j+1} > \delta_j$$

Before formalizing the MPC problem , we will define two operators to ease the notations and the understanding.

3.1.2.1 Operators

The following operators are introduced and will be used to formalize the resolving methods.

The Sampling operator *Samp* Given a function $u(t)$, $t_0 \leq t \leq t_N$, a collection of time Π , such as $\forall k \in \{1, \ldots, N\}$: $t_k > t_{k-1}$.
We define the operator *Samp* :

$$\overline{u}(\{1, \ldots, N\}|t_0) = Samp(u(t), t_0, \Pi) \tag{3.49}$$

such that $\forall i \in \{1, \ldots, N\}$:

$$\overline{u}(i|t_0) = \frac{1}{(t_i - t_{i-1})} \int_{t_{i-1}}^{t_i} u(\tau) d\tau$$

The Zero-holder operator *ZO* Given a sequence $u(\{k\})$, $1 \leq k \leq N$, and a collection of time Π we define the operator *ZO*:

$$\underline{u}(t|t_0) = ZO(u(\{1, \ldots, N\}), t_0, \Pi) \tag{3.50}$$

such as $\forall t \in [t_0, t_N]$ and $\forall i \in \{1, \ldots, N\}$:

$$\underline{u}(t|t_0) = u(i) \text{ if } t_{i-1} \leq t < t_i$$

Thus $\underline{u}(t|t_0)$ is a constant piecewise function, $\in S(\Pi)$.

3.1.2.2 Problem definition

To formalize the General MPC problem, we still have to define the piecewise data profile needed to prediction and the solution of the states differential equations 3.1.

– Thanks to the previous operator definition, whatever the data profile available $w_{NC}(t)$, we transform it into a piecewise constant function $\langle w \rangle_{NC}$. Let's consider a continuous available data profile $w_{NC}(t)$. First we use the *Samp* operator to define its values at the sampling time collection $\{tk\}_N$ such as:

$$\overline{w}_{NC}(\{t_k\}_N|t_0) = Samp(w_{NC}(t), t_0, \{t_k\}_N) \tag{3.51}$$

Then, the *ZO* operator is used such as:

$$\langle w \rangle_{NC}(t|t_0) = ZO(\overline{w}_{NC}(\{t_k\}_N|t_0), t_0, \{t_k\}_N) \tag{3.52}$$

– The solution of the states differential equations 3.1 of the problem is:

$$\tilde{x}(t) = x_0 + \int_{\delta_j}^{t} f(\tilde{x}(\tau), u(\tau), \langle w \rangle(\tau|\delta_j)) d\tau \tag{3.53}$$

Now, it is possible to formalize the General MPC problem that we aim to resolve:

General MPC problem At a time δ_j.
Known $\Pi = \{t_k\}_N$ and given

- $x_0 = x(\delta_j)$
- $\langle w \rangle_{NC}(t|\delta_j)$: the uncontrollable prediction disturbance vector

The optimization problem is:

$$\tilde{u} = \min_{u \in S(\Pi)} \int_{\delta_j}^{H+\delta_j} J(\tilde{x}(\tau), u(\tau), \langle w \rangle(\tau|\delta_j))d\tau \tag{3.54}$$

s.t.

$$\tilde{x}(t) = x_0 + \int_{\delta_j}^{t} f(\tilde{x}(\tau), u(\tau), \langle w \rangle(\tau|\delta_j))d\tau \tag{3.55}$$

and $\forall \{t_k\}_N \in \Pi$

$$g(\tilde{x}(t_k), u(t_k), \langle w \rangle(t_k|\delta_j), t_k) \leq 0 \tag{3.56}$$

and

$$C(u(t_k), \langle w \rangle(t_k|\delta_j)) \leq 0 \tag{3.57}$$

and with $\tilde{x}$ the predicted states behaviour.

Solving the General MPC problem provides the optimal control sequence $\tilde{u}$. Similarly to the problem resolution, this sequence is used to define the piecewise constant optimal function $u^*(t)$ apply to the systems. It is defined such as $\forall t \in [\delta_j, \delta_j + H[$ and $\forall i \in \{1, \ldots, N-1\}$:

$$u^*(t|\delta_j) = \tilde{u}(t_i) \tag{3.58}$$

$$\text{for} \qquad t_i \leq t < t_{i+1} \tag{3.59}$$

$u^*(t|\delta_j)$ corresponds to the piecewise constant optimal control functions calculated at time δ_j. The term δ_j enables to differentiate the solution function calculated at the different times δ_1, δ_2, ...

As explained in chapter 2, the optimality of the MPC relies on several things:

- The quality of the prediction which depends on the system models and the exactness of the prediction data profiles. However, these do not depend of the MPC problem formalization parameters and so will be treated in Chapter 4.
- The MPC problem parameters settings. Amongst these we principally have the prediction horizon H, the sampling time sequence Π and the solving times δ_j.

In the following part, we will focus on the parameters settings and perform studies on mono-layer control before presenting the hierarchical control structure developed.

3.2 MPC controllers

In this part, we will explore the various ways to solve the MPC problem as well as doing a parameter study to find the most adapted configuration to the problem.

Illustrative examples

In order to assess the proposed control, we will consider a global system composed by the two linear sub-systems (1 and 2) which are the battery and the heating system previously defined, associated to an electrical coupling point between the building and the grid (P_{grid}). The model parameter values are presented in the tables 3.1, 3.2 and 4.3, which correspond to the heating system, the battery and the grid connection respectively.

Parameter	Value
Window area	2 m^2
Wall area	70 m^2
C_a	1e8 $J.K^{-1}$
C_w	1e5 $J.K^{-1}$
UA	10 $W.K^{-1}$
K_i	20 $W.K^{-1}$
K_{w1}	2000 $W.K^{-1}$
K_{w2}	100 $W.K^{-1}$
K_e	0.1 $W.K^{-1}$
Occupancy period	3pm to 8am
Occupancy Temp. range	19-22 °C
Inoccupancy Temp. range	15-28 °C

Table 3.1: Heating system example model parameters

Parameter	Value
$\eta_{loss,batt}$	1 min
$P_{batt}^{[up]}$	1.5 kW
$P_{batt}^{[down]}$	-1.5 kW
$SOC^{[up]}$	0.7 % × 10 kW.h
$SOC^{[down]}$	0.3 % × 10 kW.h

Table 3.2: Battery example model parameters

Parameter	Value
$P_{grid}^{[up]}$	3 kW
$P_{grid}^{[down]}$	-3 kW

Table 3.3: Electrical manager parameters

In this demonstration case, the common constraints of the illustrative example are, $\forall t_k \in \{t_k\}_N = \Pi$:

$$P_{grid}(t_k) = u_r(t_k) + u_{batt}(t_k) \tag{3.60}$$

and the additional grid power bound constraints:

$$P_{grid}^{[down]} \leq P_{grid}(t_k) \leq P_{grid}^{[up]} \tag{3.61}$$

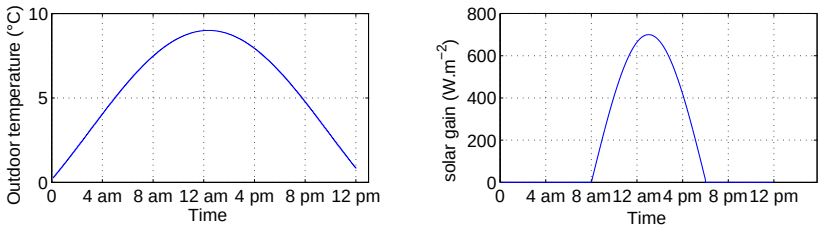

(a) Temperature profile (b) Solar gain profile

Figure 3.4: Distubances profiles

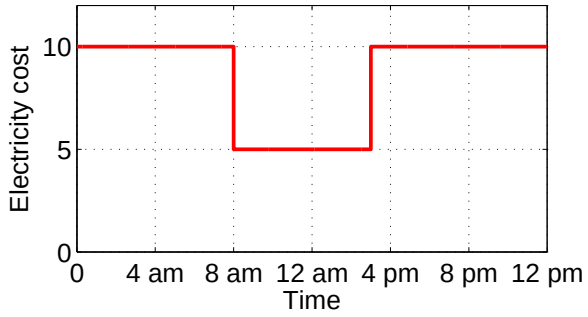

Figure 3.5: $w_{buy}(t)$ profile of the illustrative case. $w_{sell}(t)$ *is set equal to* $w_{buy}(t)/2$.

Moreover, we suppose that the disturbances w_{NC} are known on the horizon H at each computing time δ_j. Profiles are defined on Figure 3.4 (a) and (b).

In addition, in the illustrative cases and in throughout all this work, we will consider varying energy tariff periods over the day. Here, the electricity buying price is displayed in Figure 3.5. We set the selling electricity price so that it equals half of the buying ones.

In the following part the BEMS aims to reduce the energy cost consumption of the building J_{glo}. The cost function is defined such as:

Objective cost function Known $w_{sell}(t)$ and $w_{buy}(t)$, the sale and purchase prices of electricity on the grid, we have

$$J_{glo} = \int_0^{\infty} \begin{cases} w_{buy}(\tau).P_{grid}(\tau)d\tau & \text{if } P_{grid}(\tau) > 0 \\ w_{sell}(\tau).P_{grid}(\tau)d\tau & \text{if } P_{grid}(\tau) < 0 \end{cases} \tag{3.62}$$

The variables $P_{grid,buy}$ and $P_{grid,sell}$ correspond to the buying and selling power.

The choice of a linear cost function J arises from the fact that:

- A linear cost function enables to keep a real meaning of the cost function.
- On a technical aspect, due to the constraint, it leads to better efficiency.

Moreover, due to the fact that the problem has constraints, slack variables are added in the cost function. It is because the constraints lead to infeasibility. And when there is infeasibility, no solution can be found. To overcome that, slack variables are added to relax the constraints (see Appendix A) and are heavy penalized in the cost function. In our case, no compromise is done on the user's comfort and requests which mean that each slack variable is heavily penalized. Thus, whatever the energy cost, the control aims to respect the constraints.

Comparison criterion

To differentiate the configurations, we will compare them paying attention to three aspects:

- The control optimality.
  The control optimality defines the values of the cost function post control. It enables to compare the performance of the MPC configurations.
- The respect of the constraints.
  As said in the illustrative example specifications, the constraints are relaxed to ensure the solution feasibility. In consequence, failure to the states constraints respect can occur. We look for the more "robust" MPC configuration in order to reject as much as possible the disturbances. This aspect is assessed post control.
- The computing time burden.
  Remember that due to the long time constant of some building systems and the fast dynamic of the electrical power of other system, the building controller has to deal with a long horizon (almost 12 hours) and fine sampling time (e.g. 10 to 60 seconds). Due to its large complexity and so as to implement the controller, we look for the lower MPC configuration computing time burden.

In the following part, we will first examine a mono-layer structure in order to assess open loop and closed loop efficiencies. Then, we will study different sampling time vectors and the prediction horizons. In a second part, we will present and detail the BEMS developed which uses the first part results and offers advanced possibilities to integrate a smart grid. This BEMS has multi MPC layers architecture, it is composed of two control modes. The last part of this section is about the BEMS implementation. It presents a cooperative method enabling to distribute the problem resolution and so bring modularity and adaptability to the BEMS.

3.2.1 MPC configurations studies

In this part, we suppose that the MPC programming is composed of a unique layer noted Centralized controller (C) in order to define the most efficient parameters values for our problem. We will start with an open loop control before testing a closed loop control. Both controls will use constant sampling time intervals. Then we will assess the impact of the sampling time vector and finish with the horizon impact.
Let's note that in all the manuscript, the CPLEX solver with the MATLAB interface is used to solve the optimization problem.

3.2.1.1 Centralized Open Loop (C-OL)

The C-OL corresponds to a scheduling control which computes the optimal problem solution at time δ over a horizon H. For this configuration, the next optimization occurs only at time $\delta + H$. So for this control, the optimal control sequence is applied over all the horizon without being recalculated. With the introduced notation for the General MPC problem 3.1.2.2 this means that we have $\forall j \in \mathbb{N} - \{0\} : \delta_j = j.H$.

For this control configuration, we use a resolution sampling time vector with constant intervals (time slots) which is often used in the MPC controller. It results the C-OL sampling time vector noted Π^{Δ_L} such as $\forall t_k \in \{t_k\}_N$:

$$t_k = \delta_j + k.\Delta_L \tag{3.63}$$

with Δ_L a constant value.

This C-OL mode is called "scheduling" mode in the literature because the optimization is repeated with a "frequency" H.

The main parameter of this control configuration is the value Δ_L. That is why, we will first study its effect before assessing the C-OL control configuration performance.

3.2.1.1.1 Impact of Δ_L on computing time Δ_L is the time slot of the optimization problem. To assess its impact on the computing burden, we have to introduce the number N_{opti} which is the decision variables number of the optimization problem. It is defined such as:

$$N_{opti} = N_{var} \times \frac{H}{\Delta_L} = N_{var} \times N \tag{3.64}$$

N_{var} is the number of variable and H is the horizon fixed at 24 hours. Both values are fixed, therefore N_{opti} is proportional to Δ_L.

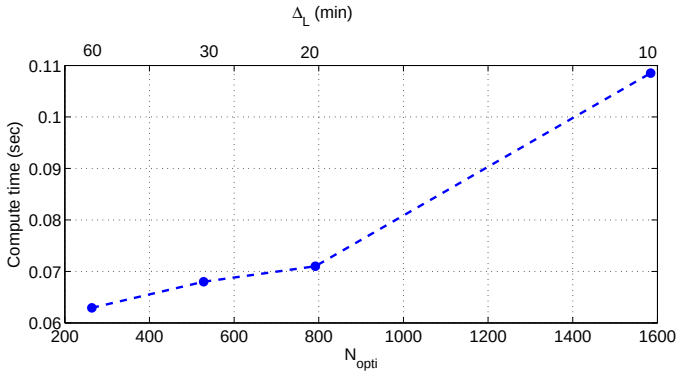

Figure 3.6: Resolving computing time function of N_{opti}. *The N_{opti} values is displayed in the bottom axis and the Δ_L constant sampling time on the top axis.*

In this case, the optimization problem is composed of eleven variables. There are P_{grid}, u_r, u_{batt}, plus fourth linearising variables $\lambda_{1,2,3,4}$ which enable to linearize the complementary constraints (eq. 3.25 and 5.5) and plus fourth slack variables for the relaxation of the temperature constraint equation 3.17 and the battery state of charge constraint equation 3.27 (see Appendix A for details).

Figure 3.6 shows the computing time in function of the number N_{opti}. Each value displayed corresponds to the average computing time of 500 simulations with different initial states values. We note that the computing time increases when N_{opti} grows. Here, no bigger value ofN_{opti} could be performed because the computer capacity was saturated. As displayed in Figure 3.6, the biggest value is $N_{opti} = 1584$ corresponding only to $\Delta_L = 10$ min. We notice that the computing time seems not very big, but the illustrative case example involves only three controllable variables. Many more variables are needed to describe the whole building control.

3.2.1.1.2 Illustrative robustness performance Another important point is the robustness performance. To illustrate the C-OL MPC one we will disturb the control by introducing biased prediction profiles.

First, we define a benchmark. We considered the optimal solution of the optimization for $\Delta_L = 10$ min where prediction profiles and those of the simulation process are identical ($\langle w \rangle_{NC}(t_k|\delta_j) = w_{NC}(t_k)\ \forall \{t_k\}_N \in \Pi$ and $\forall j$). The resulting indoor temperature benchmark trajectory is displayed in Figure 3.7.

Now we suppose that the prediction solar gain profile is biased as de-

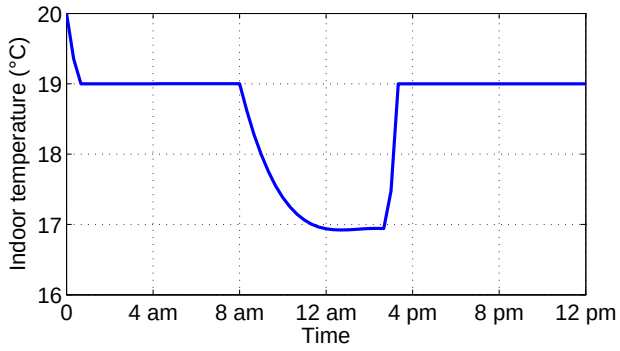

Figure 3.7: Benchmark indoor temperature trajectory

scribed in Figure 3.8. The resulting temperature profile trajectory displayed

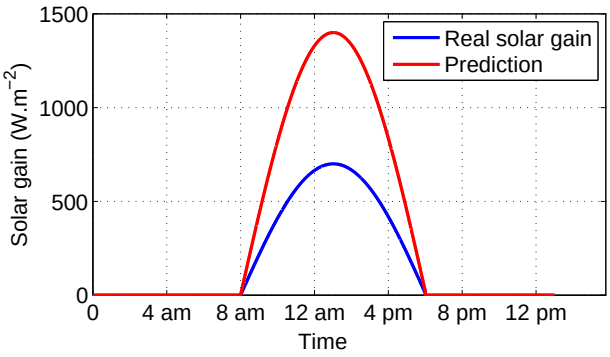

Figure 3.8: Prediction disturbance of the simulation example

in 3.9 shows a temperature regulation error. As said in chapter 2, for build-

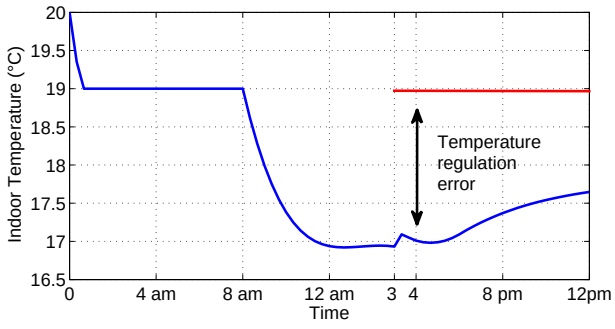

Figure 3.9: Indoor temperature trajectory with disturbance

ing regulation, the prediction profiles are very hard to predict and so control

robustness is essential.

Before studying another control mode, let's note another drawback of this one. It is not illustrated here but let's explain it. To optimize the control, the MPC method aims to anticipate the needs and to shift the consumptions. With the C-CL mode. If a need occurs at time $\delta_j + H + \epsilon$, the control will be informed only at the next optimization time $\delta_{j+1} = \delta_j + H$. As a consequence, it will have sadly only a time interval of ϵ to anticipate it. It results a suboptimal optimization.

To conclude the OL MPC does not provide enough "robustness" and efficiency that is why the following receding control is studied.

3.2.1.2 Centralized Closed Loop (C-CL)

Similar to the previous mode, the C-CL corresponds to a scheduling control which computes the optimal problem solution at time δ_j over a horizon H. However, contrary to the C-OL mode, the next optimization occurs at time $\delta_{j+1} << H$. This means that only a part of the first optimal control sequence is applied to the process. This enables to update the current systems' states and also adjust the prediction data, if available. Thereby, the prediction error can be adjusted and the objective cost function is re-optimized over the receding horizon.

The C-CL MPC problem is the same as the C-OL problem but, however instead of having $\delta_j = j.H$, the C-CL principle consists in repeating the calculation at each sampling time Δ_L such as $\delta_j = j.\Delta_L$.

3.2.1.2.1 Illustrative example Figure 3.10 shows the indoor temperature trajectory without considering unpredicted disturbance. The results are similar to the C-OL mode and the objective function values are identical.

Then, as in the previous study, we simulate control with unpredicted disturbance. Indoor trajectory result is displayed in Figure 3.11. The unpredicted disturbance is rejected and the temperature is regulated at 19 °C.

In comparison to the C-OL control, we note that the C-CL method is more adapted to our problem when feedback state values T_a and SOC and updated information and predictions are available.
Moreover, the situation explained in the previous paragraph where a need occurs at time $\delta_j + H + \epsilon$ is treated efficiently. Because the controller will take into account the need at the next optimization time $\delta_{j+1} = \delta_j + \Delta_L$.

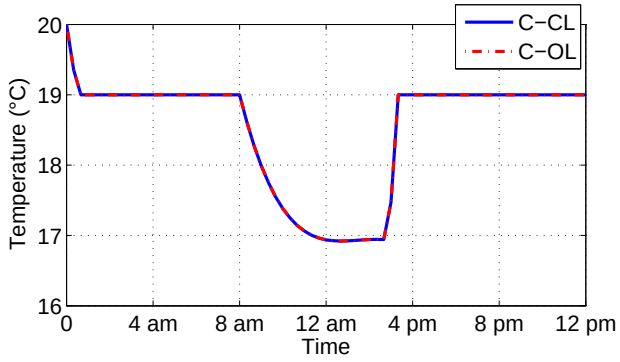

Figure 3.10: Indoor temperature trajectory without unpredicted disturbance

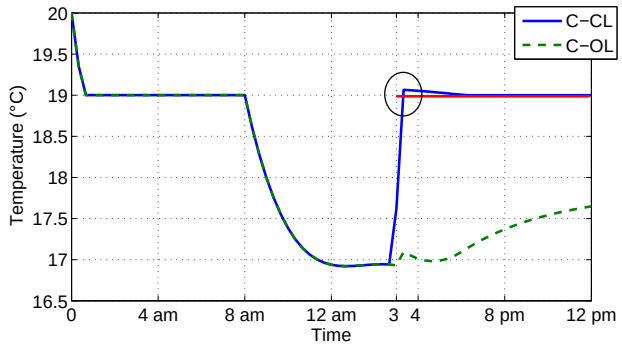

Figure 3.11: Indoor temperature trajectory with unpredicted disturbance (C-CL)

Thus, the anticipating interval size is $\delta_{j+1} + H + \epsilon - \Delta_L$.

However, compared to the previous mode, the computing time is not improved (same number of variable). In this case, this is especially important because the receding mode proceeds repeated optimization. Moreover, due to this large complexity, the sampling time cannot be finer than 10 min as in the C-OL.

To reduce the computing time while using finer sampling time, it exists several solutions:

- Decrease the horizon.
  The optimal horizon is complex to be, right from the beginning, determined. It depends on many things such as the building need, the system time constants, the power bounds or also the tariff profile alias it depends on the simulation case.
- Use hierarchical architecture.

The principle is to have different layers working with different time scale. The higher the layer is, the longer the horizon is and the bigger the sampling time is.

– Work with a varying sampling time.
Advantage is that it keep the same horizon and used adaptive sampling time over it deals with the different dynamics.

In the following part we will test the varying sampling time vector method.

remark We may find another interest to reducing the variables number, that way, indeed the control aims to be distributed. As a consequence, the smaller the variables number is, the smaller exchanged information quantity between the future local controllers is. Thus it improves the algorithm time convergence.

3.2.1.3 Centralized Closed Loop with varying sampling time (C-VCL)

Due to the high computing time of the C-CL mode for fine sampling time with long horizon, we propose the following modes to alleviate real time computation load. As seen in Figure 3.12, the sampling times are no more constant but vary.

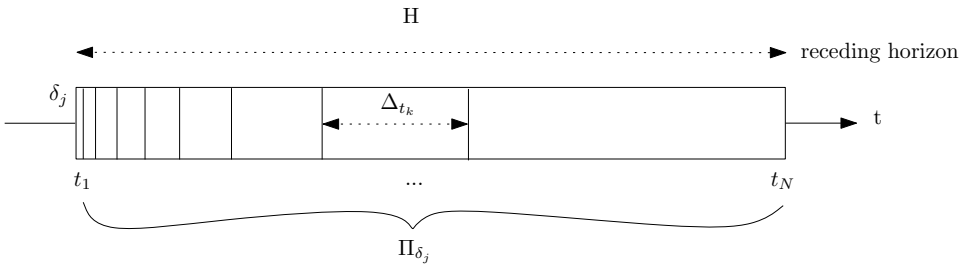

Figure 3.12: Scheme of the C-VCL sampling time distributions

To avoid the computing time problem while keeping the control efficiency and even reducing the sampling time, we propose to work with a varying sampling time such as $\forall k \in \{1, \ldots, N-1\}$ and $\forall \{t_k\}_N \in \Pi^{VCL}$:

$$\Delta_{t_k} \leq \Delta_{t_{k+1}} \tag{3.65}$$

with

$$\Delta_{t_k} = t_{k+1} - t_k \tag{3.66}$$

The C-VCL problem is identical to the C-CL problem. The optimization is repeated at each sampling $\delta_j = j.\Delta_{t_1}$. However, the decision variable number N_{opti} is not equal to the equation (3.64) but is defined such as:

$$N_{opti} = N_{var} \times N \tag{3.67}$$

Let's note that N_{opti} is no more function of the finer sampling time but depends on the times slots number N wished.

3.2.1.3.1 Illustrative example Many time slots distribution can be used, using specific systems time or problem constraints. In our case, we will test several distributions (linear, exponential, and so on) and see that their efficiencies are equivalent. In order to take into account the slow and fast dynamic, we propose a varying sampling time composed of two different times slots Δ_f fine and Δ_s bigger constant values such as:

$$\begin{aligned} \text{for } t_k \leq \delta_j + 2\text{h} \quad &, \Delta_{t_k} = \Delta_f \\ \text{and } t_k > \delta_j + 2\text{h} \quad &, \Delta_{t_k} = \Delta_S \end{aligned}$$

To assess the mode efficiency, we performed simulations. We set $\Delta_s = 1$ hours and tested several Δ_f values.
As in the previous study, we assess its robustness by considering unpredicted disturbance (see Figure 3.8). The temperature regulation results in Figure 3.13 shows that, like in the C-CL control mode unpredicted disturbances are rejected more or less quickly. We remark that, with a horizon $H = 24$ hours, it is possible to work with finer sampling time $\Delta_f = 5$ min and that the finer Δ_f is, the better the temperature regulation is and as a consequence the control robustness.

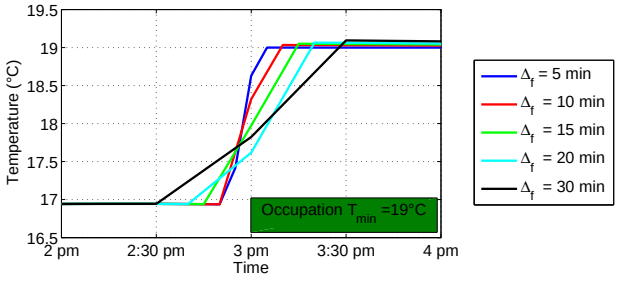

Figure 3.13: Temperature regulation with unpredicted disturbances in function of Δ_f.

Figure 3.14 shows the computing time in function of N_{opti} and Δ_f. Each time displayed corresponds to the average computing time of 500 simulations with different initial states values. We note that in comparison with the other mode, varying time slot method enables to reduce significantly the computing time, e.g. 39 % for $\Delta_f = 10$ min.

To sum up, the varying sampling time configuration seems to be adapted to the BEMS problem. Nevertheless, considering the interface with the grid, changing the energy plan at each fine sampling time is not thinkable. To overcome this issue, we propose to combine the varying sampling time

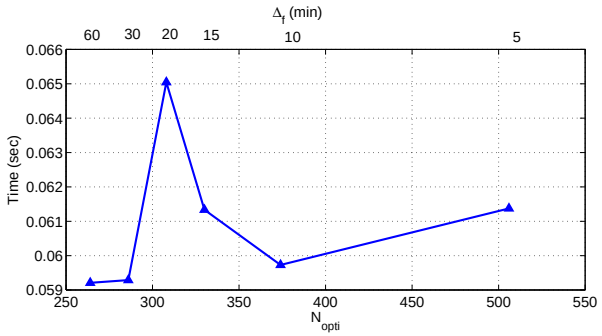

Figure 3.14: Computing time function N_{opti} (Δ_f). *The N_{opti} values is displayed in the bottom axis and the Δ_f finer sampling time on the top axis.*

method with a hierarchical control structure. This is presented into the part 3.2.2.

Before presenting it, we will study first the horizon impact in order to close our MPC configuration investigations.

3.2.1.4 Varying horizon and horizon size impact

Rather than varying the sampling time, another method, used in [63] for the thermal regulation, is also to use a varying horizon. In the cited work, the choice of horizon was to use long horizon during the inoccupancy period and to use a short horizon during occupancy period in order to regulate temperature as fast as possible and during the preheating phases. In this work, the horizon is fixed according to application specificities. In our case, it seems very hard to define this kind of rules because our application combined many systems and information (occupancy/inoccupancy period, battery, different cost periods, etc).
However, the impact of the horizon on the cost function can be assessed. In one of our study, we show that for the study case, a horizon of eight hours was enough to minimize the cost function (see Figure 3.15). In this study, detailed in [64], we considered varying electricity prices profiles and one building composed of a solar panel, an electrical battery, electric radiators and a hot water tank. A C-CL control with constant sampling time Δ_S was used.

These results do not establish an optimal horizon for all the building but gives us an idea of the anticipative horizon needed to anticipate the price variations and optimize the building consumption. We can say with caution that a horizon of 24 hours is unnecessary and that a horizon of about 12 hours or a little bit more is enough for the residential building.

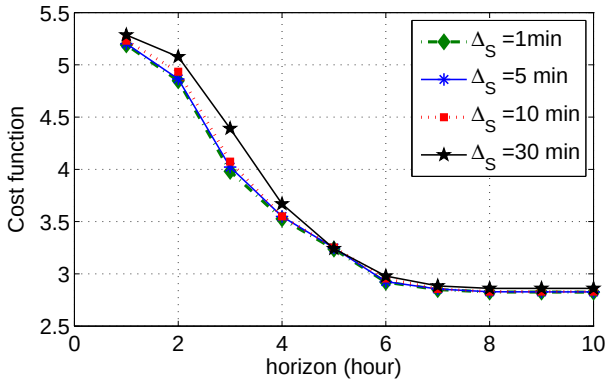

Figure 3.15: Impact of the horizon on the objective cost value

3.2.1.5 Conclusion

In this part, we performed a study on centralized optimization. We studied different techniques to improve the robustness of the control and reduce the computing time. Among the results, the C-VCL mode using receding control and varying sampling time seems the most adapted control, offering the best compromise, to deal with large scales of dynamic time constants while requiring low computing capacity. This advanced technique enables to fine the sampling time to 5 or 1 min while having adapted horizon which is about 12 hours for the residential building energy control.

However, as explained in chapter 2, the BEMS is not anymore limited to the building energy consumption optimization, but has also to deal with the grid constraints and demands, arising from global electricity network or local network (district, quarter). That is why, to go further we look for a BEMS architecture enabling to take into account more specific grid demands.
In the next part, the developed multi MPC layers control architecture is presented. These different configurations arise from the mono-layer control modes described previously.

3.2.2 The Multi-layers BEMS architecture

In this part we will present a structuring multi MPC layers BEMS proposing advanced interface between building and grid (see Figure 3.16).

These multi MPC layers approach is proposed for two reasons. First, it is a structuring approach often used in building control and which corresponds to the actual building control with a supervisor layer at the top and local controllers at the bottom. Secondly, this architecture will enable to develop specific controls configurations in order to integrate the global network challenges considering that the energy building consumption (electrical

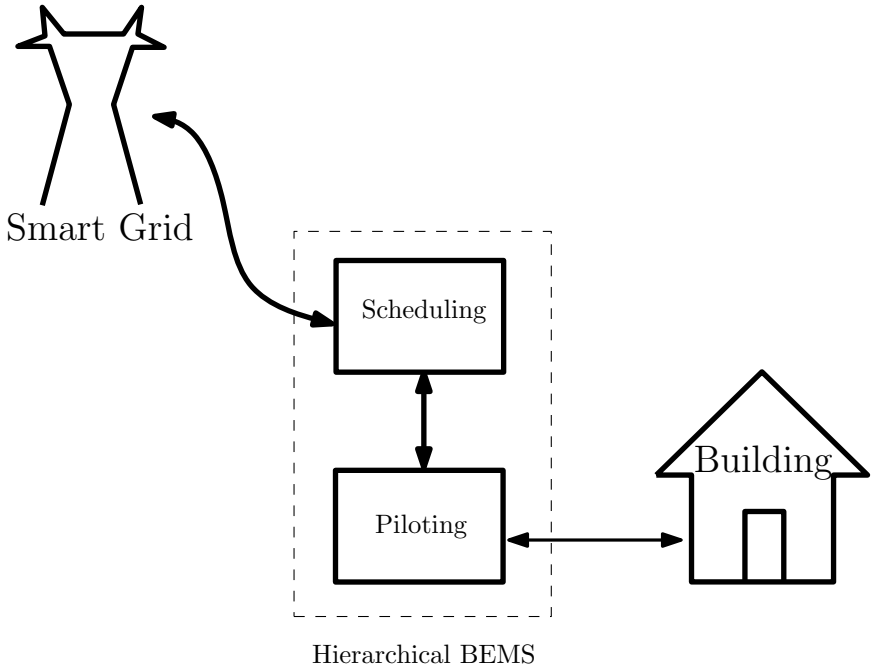

Figure 3.16: Hierarical BEMS scheme

or other) is supported by the global network through the common coupling point. In this part, we will first explain the hierarchical control principle and then detail the two developed BEMS modes.

3.2.2.1 Hierarchical Architecture Principle

The BEMS architecture is composed of two MPC layers, its principle is:

– At the Scheduling layer, the BEMS receives the grid information and has for objective to minimize the global economic objective function J (plan the energies consumptions) over a long time scale horizon H_S, so $J_S = J$. At this level, only the slow dynamics are taken into account to obtain the tendencies that have to be respected in order to minimize the objective cost. Then, a part of the solution or all the solutions, depending on the BEMS modes, is sent to the lower level in order to be respected.

– At the Piloting layer, the objective is to manage energies over a shorter horizon h_P, while fulfilling commands orders given by the higher level. At this layer, finer and varying sampling time is used in order to be as robust as possible.

To add clarity, it results that the high layer (scheduling layer) has two important functions. Firstly, it optimizes the economic cost function of building by working over a long horizon. Then, it provides the energy plan to the lower MPC layer. Secondly, it interacts with the grid. This means that it receives grid demands and tariff information and, depending on the mode, will provide information back.
At the lower level, the difficulty is to respect the systems and users' constraints while following the higher level command in order to be as close as possible to the optimal plan.
This architecture has two main advantages. First, it is a structuring architecture. It is made of two layers with their own functionality. One is to plan consumptions and to deal with the interface building-grid, and the other one serves to pilot the building energies flows. Secondly, the two time scales of the layers combined with the varying sampling time enable to propose a BEMS with anticipation and reactivity.

Important aspects for the hierarchical control are how the higher commands are transmitted and interpreted at the lower level and how they are executed. The main idea is to transmit the state trajectories planned together with the energy stage consumption associated. Thus, it is possible to weigh differently each constraint to obtain different BEMS objectives in order to either promote the trajectories tracking or promote the energy stage consumption respect. Details are given follows.

Scheduling layer (S)
We consider that, at the Scheduling layer, we have:

- δ_j : the scheduling optimization computing times which are explicit in the different control modes.
- $\forall \delta_j$, $\Pi^S_{\delta_j} = \{t_K\}_{N_S}$: the scheduling sampling time vector, $t_0 = \delta_j$, $t_{N_S} = \delta_j + H_S$
- H_S: the scheduling long horizon
- J_S, the global objective cost function.
- $\langle w \rangle_{NC}(\{1, \ldots, N_S\}|\delta_j)$: the uncontrollable prediction disturbance profile

Solving the S problem provides the optimal control sequence functions $\tilde{u}^*$. From it, the optimal control continue function $u^*(t|\delta_j)$, $\forall t \in [\delta_j, \delta_j + H_S[$ is created.
These functions are used to generate the profile of each subsystem state $x^*(t|\delta_j)$ according to their continuous dynamical equations.
Moreover, in order to constrain the energy spent by the piloting layer, the energy stages functions E^*_S are defined such as, $\forall \{t_K\}_{N_S}$ and with $t_0 = \delta_j$:

$$E_S(t_K) = \int_{t_{K-1}}^{t_K} u^*_{grid}(\tau|\delta_j) d\tau \tag{3.68}$$

Then, the ZO operator is used and provides:

$$\underline{E}_S(t|\delta_j) = ZO(E_S(\{t_1, \ldots, t_{N_S}\}), \delta_j, \{t_K\}_{N_S}) \tag{3.69}$$

We note χ the resulting command function composed by the state trajectories and the energies time slot consumptions over the horizon H_S, such as:

$$\chi(t|\delta_j) = \left[x^*(t|\delta_j) \quad \underline{E}_S(t|\delta_j)\right]^T \tag{3.70}$$

Then, $\chi(t|\delta_j)$ is sent to the lower layer. The choice of used energy stage cost is due to the impossibility to control the real time power. The energy cost stage enables to take into account energy consumption plan without forcing power to be constant. The smoothing of the power is brought with the states trajectories commands which are built considering constant piecewise inputs.

Piloting layer (P)

At the Piloting layer we have:

- ρ_p : the piloting optimization computing time
- $\chi(t|\delta_j)$: the command profiles
- h_p: the piloting horizon
- $\forall \rho_p$, $\Pi^P_{\rho_p} = \{t_k\}_{N_p}$: the piloting sampling time vector at time ρ_p, $t_0 = \rho_p + h_p$
- $\langle w \rangle_{NC}(\{1, \ldots, N_p\}|\rho_p)$: the uncontrollable prediction disturbance profile
- For this layer, we define a multi-objective function J_p. We set $\forall t_k \in \Pi^P_{\rho_p}$:
  - $|\sigma_X(t_k)|$ the absolute trajectories tracking errors
  - $|\sigma_E(t_K)|$ the absolute energy stage errors

  The absolute trajectories tracking error is defined such as $\forall t_k \in \Pi^P_{\rho_p}$:

$$|\sigma_X(t_k)| = |(x(t_k) - overline x^*(t_k|\delta_j))| \tag{3.71}$$

  with:

$$\overline{x}^*(t_k|\delta_j) = Samp(x^*(t_k|\delta_j), \rho_p, \Pi^P_{\rho_p})) \tag{3.72}$$

  The absolute energy stage error is more complex to define. To ease the understanding, you may refer to Figure 3.17 during the definition.

  The principle is to constrain the used piloting energy grid consumption during each high layer sampling interval. As a consequence, the scheduling sampling time vector associated to the energy state profile command is known ($\Pi^S_{\delta_j)}$).
  At the piloting time ρ_p, the energy stage errors taken into account are only those included in $\Pi^P_{\rho_p}$. As a consequence, $|\sigma_E(t_K)|$ is defined only $\forall t_K \in \Pi^S_{\delta_j} \cap \Pi^P_{\rho_p}$. This sequence of times depends on ρ_p, it is defined

as $\Xi(\rho_p) = \{t_i, t_i \in \Pi^S_{\delta_j}, t_i \in Pi^P_{\rho_p}\}$

In order to define the first energy stage error, we introduce T_{ρ_p} corresponding to the first energy stage time. Thus, we can define the energy stage error such as $\forall t_K \Xi(\rho_p)$:

$$|\sigma_E(T_{\rho_p})| = |E_S(T_{\rho_p}|\delta_j) - \int_{T_{\rho_p-1}}^{\rho_p} u_{grid}(\tau|\rho_p).d\tau - \sum_{t_k=t_1}^{T_{\rho p}} E_p(t_k|\rho_p)| \tag{3.73}$$

$$|\sigma_E(t_K)| = |E_S(t_K|\delta_j) - \sum_{t_k=t_{K-1}}^{t_K} E_p(t_k|\rho_p)| \tag{3.74}$$

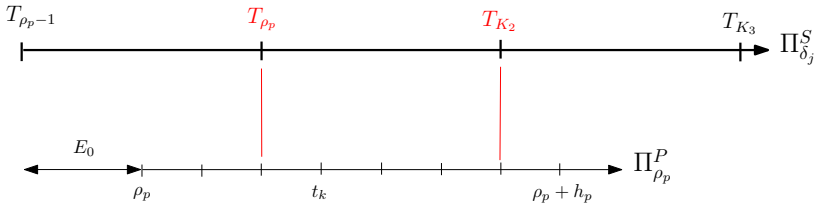

Figure 3.17: Scheme of the piloting energy stage time

Thus, we can express the piloting objective function J_p in the discrete form:

$$J_p = P \sum_{i=1}^{N_p} |\sigma_X(i)| + Q \sum_{t_K \in \Xi(\rho_p)} |\sigma_E(t_K)| \tag{3.75}$$

The parameters P and Q define the weights of each objective;These two weights are used to define the two BEMS modes which are detailed in the following parts.

An important characteristic is that, at the piloting layer, we use a varying sampling time vector $\Pi^P_{\rho_p}$. This choice results from the centralized MPC study. Its sampling time vector is the one developed in the part 3.2.1.3. If the piloting horizon h_p is smaller than 2 hours, then $\Pi^P_{\rho_p}$ is only composed of 5 minutes constant sampling times intervals. Otherwise, the sampling times intervals are 5 minutes during 2 hours and then 1 hour.

3.2.2.2 Hierarchical Tracking mode (H-Track)

The Hierarchical Tracking BEMS mode aims to minimize the occupant's objective only. It takes into account the prediction profile update to periodically modify its behaviour in order to offer an optimal control.

The Hierarchical tracking (H-Track) mode has the following aim:
- Function of the information provided by the grid, the scheduling layer (S) plans the energy consumptions and flows over a long horizon H_S matching the grid information while fulfilling the constraints. It is assumed that the grid information has constant time slots (Δ_S). We take the same sampling time interval for the scheduling layer (S) optimization. Then the states trajectories arising from the optimization are extrapolated and sent to the lower layer.
- At the lower level, the piloting control (P) has to track the states prediction trajectories while fulfilling the users and systems' constraints. In terms of weight factor, it consists in setting $P = 1$ and $Q << 1$. The P control uses a receding horizon h_p.

At the S layer, we consider closed loop optimization such as, considering a tariff profile with a constant time slot value Δ_S:

$$\delta_{j+1} = \delta_j + \Delta_S \tag{3.76}$$

The optimization horizon is noted H_S, and is equal to 24 hours if the tariff profiles are available, otherwise it corresponds to the tariff profile horizon (always supposed greater than 12 hours). The sampling time vector is noted $\Pi^S_{\delta_j} = \{t_K\}_{N_S}\ \forall K \in \{1, \ldots, N_S\}$.

At the P layer, similarly to the S layer, we consider a closed loop optimization. The piloting is performed at the times ρ_p such as:

$$\rho_{p+1} = \rho_p + \delta_f \tag{3.77}$$

with δ_f a constant value integer divider of Δ_S.
At a piloting optimization time ρ_p, we note by $\chi(t|\delta(\rho_p))$ the last Scheduling optimization result used. $\delta(\rho_p)$ function is illustrated in Figure 3.18. For instance, with $\Delta_S = 5.\delta_f$ then $\delta_j(\rho_{1,2,3,4}) = \delta_1$, $\delta(\rho_{5,6,7,8}) = \delta_2$, etc.
The optimization horizon is noted h_p and has to respect the constraint:

$$H_S \geq h_p \tag{3.78}$$

which is understandable otherwise $\chi(t|\delta(\rho_p)$ is not defined. Characteristics are in Figure 3.19.

3.2.2.2.1 Impact of the piloting horizon From the centralized MPC study, we know that varying sampling time is the most adapted configuration for piloting layer. However, it remains to know which horizon h_p or time t_{N_p} will bring the best performance. Thereby we will study three configurations :

1. $t_{N_p} = t_{N_s} \equiv h_p = t_{N_s} - \rho_p$: the piloting horizon vary.

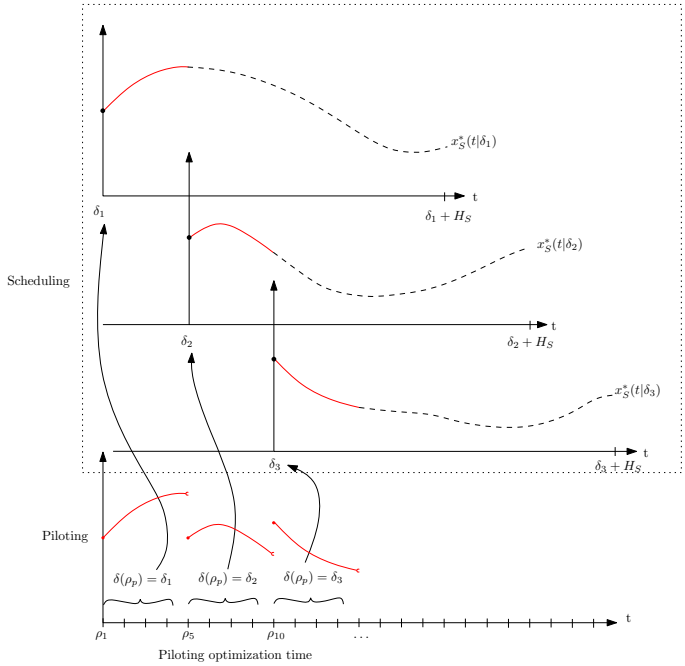

Figure 3.18: Scheme of piloting information update with $\Delta_S = 5.\delta_f$.

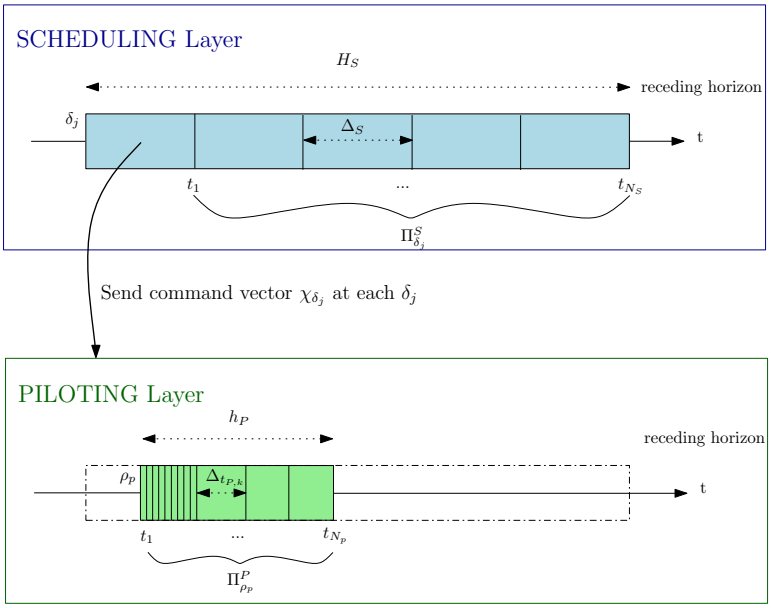

Figure 3.19: Principle of the Hierarchical Tracking mode

2. $t_{N_p} = \rho_p + \Delta_S \equiv h_p = \Delta_S$: the piloting horizon is constant.
3. $t_{N_p} = t_1$ with $t_1 \in \Pi^S_{\delta(\rho_p)} \equiv h_p = t_1 - \rho_p$: the piloting horizon vary.

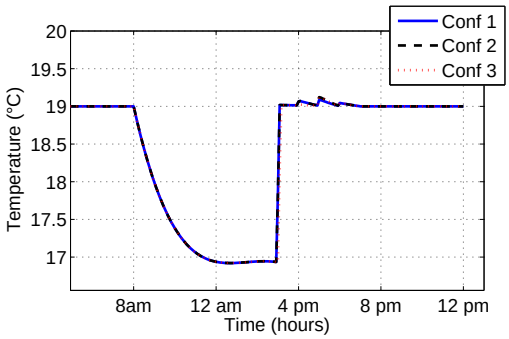

Figure 3.20: Temperature regulation for H-Track configuration - Simulation Disturbed -.

with $H_S = 24$ hours and $\Delta_S = 1$ hour for all the cases.

To summarize, in configuration 1 the piloting horizon is set to 24 hours at time $t = 0$ corresponding to the scheduling horizon, then it decreases a little before the next scheduling optimization. In configuration 2, the piloting horizon is constant and equal to 1 hour for all ρ_p. In configuration 3, the piloting horizon is set to 1 hour at time ρ_p corresponding to the scheduling horizon sampling time interval, then it decreases until 5 min before before the next scheduling optimization.

First, we perform the two simulations: the Classic simulation, in which the predicted disturbance profile and the simulation one are similar, and the Disturbed simulation, in which, as in the previous illustration, the predicted solar gain disturbance profile is biased (refer to Figure 3.8).
The results show no major differences between the configurations. The temperature regulations are similar (see Figure 3.20) and the controls reject the unpredicted disturbances while the cost function values summarized in the table 3.4 do not prove a significant over-performance of a configuration. The only difference is in term of computing time with $\text{C.time}_{conf1} > \text{C.time}_{conf2} > \text{C.time}_{conf3}$.

Secondly, to try to distinguish the configuration performance while keeping close to our application, we suppose that the BEMS receives a new occupation profile at a time t_i. This new profile is transmitted to the BEMS and so $w_{O_{cc}}$ is updated. As a result, a new consumption strategy is calculated because the building will now be occupied between 12pm and 2pm and the initial strategy was to regulate the air temperature at 16 ° C. The fourth columns of the table 3.4 and Figure 3.21 summarize the results. As previously, for our example case study no important differences can be seen.

Conf./Simu.	Classic	Disturbed	Informed
1	7.1177	7.0126	7.4193
2	7.1179	7.0136	7.4193
3	7.2225	7.1383	7.4193

Table 3.4: Cost function values. *Simulation noted Disturbed refers to the unpredicted disturbance case and simulation noted Informed refers to update occupancy profile case.*

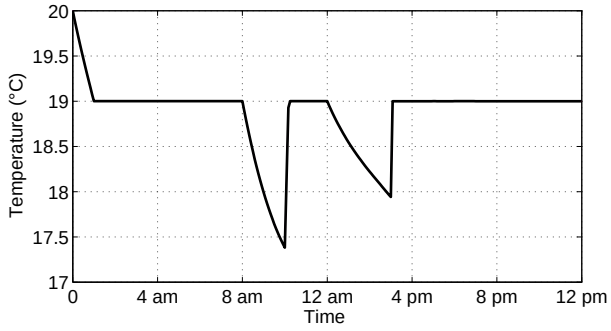

Figure 3.21: Temperature regulation for H-Track configuration - Simulation Informed -.

Hence, we conclude that, in our study case, there is no impact of the piloting horizon for H-Tack developed mode. For our BEMS H-Track mode we choose to set the configuration 3 : $t_{N_p} = t_1$ with $t_1 \in \Pi^S_{\delta(\rho_p)}$ having the advantage to have the smallest computing time burden because it has the smallest configuration horizon.

3.2.2.3 Hierarchical Commitment mode (H-Cmt)

In this part, we will describe the second developed BEMS mode. The Hierarchical Commitment mode is developed for an advanced energy and building context where the BEMS aims to minimize the occupant's objective but takes also a role in the smart grid by committing itself on its grid energy consumption profile.

From a grid point of view, an advanced BEMS which optimizes its own energy consumption has not much interest. Discussion on the BEMS impact will be done in chapter 4. However, as the grid challenge is to match the consumption and demand, it seems more interesting to know the building grid consumption. That is why, we propose here, a BEMS mode which tries as much as possible over a certain horizon to respect its initial grid energy consumption profile sent to the grid aggregator.

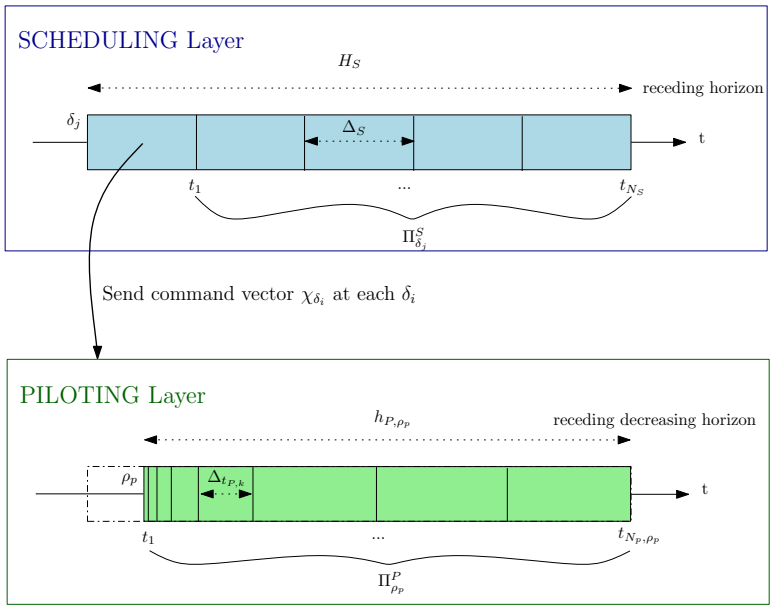

Figure 3.22: Principle of the Hierarchical Commitment mode

The Hierarchical Commitment (H-Cmt) mode has as principle:

- As supposed in the previous mode, the BEMS receives the grid information and then the scheduling layer (S) plans the energy consumptions and flows over a long horizon H_S. Then, instead of sending the result consumption profile only at the lower control layer, we suppose that the BEMS provides it to the grid over a horizon H_C.
- At the piloting layer (P) the objective is double. It has to follow the states' trajectories but mainly to respect the energy consumption profile. In terms of weight factors, it consists in setting $P < Q$. The P control uses a receding horizon h_p.

Since respecting a power load profile seems to be compromised by the complexity of the load systems prediction, we propose a commitment to a power consumption stage profile. The scheduling problem is identical to the previous mode except that here $P << Q$. About the piloting horizon, we set $h_p = H_C$ and the sampling time distribution is the one established previously.

The H-Cmt mode performance will be investigated in chapter 4.

3.2.3 Conclusion

To summarize, we present a generic systemic view where each system is independently described in order to solve the building energy manage-

ment problem. Then, we study various MPC resolution configurations and choose the receding control mode combined with a varying sampling time to reduce the computing time burden while ensuring a robust control. Finally, to respond to the BEMS needs, we present a hierarchical architecture with two control modes (H-Track and H-Cmt). The H-Track mode focuses on building optimization whereas the H-Cmt mode provides a new option with an energy stage commitment from the building to the grid. These BEMS modes will be assessed by simulations in chapter 4.
We will use the systemic view to distribute the resolution of the problems. More precisely, the global problem is composed of several subproblems linked to various common constraints. Distribution techniques can be used, not only to solve the problem more efficiently, but also to define structured controllers. This architecture will allow modularity.
In the following part, we will briefly present one of these techniques, dedicated to linear optimization: The Dantzig-Wolfe Decomposition.

3.3 Modular aspect ensured by decomposition

In the previous part, we presented our BEMS modes. Until now, we did not mention the implementation method. However, as said in chapter 1, the building problematic involves being generic and modular in order to be adaptable and perdurable. The idea is to use a decomposition method in order to distribute the control and so obtain a "plug-and-play" infrastructure adaptable for all buildings. This means that rather than centralizing all data, system models and controller devices into a unique controller, we propose to use a decomposition technique to define local controllers linked by a coordinator agent that have to manage the global objective and constraints. For example, we work under linear assumptions and we use the Dantzig-Wolfe (DW) decomposition method to distribute the optimization problem.This cooperative resolution method brings modularity and adaptability to the BEMS while providing the optimal solution.
The DW decomposition works with linear problem with a block angular structure which corresponds to the problem formulation [65].

In the next part, we will firstly re-write the linear BEMS problem into a block matrix form in order to explain the decomposition. Then we will present the DW resolution principle. Afterwards, we will test the algorithm behavior by performing some simulations.

3.3.1 Block matrix problem formulation

In order to ease the understanding and the similarities between the DW resolution method structure and our BEMS problem, in this part the global

BEMS problem is re-written explicitly into a linear formulation.

Let's restart from the generic global system composed by s subsystems coupled, as presented in the paragraph 3.1.1.2.2. To be as generic as possible the coupling variables and the common constraint (3.57) are considered.

To operate the Dantzig-Wolfe method the problem has to satisfy two main things:

– the objective has to be a linear function, as well as the constraints,

– the problem has to be written under block-angular structure.

In the previous part, we considered a linear global economic cost function $J_{glo}(u, w)$ and linear functions f_i, g_i and C. Figure 3.23 schematizes the BEMS problem.

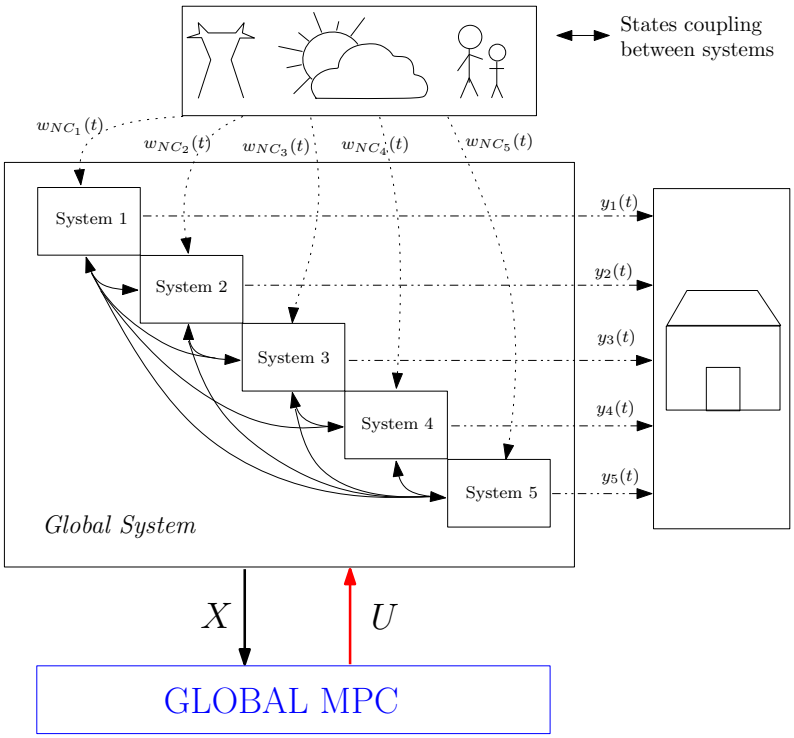

Figure 3.23: Diagram of the global BEMS with 5 systems

Even if the formulation proposed in the previous section is general, we shall explicit the linear formulation to be as clear as possible.

– Each subsystem i is described by the dynamical equation

$$\dot{x}_i = A_i.x_i + B_i.u_i + K_i.w_{NC_i} + L_i.w_{C_i} \tag{3.79}$$

– Its local constraints:

$$G_i.x_i + H_i.u_i + F_i.w_{NC_i} + R_i.w_{C_i} \leq 0 \tag{3.80}$$

– Its interaction variables are described by:

$$w_{C_i} = \sum_{j \in N_i} (W_{ij}.x_j + \Gamma_{ij}.u_j) \tag{3.81}$$

in which N_i is the set of all system that act on i.

– All the s systems are linked by the common constraints:

$$\sum_i (C_i.u_i + M_i.w_{NC_i} + E_i.w_{C_i}) \leq 0 \tag{3.82}$$

With these new notations, we can formalize the General BEMS MPC problem in order to highlight its block matrix structure.

General matrix BEMS MPC problem

From the previous matrix equations, the General MPC problem 3.1.2.2 can be re-written into:

General matrix BEMS MPC problem At a time δ_j, with $\Pi_{\delta_j} = \{t_k\}_N$ and given $\forall i, j \in \{1, \ldots, s\}$,

– $\tilde{x}_i(0) = x_i(\delta_j)$

– $\langle w \rangle_{NC_i}(\{1, \ldots, N\}|\delta_j)$: the uncontrollable prediction disturbance vector

The optimization problem is:

$$J_{glo} = \min_{\mathbf{u}(\{0,\ldots,N-1\})} \sum_{i=1}^{s} \left(\sum_{k=0}^{N-1} J_i(k+1) \right) \tag{3.83}$$

where:

$$J_i(k+1) = C_{x_i}^{k+1}.\tilde{x}_i(k) + C_{u_i}^{k}.\mathbf{u_i}(k) + C_{\langle w \rangle_{NC_i}}^{k}.\langle w \rangle_{NC_i}(k|\delta_j) + C_{w_{C_i}}^{k}.w_{C_i}(k) \tag{3.84}$$

s.t. $\forall k \in \{0, \ldots, N-1\}$, $\forall i \in \{1, \ldots, s\}$:

$$\tilde{x}_i(k+1) = A_i^k \tilde{x}_i(k) + B_i^k \mathbf{u_i}(k) + K_i^k.\langle w \rangle_{NC_i}(k|\delta_j) + L_i^k.w_{C_i}(k) \tag{3.85}$$

$$G_i^k \tilde{x}_i(k) + H_i^k \mathbf{u_i}(k) + F_i^k.\langle w \rangle_{NC_i}(k|\delta_j) + R_i^k.w_{C_i}(k) \leq 0 \tag{3.86}$$

and also:

$$w_{C_i} = \sum_{j \in N_i} W_{ij}.\tilde{x}_j(k) + \Gamma_{ij}.\mathbf{u_j}(k) \tag{3.87}$$

and the common system constraints:

$$\sum_{i=1}^{s} \left(Q_i^k.\mathbf{u_i}(k) + M_i^k.\langle w \rangle_{NC_i}(k|\delta_j) + E_i^k.w_{C_i}(k) \right) \leq 0 \tag{3.88}$$

3.3.2 Dantzig-Wolfe Decomposition

In previous global formalization, we noted that all equations excepted the common equation (eq. 3.88) and the coupling equation (eq. 3.87) constraints are independent of systems. The objective function (3.83) is a sum of local cost function, the system dynamics (3.85) are subject to local variables as well as constraints (3.86).

The DW decomposition consists in making all the systems independent by adding a coordinator agent (see example in [66] or in [67]). Each local system or subproblem is composed only of its local constraints and objectives. Thereby, each local system only interacts with the coordinator agent but not with other agents (see Figure 3.24). In this approach, all the global

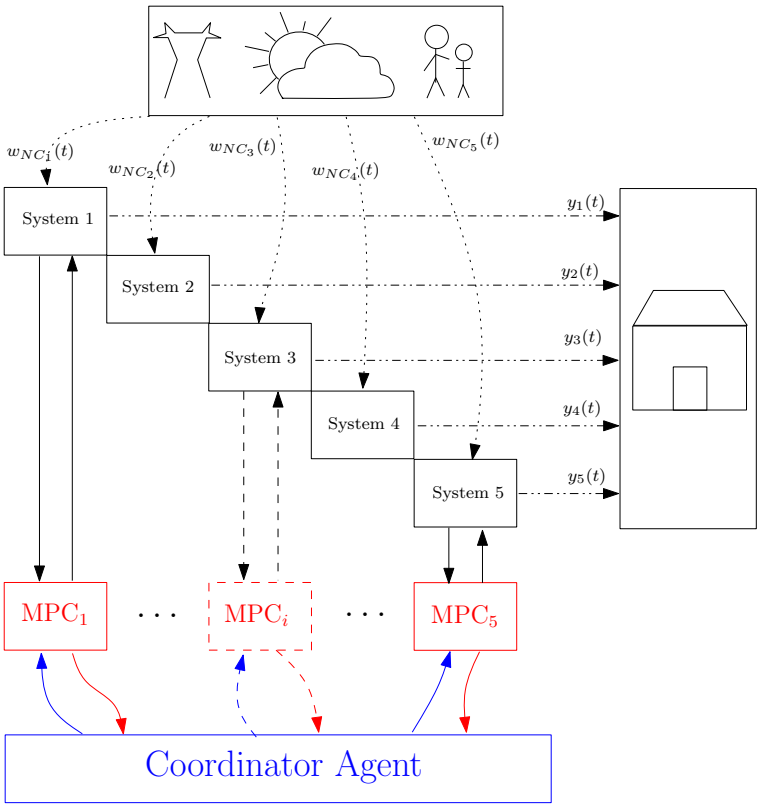

Figure 3.24: Diagram of independent systems linked to the Dantzig-Wolfe coordinator with five systems

aspects are taken into account by the coordinator. This means, in our problem formulation, that it is the coordinator which will have to ensure the respect of the common system constraints (eq. 3.87) and the coupling equation constraints (eq. 3.87). It results that the disturbance vector w_{C_i} of the system i becomes an optimization variable so that the system i input vector

becomes:

$$\mathbf{u_i}' = \left[\mathbf{u_i}, w_{C_i}\right]^T \tag{3.89}$$

In addition, it is also the coordinator which takes into account the global cost function. For this reason, information provided by the system i to the coordinator is $\mathbf{u_i}'$ and J_i. In Figure 3.24, the blue and red arrows schematize the system communications with the coordinator agent.

From a formalization point of view, the decomposed problem is identical to the previous formulation. However, the former local coupling equation (eq. 3.87) is now part of the common constraint (eq. 3.88).

In the next part the DW resolution principle and its modularity aspect will be explained.

3.3.3 Resolution principle

The principle of the Dantzig-Wolfe method, described in [65], is to decompose a linear problem including a big number of equations, in independent subproblems (SP), all coordinated by a unique master problem (MP). In the decomposition method, the master problem (MP), supported by the coordinator, defines an optimal composition of the solutions, provided by the relaxed independent subproblems (SP), which minimize the global cost function J_{glo}. Then, the MP affects the weight vector function Λ_i to each subproblem corresponding to the dual variables of the MP problem resolution associated with common constraints ignored in the SP.
After resolution with the weight factors, the SP will provide, a new partial solution which will enable to improve the global solution. The algorithm iterates until the difference between the lower and higher solution bounds converges to zero, which means that the optimal global solution is reached. The principle is summarized in Figure 3.25.

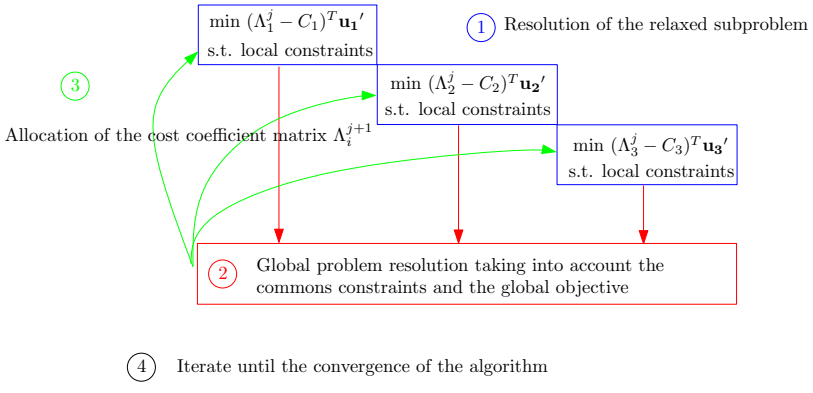

Figure 3.25: Algorithm resolution iterative principle

The optimal solution is ensured by the MP primal and dual approach. The dual solution of the MP is then used to update the local cost of the SP.

3.3.3.1 BEMS Modularity

A schematic explanation can be given in Figure 3.24 where $s = 5$. To add a new system to the BEMS we only have to add a System 6 and MPC_6 blocks, as well as add its associated common constraints into the coordinator.

To illustrate the method and show its simplicity, let's consider the previous thermal heating system 1 and the battery system 2. The global objective is to minimize the energy consumption cost such as considering an electrical coupling point P_{grid} between building and grid. If the sale $w_{sell}(t)$ and purchase $w_{buy}(t)$ prices of electricity on the grid are known, we have

$$J_{glo} = \sum_{k=1}^{N} (w_{buy}(k).P_{grid,buy}(k) + w_{sell}(k).P_{grid,sell}(k) \tag{3.90}$$

The variables $P_{grid,buy}$ and $P_{grid,sell}$ correspond to the power bought and sold such as:

$$P_{grid} = P_{grid,buy} + P_{grid,sell} \tag{3.91}$$

and subject to:

$$P_{grid}^{[down]} \leq P_{grid} \leq P_{grid}^{[up]} \tag{3.92}$$

In this illustrative case, the common constraints are:

$$P_{grid} = u_r + u_{batt} \tag{3.93}$$

From a global view, the electrical coupling is seen as an additional system 3 which has its local constraints and objective. It results in three systems with their local dynamics functions, constraints, and objectives, which have to respect a global common constraint (eq. 3.93) and to minimize a global objective cost (eq. 3.90) as summarized in:

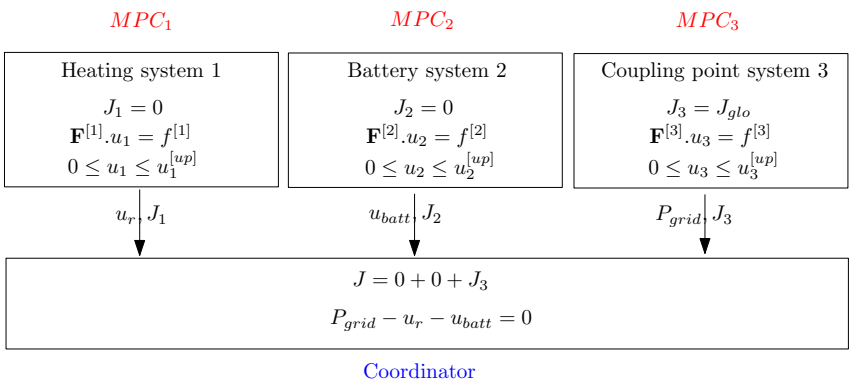

With this structure, integrating a new system consists in adding an extra MPC subproblem specifying its common constraints and objectives to the building coordinator. With the same simplicity, modifying a system model or constraint is performed locally. This does not change the control architecture.
In our hierarchical architecture, the distribution is used at the two MPC layers. The difference between the layers is the definition of the local objective functions. For instance, in the illustrative case, at the piloting layer, the heating system 1 objective is to follow the thermal temperature tendencies while fulfilling the energy stage profiles provided by the high level. Other examples can be found in [68] and [69].

3.3.4 Algorithm behaviour

To study the algorithm behaviour, we consider s linear systems all identical composed by the input variable u_i, their state variable x_i, their dynamic matrix function A_i and B_i and their bounds $u_i^{[down]}$, $u_i^{[up]}$, $x_i^{[down]}$ and $x_i^{[up]}$. The objective cost function is to minimize J the sum of the input u_i with $i \in \{1, \ldots, s\}$.The common constraint is supposed to be:

$$\sum_{i=1}^{s} u_i \leq u_{glo}^{[up]} \tag{3.94}$$

In figure 3.26, we can see the convergence criterion until the optimal values 0 proving the algorithm optimality. The convergence has the particularity to jump frequently and then decrease slowly which leads to increase the number of algorithm iteration exchange. Figure 3.27 displays the number of algorithm iterations required in function of the number of optimization variables. The iteration corresponds to the number of communications between the coordinator and the subproblems. A high number leads to increase the problem computing time, this inconvenient has to be taken into consideration for the implementation aspect. A solution to efficiently reduce this number would be to stop the algorithm at a criterion value near to zero ($0 + \epsilon$ with $\epsilon << 1$). Further study on the algorithm would be necessary to determine the interest of this idea, but working on the distributed method was not the focus of the work.

About the computing time, as the MP variables number depends on the number of algorithm iterations, it does not depend on the number of systems, the coordinator optimization problem complexity will not increase in comparison with a centralized resolution as it is shown in [70], where a comparative study on the computation burden between the DW cooperative and a centralized resolution using the solver CPLEX is presented for a plant

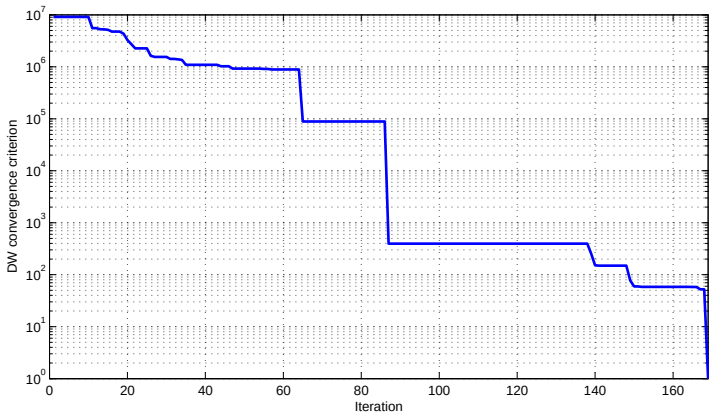

Figure 3.26: Dantzig Wolfe algorithm criterion convergence to optimale values 0 . *Value 0 has been changed in 1 on order to use logarithmic scale.*

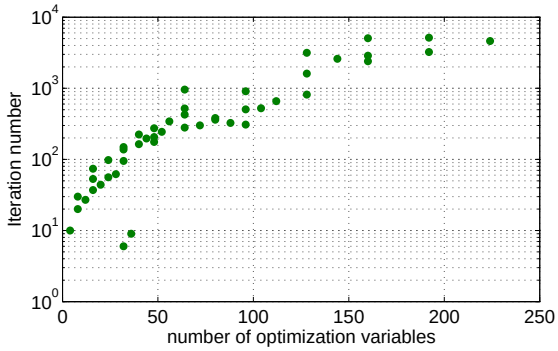

Figure 3.27: Dantzig Wolfe algorithm iteration number in function of N_{opti} .

optimization.
This last aspect enables to ensure that, if the number of system becomes very big, the computing time will not increase strongly. In other words, for a big number of systems, the computing time resolution of a distributed resolution will be better than the one of a centralized resolution.

Here we presented a cooperative resolving method based on Dantzig-Wolfe decomposition algorithm. We structured the BEMS MPC problem in order to adapt it with the algorithm form. As a result, we obtained a decentralized BEMS structure thanks to a coordinator agent that manages the global objective and constraint while the local specific controllers ensure their own objectives and constraints.

The decentralized structure offers a modular BEMS implementation adaptable in such a way that each system is independent of each other. We showed that the coupling parts between systems are integrated in the common constraint. Consequently, modifying or adding a new system does not change the BEMS.
It results in an adaptable and modular BEMS responding to the building control problematic.
For a nonlinear case, others distributed resolution techniques can be found, for instance based on Lagrangian method, which can also provide a structured architecture.

3.4 Conclusion

In this part, we develop a Hierarchical Distributed MPC BEMS schematized in Figure 3.28.
The hierarchical approach combined with the different MPC studied modes enables to work on long time horizon in order to anticipate the building energy consumption and storage while controlling the installation at a fine sampling time to ensure reactivity and robustness. Moreover, the two MPC layers offer a structuring control architecture adapted to the building infrastructure and enabling to take into account the new demand of the grid and exchange information.
Moreover, a generic systemic representation is presented where the system

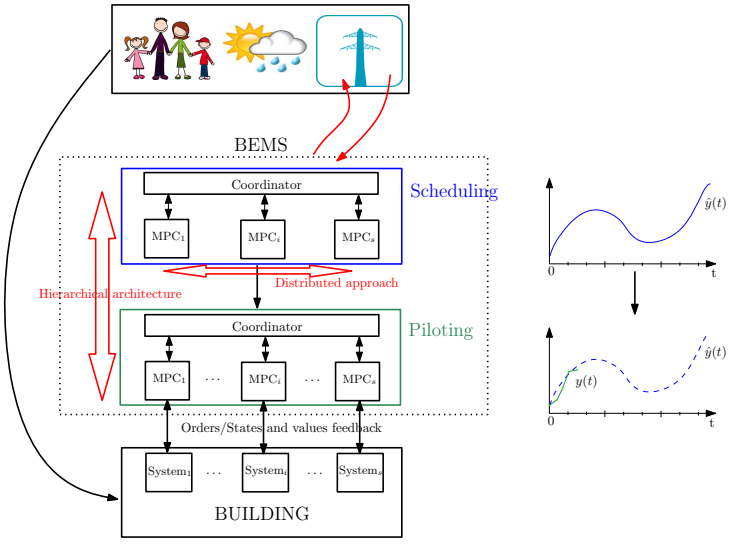

Figure 3.28: Scheme of the BEMS .

coupling are integrated by the disturbance variable. The system model enables to ease the model formalization but also enables to modify a system

model or to add a new system without any change on the other ones.
In addition, the cooperative resolution based on Dantzig-Wolfe method aims to propose an adaptable and modular BEMS which can be implemented on a wider range of buildings. This method enables to optimize the global problem and respect the common constraints while allowing independent controllers. This method is useful for linear case, but this idea may be extended to non linear cases using another decomposition technique.

In the next part, we will perform simulations in order to assess the BEMS modes presented in this chapter. Several tariff scenarios, buildings and grid interactions will be assessed.

Chapter 4

Applications

Contents

4.1 Buildings description 78
4.1.1 Home A: Low Energy 78
4.1.2 Home B: All-Electric 83
4.2 BEMS performance 85
4.2.1 Simulations conditions 86
4.2.2 Indicators 89
4.2.3 Conventional control 90
4.2.4 Qualitative results 91
4.2.5 Building strategies 93
4.2.6 BEMS improvement 101
4.2.7 Conclusion 102
4.3 Building Smart grid ready 103
4.3.1 Scenario 103
4.3.2 Indicator 104
4.3.3 Varying cost strategy 104
4.3.4 Building commitment 110
4.4 Conclusions 112

The first part of this chapter aims to assess the performance of the HD-MPC BEMS in an environment which is as close as possible as we may find in real living conditions. After detailing building cases and simulation particularities, we will compare the BEMS efficiency with conventional rule-based controls. Then, these gains and strategies will be assessed in function of buildings and with different kinds of weather conditions. Various behaviours and efficiencies will be shown. The first part will conclude with some simulations with different conditions (model accuracies, better disturbance predictions) in order to give some guidelines to improve the control. The second part is dedicated to the smart-grid integration. We will perform simulations with several varying cost profiles in order to show the impact

of the Time-Of-Use grid strategy on building behaviours. We will focus our attention on the peak consumption period and emphasize storage effect on building power load flexibility. The last study concerns the BEMS commitment mode. We will test the mode on simulations and assess its performance for a strict respect of the commitment profile and for a softer respect of the profile.

4.1 Buildings description

In order to integrate our approach in the reality scope we chose a *Low energy* house **A** approximating the new French building and a *All-Electric* house **B** expressing the integration of the new energy systems on a classical French house. The two houses have the same size and orientation (100 m^2 with 3 bedrooms, 1 living room, 1 kitchen and 1 bathroom). However, the walls components, the windows and the systems are different. For our simulations, we suppose that only a few systems are controllable (air and water heating system mainly). It is because they are the most important consumers in the residential house and they are all controllable devices. Moreover, we consider that many of the appliances are not controllable until today (auxiliary devices, lighting). Nevertheless, as presented in the previous part, additional systems can be integrated easily in the BEMS.
An attention must be given to the models description. For our simulations, there are two kinds of models: the process models which are accurate models principally coming from the SIMBAD library, a Matlab toolbox dedicated to building simulation developed by the CSTB [71], and the prediction models which are developed for the predictive controller. The prediction models are chosen as simply as possible: linear ones, determined from an energetic view.

4.1.1 Home A: Low Energy

The Home A, called *Low Energy* house is characterized by a slow thermal dynamic. It is a very inert residential house with very low thermal losses, equipped with an air/water heat pump (HP) with hydraulic radiators and a sanitary water tank which is coupled to a water solar panel. The systems characteristics are given in tables 4.1, 4.2, 4.3 and 4.4.

Process models

The thermal building process model is the Multi-zone air thermal building model from SIMBAD library. This model includes a very accurate description of the building (wall layers, windows, ventilation flow distribution ...). We can see in Figure 4.1 its step thermal response with no solar gain

Parameter	Value
Window area	1.7 m^2
nominal flow	0.02 m^3/s
$T_{in}^{[up]}$	45 °C
η_{sc}	0.85
Initial temperature	20 °C

Table 4.1: Solar collector parameters

Parameter	Value
$P_{pac}^{[up]}$	3000 W
$\hat{T}_{water,out}$	60 °C
$A_{radiator}$	2.3 m^2
radiators number	7

Table 4.2: Heating house B system parameters

Parameter	Value
$P_{grid}^{[up]}$	7 kW
$P_{grid}^{[down]}$	-7 kW

Table 4.3: Electrical manager parameters

Parameter	Value
volume	200 L
T_{init}	50 °C
number of subvolumes	3
$T_{hwt}^{[up]}$	70 °C
$T_{hwt}^{[down]}$	30 °C
$P_{elec,hwt}^{[up]}$	3000 W
T_{in}	10 °C
η_{elec}	0.8

Table 4.4: Water Tank parameters

and an external temperature drop from 20 to 0 °C. Notice that the home indoor temperature is an average temperature of the 7 rooms.

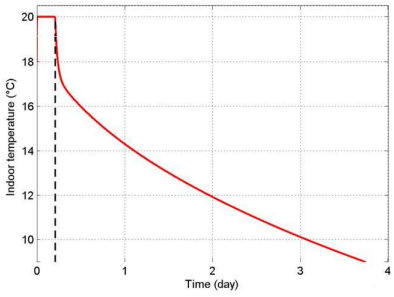

Figure 4.1: *Low Energy* house **A** thermal step response

About the heat pump system, it is a system which has for principle to take calories from the cool source (here the air) and to transfer it to the hot source (water). Thus, its energy efficiency COP strongly depends on the external temperature. Its value ranges from 1 to 4. The process energetic heat pump model and the hydraulic radiator models comes from [72].

The sanitary water tank has a free heating part offered by the sun via water tubes put on the house roof. When the renewable energy is not suf-

ficient, the auxiliary electrical resistor power ensures the occupant's needs. The average hot water drawn temperature is at 42°C and the inlet water temperature at 12°C. The solar water panel pump is activated if the water temperature is superior to the sanitary water tank one.
The hot water tank and the solar panel process models come from the SIMBAD library. The water tank dynamic is divided into three sub-volumes. The solar panel exchanger is in the second volume while the auxiliary electrical resistor is at the bottom of the tank. The modeled water solar collector is composed of a flat tube panel on the roof top of the house (the most common for residential house [73]).

Prediction models

Due to the high complexity for establishing a correct analytic model of the building temperature, we identify a simple linear model. The identification was performed on the Multi-zone SIMBAD Building model with the MATLAB identification toolbox. We propose to use a middle fit model (ARX model of order 6 with about 60 % fit) in order to highlight the control robustness and also because we think that better models won't be easy to find in practice. The input variable vector is:

$$U_{th} = \begin{bmatrix} T_{ext} & I_{sr} & Q_{in,conv} & Q_{in,rad} \end{bmatrix}^T \tag{4.1}$$

with $Q_{in,conv}$ and $Q_{in,rad}$ the convective and radiative internal loads. From building thermal load point of view, the high insulation combined to a double flows ventilation unit leads to very low needed loads. We do not control the ventilation unit and consider constant power consumption at 50W. Contrary to the simulation process, in the prediction model, we suppose a single thermal node and a unique heating power emitter for building. As a consequence, to ensure the good regulation in the rooms, we implement a controller which distributes the heating power calculated through the rooms in order to balance the temperatures.

Air heating installation For the heat pump device we suppose, in the prediction model that, the thermal heating power provided is:

$$Q_{prod,ch} = COP.P_{comp} \tag{4.2}$$

It is supposed that the output water temperature is constant T_s and that the auxiliaries electrical consumption comes from the compressor. Thus, we can express the power P_{comp} by:

$$P_{comp} = \frac{1}{\eta_{comp}}.P_{elec,ch} \tag{4.3}$$

The Coefficient of Performance COP is determined such that, considering a return temperature T_r of about 40°C:

$$COP = \eta_{PAC} . \frac{T_c}{(T_c - T_f)} \tag{4.4}$$

with T_f the external temperature and T_c the hot source temperature ($T_c = (T_s - T_r)/2$).
Equation (4.2) becomes:

$$Q_{prod,ch} = \eta_{PAC} . \frac{T_c}{(T_c - T_f)} . \frac{1}{\eta_{comp}} . P_{elec,ch} \tag{4.5}$$

All the auxiliary heat pump power consumptions (pump consumption, defrost consumption) are taken into account so that they reduce the system efficiency performance. They are included in the constant coefficients η_{PAC} and η_{comp}.
The power constraints of the model are :

$$Q_{prodmin,ch} \leq Q_{prod,ch} \leq Q_{prodmax,ch} \tag{4.6}$$

The water radiators have the particularity to have an important heat radiative part which leads to have a long thermal time constant. In the predictive model, the radiative part is set to 65 % and the convective part to 35%.

$$Q_{rad} = \begin{bmatrix} 0.65 \\ 0.35 \end{bmatrix} Q_{prod,ch} \tag{4.7}$$

Water tank installation The domestic hot water system (DHW) is composed of a solar water panel exchanger and a small electrical resistor. The proposed model considers only one stratification layer, the electrical dynamics are neglected and the resistance efficiency (η_{dhw}) does not depend on the water temperature. The water temperature dynamic equation is governed by mass and internal energy conservation law:

$$\rho V C_p \frac{dT_{tank}}{dt} = \eta_{lost,dhw} T_{tank} + \begin{bmatrix} 1 \\ \eta_{dhw} \\ -1 \end{bmatrix}^T \begin{bmatrix} Q_{sp,dhw} & P_{elec,dhw} & Q_{dhw} \end{bmatrix}' \tag{c.dhw}$$

where ρ, V, and C_p are the density, the volume of water and the heat capacity respectively. $\eta_{lost,dhw}$ is the lost coefficient, $Q_{sp,dhw}$ is solar collector panel load provided to the HWT, $P_{elec,dhw}$ is the electric load of the electric resistance and Q_{dhw} is the hot water load due to occupants' drawing.
The electric load power constraints and the water tank temperature limits are:

$$0 \leq P_{elec,dhw} \leq \overline{P_{elec,dhw}} \tag{4.8}$$

$$\underline{T_{tank}} \leq T_{tank} <\leq \overline{T_{tank}} \tag{4.9}$$

For the solar panel prediction models, it is very difficult to calculate the temperature in the tube due to the many parameters and losses (external temperature, heat removal factor, etc). Even if it exists some rather simple characterization equations with only four parameters, there still are non-linear and approximated. That is why, considering that the solar gain prediction and the water input will be approximated and thus biased, we considered that the water solar collector power is given by:

$$Q_{sp,hwt}(t) = I_{sr}(t).A.\tau.\alpha \tag{4.10}$$

with I_{sr} the radiative solar gain, A the solar panel surface and $\tau.\alpha$ the absorption and transmission gains.

Extra consumption

In addition to these systems, building includes an uncontrollable power consumption P_f (washing machine, computer, light, ventilation unit etc) which provides an uncontrollable heating and consumes electrical power. This fatal power consumption is defined by a disturbance profile. Details are given in the scenarios descriptions.

Controller variables

To sum up the control variables are:
- the grid power : P_{grid}
- the heat pump power : P_{hp}
- the auxiliary hot water tank power: P_{hwt}

The disturbance variables are:
- the solar gain : I_{sr}
- the external temperature : T_{out}
- the fatal power consumption: P_f
- the occupancy: O_{cc}
- the hot water draw: q_{hwt}

The system state values which have to be managed are:
- the sanitary water tank temperature: T_{hwt}
- the indoor temperature : T_a

It results in an electrical balance constraint such as:

$$P_{grid} = P_{hp} + P_{hwt} + P_f \tag{4.11}$$

The system state constraints are:

$$30 \leq \quad T_{hwt} \leq 70 \tag{4.12}$$

$$T^{[down]}(O_{cc}) \leq \quad T_a \leq T^{[up]}(O_{cc}) \tag{4.13}$$

The internal temperature bounds depend on the occupant's profile. Details are given in the scenarios descriptions.

4.1.2 Home B: All-Electric

The Home B is called *All-Electric* house. It has a smaller inertia than the house A, and it is equipped with electrical appliances which are : an electric battery P_{batt}, electric radiators P_{rad}, an electric sanitary hot water tank P_{hwt} and an electric solar panel. Their characteristics are given in the table 4.5, 4.6, 4.7 and 4.8.

Parameter	Value
Area	2 m^2
Orientation	South
Performance ratio	0.85

Table 4.5: Solar Panel parameters

Parameter	Value
τ_2	1 min
$P_{batt}^{[up]}$	1.5 kW
$P_{batt}^{[down]}$	-1.5 kW
$SOC^{[up]}$	0.7 % × 10 kW.h
$SOC^{[down]}$	0.3 % × 10 kW.h

Table 4.6: Battery model parameters

Parameter	Value
$P_{grid}^{[up]}$	11 kW
$P_{grid}^{[down]}$	-11 kW

Table 4.7: Electrical manager parameters

Parameter	Value
volume	200 L
T_{init}	50 °C
number of subvolumes	3
$T_{hwt}^{[up]}$	70 °C
$T_{hwt}^{[down]}$	30 °C
$P_{elec,hwt}^{[up]}$	3000 W
T_{in}	10 °C
η_{elec}	0.8

Table 4.8: Water Tank parameters

Process models

Similarly to the house A, the process model is the Multi-zone air thermal building model from SIMBAD library. This model includes a very accurate description of the building (walls layers, windows, ventilation flow distribution ...). We can see in Figure 4.2 its step thermal response with no solar gain and an external temperature drop from 20 to 0 °C.

The electrical radiator,the hot water tank and the electrical solar panel come from the SIMBAD library. The auxiliary hot water electrical resistor

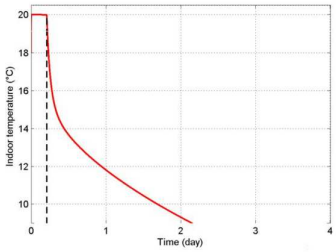

Figure 4.2: *All electrical* house **B** thermal step response

is at the bottom of the tank.
To consider the fast dynamics of a battery, a simple RC model is used. In the dynamical model of the energy stored in the battery (SOC), the charge ($\eta_{ch,batt}$) and discharge ($\eta_{dis,batt}$) efficiency factors are supposed to be distinct whereas the loss factor ($\eta_{ch,loss}$) is constant:

$$\frac{dSOC(t)}{dt} = \eta_{ch,batt} P_{batt,ch}(t) + \eta_{dis,batt} P_{batt,dis}(t) - \eta_{loss,batt}.SOC(t) \quad \text{(c.el1)}$$

Prediction models

Similarly to House A, a simple thermal predicted linear model of the building is created. Its fit is about 60% and it is an ARX model of order 4. Like in the first model, we implement a heating controller which distributes the heating power calculated into the rooms in order to balance the temperature.
The electric radiators have the particularity to have an important heat convective part which leads to have a short thermal time constant. In the predictive model, the convective part is set to 85 % and the radiative part to 15%.

$$Q_{rad} = \begin{bmatrix} 0.15 \\ 0.85 \end{bmatrix} P_{rad} \tag{4.14}$$

The hot water tank is the same as in the house A. However, contrary to the previous model, in this model, all the hot water power need is provided by a electrical resistor.

In addition, solar panel and battery prediction model are defined.

Electrical Solar Panel Instead of taking into account the physical effect of the solar panel which leads to complex equations with many parameters, that are hard to determine, the solar panel is described by the equation:

$$P_{sp}(t) = A_{sp}.\eta_{sp}.((\alpha_1 + \alpha_2).I_{sr}(t) + \alpha_3.\beta_{az}(t)) \tag{4.15}$$

with I_{sr} and $\beta_{az}$the solar gain radiation and the sun azimuth angle respectively. A_{sp} the square meter of the panel and η_{sp} the performance ratio. $\alpha_{1,2,3}$ are used to calculate the solar flow received by the panel. Here we set $\alpha_1 = 0.36$, $\alpha_2 = 2.6863$ and $\alpha_3 = 0.44$ determined via a roughly identification over a year with the MATLAB identification toolbox (43% fit). This choice was done considering that the major error will be brought by the solar gain prediction.

Battery For the battery, we suppose the same model for process and prediction.

Extra consumption

In addition to these systems, building includes an uncontrollable power consumption P_f (washing machine, computer, light, ventilation unit etc) which provides uncontrollable heating and electrical powers.

Controller variables

To sum up the control variables are:
- the grid power : P_{grid}
- the radiator power : P_{rad}
- the hot water tank power: P_{hwt}
- the battery power: P_{batt}

The disturbance variables are the same as in the first building: I_{sr}, T_{out}, P_f, O_{cc} and q_{hwt}. As previously, the system state values which have to be managed are T_{hwt} and T_a.

It results in an electrical balance constraint which is:

$$P_{grid} + P_{sp} = P_{batt} + P_{hwt} + P_f \tag{4.16}$$

4.2 BEMS performance

In this part the BEMS is compared to conventional rule-based control in order to show its pure performances. We perform the comparison under three different weather conditions. Then, the resulting BEMS strategies for the two houses are described, emphasizing the impact of the system type on operating cost gains and on building control flexibilities. In the last part, we will assess the impact of the thermal building model, the outdoor predicted profile and the fatal consumption profile accuracies on control efficiency to give some improvement guidelines for the BEMS.

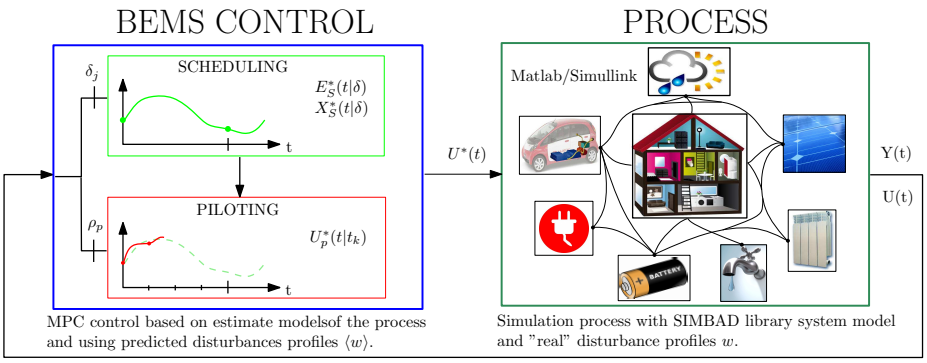

Figure 4.3: Simulation scheme

To optimize the building objective, we used the H-Track mode. We set the high constant sampling time $\Delta_S = 1$ hour and work with a horizon $H_S = 12$ hours. At the piloting level, the sampling time is constant $\Delta_f = 5$ min because the varying piloting horizon is always smaller than 2 hours ($h_p \leq 1$hour).

4.2.1 Simulations conditions

In the simulation, we concentrate on the building energy consumption cost also called the operating cost. Doing the same as in the previous chapter, we suppose selling and buying price so that the cost function is:

$$J_{glo} = \int_0^{\infty} \begin{cases} w_{buy}(\tau).P_{grid}(\tau)d\tau & \text{if } P_{grid}(\tau) > 0 \\ w_{sell}(\tau).P_{grid}(\tau)d\tau & \text{if } P_{grid}(\tau) < 0 \end{cases} \tag{4.17}$$

The simulations are performed with SIMULINK/MATLAB while the optimization uses the CPLEX solver interfaced with Matlab. The simulation scheme principle is displayed in Figure. 4.3.

Note that simulations scenarios have been performed considering bias on the control disturbances profiles. This means that, the predicted and the process disturbance profiles are not the same[1]. To assess the control robustness and its adaptability, three weather conditions are considered: a summer, a winter and a spring week, in order to prove that BEMS offers good performances for all kind of conditions. The disturbances profiles are displayed in Fig 4.4 (a,b and c) for winter and 4.5 (a,b and c) for summer and 4.6 (a,b and c) for spring. The winter and summer week chosen for the simulation include the extreme temperature of the year 2007 in Paris. The prediction disturbances profiles arise from a classical statistic method based on the mean values of each hour of the day, for each day of the week and for each month.

1. The predicted disturbance profiles are created via historical data.

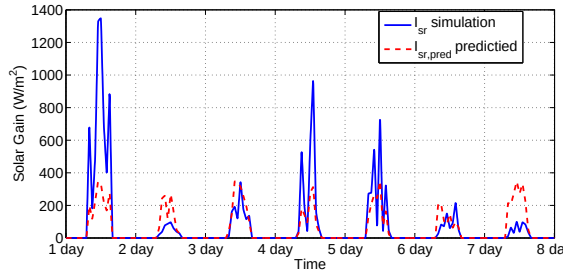

(a) Solar gain

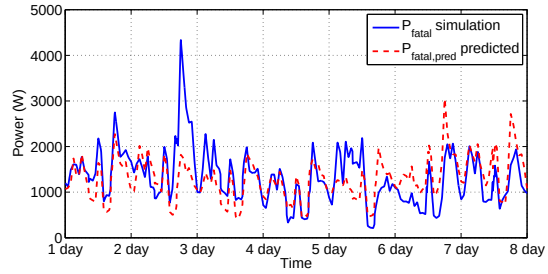

(b) Fatal power consumption

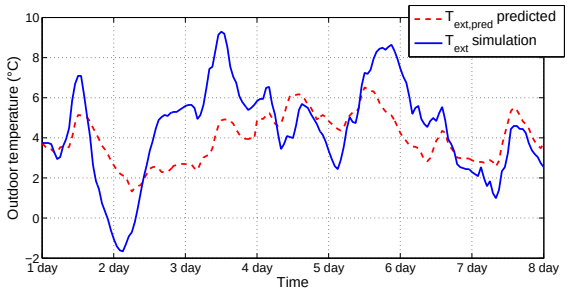

(c) Outdoor temperature

Figure 4.4: Difference for a winter week data between the predicted and the real disturbances profiles.

For the following simulations, the tariff profiles are based on the basic two tariff French period scenario. The low price and the high price correspond to the French tariff scale, considering a contract of 12 kVA. The tariff profile is plotted in fig. 4.7. The timeslots prices are piecewise constant with a time step of one hour.

The air temperature regulation limits depend on the occupancy profile. In all simulations we will suppose that during the occupancy period $T^{[down]} = 20°\text{C}$ and $T^{[up]} = 25°\text{C}$ and that during the inoccupancy period $T^{[down]} = 16°\text{C}$ and $T^{[up]} = 29°\text{C}$. Moreover, due to the complexity of the blind control, we set that occupants close them at 9 pm and open them at 7 am. No other changes are done.

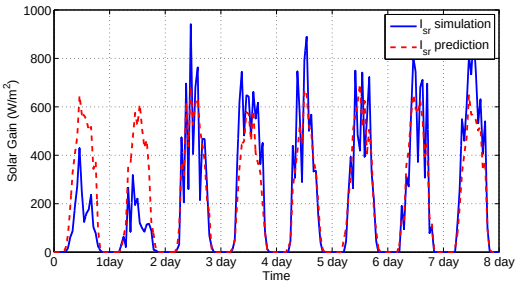

(a) Solar gain

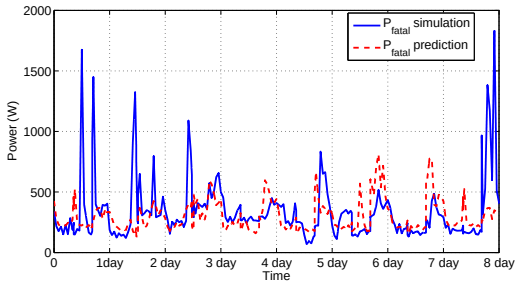

(b) Fatal power consumption

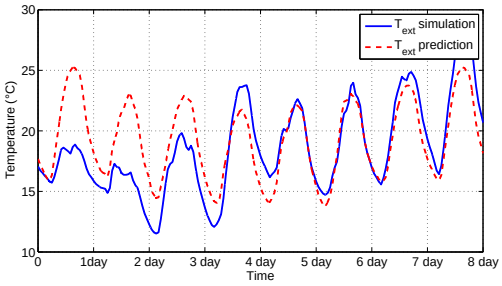

(c) Outdoor temperature

Figure 4.5: Difference for summer week data between the predicted and the real disturbances profiles.

A last important point is the physical system constraints. In the optimization, the physical systems constraints are taken into account via the optimization constraints. In the simulation process, the physical constraints are either included in the model or manually implemented. For instance, the battery state of charge could not exceed its upper bound or be under its lower bound even if BEMS control orders are contradictory.

Before presenting the studies, performance indicators are introduced in order to compare the results.

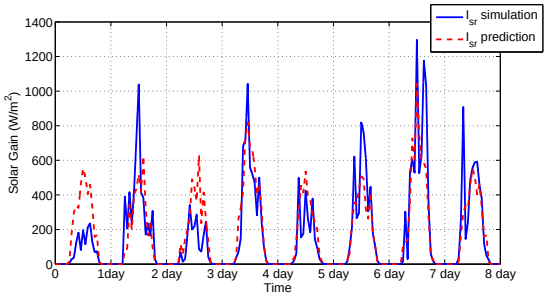

(a) Solar gain

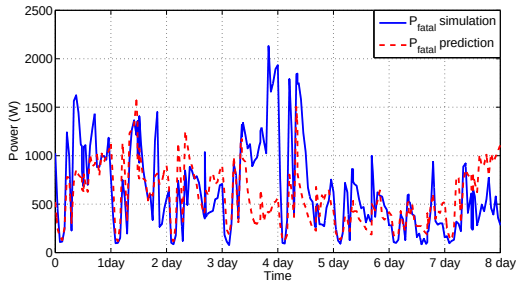

(b) Fatal power consumption

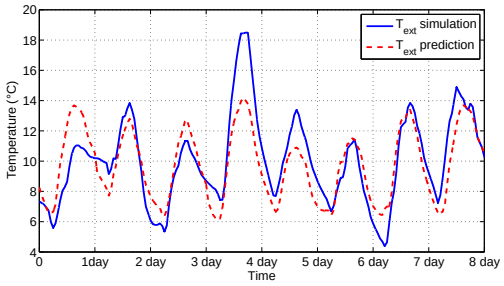

(c) Outdoor temperature

Figure 4.6: Difference for spring week data between the predicted and the real disturbances profiles.

4.2.2 Indicators

A first one is dedicated to the constraints violation, the second one is linked to the operating cost while the last one concerns the energy building consumption.

– The dissatisfaction indicator quantifies the unfulfilled bounds constraints. For each constraint $g_i(x_i, \mathbf{u_i}', w_i, t) < 0$ with $i \in \{1, \ldots, n_P\}$ and n_P the number of bounds constraints we have:

$$I_{dis-i} = \alpha_i \int_0^{t_{end}} \max(0, g_i(x_i, \mathbf{u_i}', w_i, t)) \tag{4.18}$$

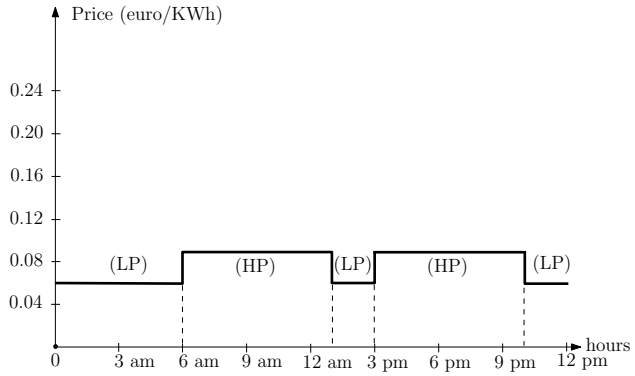

Figure 4.7: Hourly electricity tariff with low price (LP) period (6.14 c€.kWh^{-1}) and a high price (HP) (9.91 c€.kWh^{-1}).

Thus, the dissatisfaction indicator is defined as:

$$I_{dis} = \sum_{i=1}^{n_P} I_{dis-i} \tag{4.19}$$

Associated to this indicator, we note T_{dis} the violation time defined such as:

$$T_{dis-i} = t.\gamma_{I_{dis-i}>0} \tag{4.20}$$

with

$$\gamma_{x>0} = \begin{cases} 1 & \text{if} \quad x > 0 \\ 0 & \text{if} \quad x \leq 0 \end{cases} \tag{4.21}$$

where the time $t \in [0, \ldots, t_{end}]$.

– the operating cost indicator used I_{cost} is the values of the objective function at the end of the simulation corresponding to building energy consumption cost.
– the last factors $E_{tot,grid}$ quantify the building energy grid consumption.

$$E_{tot,grid} = \int_0^{t_{end}} P_{grid}(\tau) d\tau \tag{4.22}$$

4.2.3 Conventional control

In the next part, the BEMS is compared to conventional rule-based house control equipped with the same devices. For this study, we will perform simulations on both houses. The conventional rule-based controls considered are:

– the room temperatures regulations are ensured by PI controllers. The temperature is set to 20 °C during the occupation period and to 16 °C during the inoccupation period.

Weather	Summer		Winter		Spring	
Control	Conv.	BEMS	Conv.	BEMS	Conv.	BEMS
I_{cost}(€)	1.09	1.05	5.20	5.26	2.45	2.43
I_{dis}	2.1	0	2.6	0.24	0.2	0.14
$T_{I_{dis}}$ (min)	24	0	24	0.35	23	4
$E_{tot,grid}$ (kWh)	88	88	437	458	205	208

Table 4.9: Comparison to conventional rule-based control for the House A

Weather	Summer		Winter		Spring	
Control	Conv.	BEMS	Conv.	BEMS	Conv.	BEMS
I_{cost} (€)	0.86	0.80	6.62	6.57	2.59	2.30
I_{dis}	0.53	0	0.88	0.27	0.64	0.55
$T_{I_{dis}}$ (min)	0.3	0	7	3.7	0.29	0.30
$E_{tot,grid}$ (kWh)	69	54	576	585	233	212

Table 4.10: Comparison to conventional rule-based control for the House B

- the sanitary water tank is heated only during the Low Price (LP) period and the order temperature is 55 °C.
- the battery is charged during the Low Price (LP) periods and discharged during the High Price (HP) periods when energy is required.
- the solar panel production is consumed by the house or stocked in the electrical battery if possible. Otherwise it is sold to the grid.

4.2.4 Qualitative results

The results summarized in tables 4.9 and 4.10 show that BEMS control is equivalent or better than the conventional control for both houses while offering similar satisfaction.

For both houses, the dissatisfaction indicator I_{dis} values are almost zero. It shows that the BEMS can efficiently control the devices even with rough models and predicted profiles.

One general outcome is the following one: while considering standard tariff profile and supposing a good conventional rule-based control, the BEMS gains are small. The optimal BEMS predictive control leads to very low energy cost gains, between 0 and 0.11 %.
We note that, for the House A in winter, the operating cost is worst for the BEMS. This reflects the tradeoff between the operating cost and comfort. For the BEMS control, the dissatisfaction indicator is lower. For the conventional control there is a water temperature discomfort of 24 min.

Explanations to these observations are:

– French energy tariffs are very cheap (only two prices) and systems are efficient and well sized.

– Winter and summer simulation conditions are extreme cases.
For instance, for the house A, the heat pump COP values vary little in winter (see Figure 4.8).

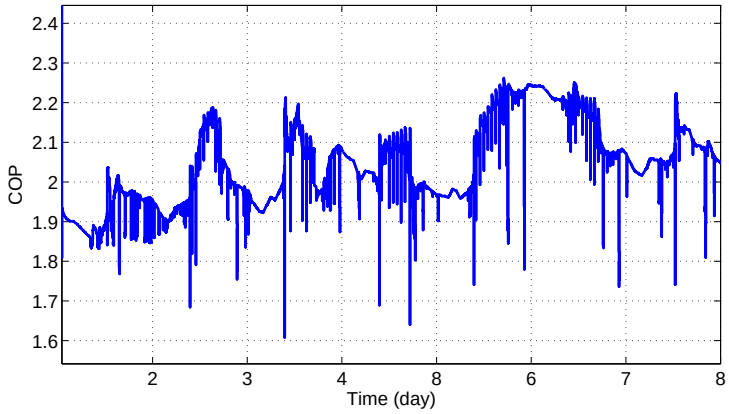

Figure 4.8: Winter heat pump energy efficiency factor *(COP)*

– In this configuration, we proceed to receding optimization without any change on the predicted profiles, even if the predicted value does not correspond to the real one.
For instance, as we see in the Figure 4.4 (c) the predicted temperature during the third morning is 2°C and the real one is -2°C. To improve the BEMS, it could be considered that the piloting layer disposes of a better prediction over a 1 hour horizon. The problem is how profiles could be improved, and which complexity they require.

To investigate more precisely the effect of the prediction error and by the same way, to improve the performance of the BEMS, we will assess the impact of some of them in part 4.2.6.

The study shows that the BEMS has the potential to efficiently manage house energies. Moreover the results are established to be as close as possible to the real living conditions, showing that the presented BEMS is adapted to building control issues. In addition, the two house cases highlight the good modularity of the advanced building controller.
In the following part we will assess building behaviours in order to explain the BEMS performances and strategies.

4.2.5 Building strategies

To understand the BEMS performances and highlight its efficiency and weakness we will detail in this part the resulting control behaviour. The objectives are to distinguish and to explain the optimal strategies according to building cases in a view to conclude on the BEMS interest.

Here we took the same simulations than previously. We will focus on the grid consumption distribution and on the storage system behaviours.

Low Energy house behavior.

The grid consumption and power distribution for a winter and a summer and a spring day are given in Figure 4.9 , 4.10 and 4.11 respectively.

Season strategies:

- In winter, comparing to other seasons, there is more power consumption because the external temperature is low which leads to bigger air heating needs combined with smaller heat pump efficiency factor. If we look at the temperature regulations in Figure 4.9, we see that it does not vary a lot in winter.
- About the summer period, we see that the temperature increases to about 23°C only with free heating power (see Figure 4.10).
  It is principally due to solar and internal gains and also due to the occupant and the devices gains. The weather chosen for the study is the one in Paris where summer temperatures are low compared to other areas and thus highlight the new needs for the high insulated building : the cooling or refreshing of the house during hot temperature long period. Knowing that the windows blinds are opened at 7 am, the blind control integration may assist in regulating the temperature.

- During the spring period the temperature regulation range is between 19 °C and 21 °C (see Figure 4.11).
  We remark that the BEMS does not have indoor temperature strategy depending on cost period (excepted for the first day). It regulates the indoor temperature at 20°C during occupancy periods and takes advantages of solar and internal device heat gains during the afternoon. Similarly to winter time, the indoor temperature never decreases under 19 °C.

From a control point of view, the high insulated house A leads to a smoothing strategy where there is no important increase or decrease indoor temperature during the inoccupancy period. This is explained by three points: firstly for a heat pump, the closer the external and indoor temperature are, the better the efficiency is and so the system is used during the

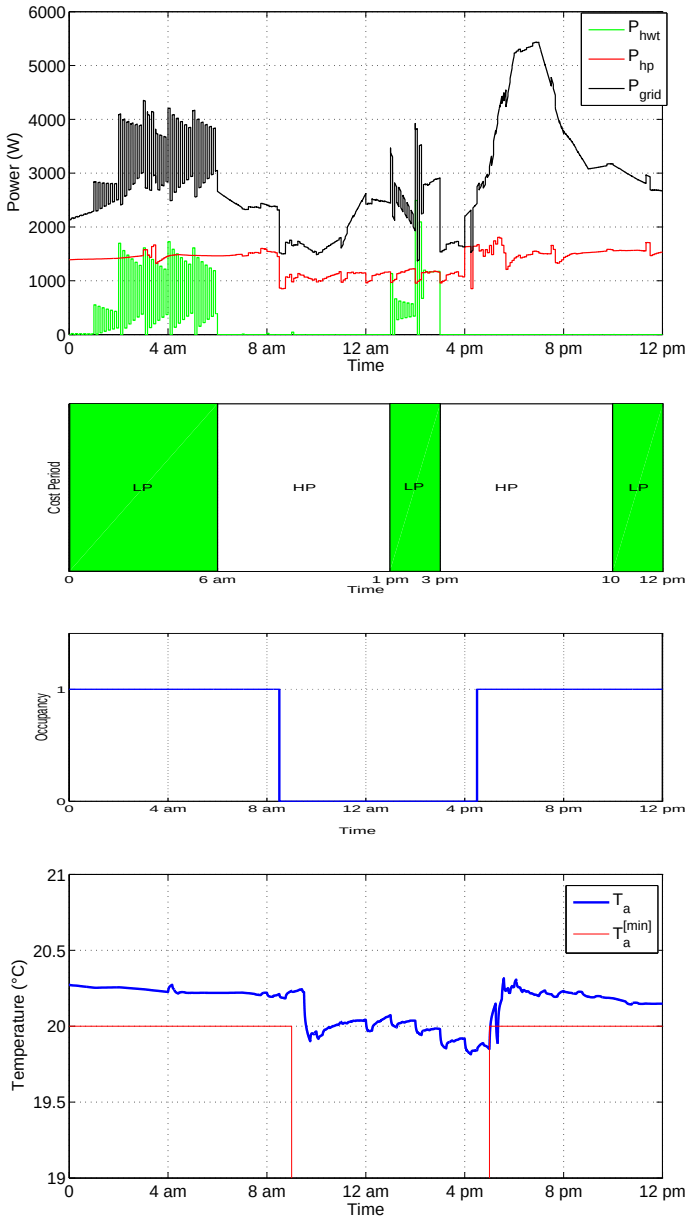

Figure 4.9: House A behavior in winter day

middle of the day when, in our case, nobody is present. Secondly, building has a slow air thermal dynamic time constant and the heat pump has a low power capacity which is not able to heat the temperature quickly. As a consequence, the controller does not let the temperature get down lower otherwise the comfort could not be insured on time. Thirdly, the inoccupancy period matches with the free solar gain which provides free heating

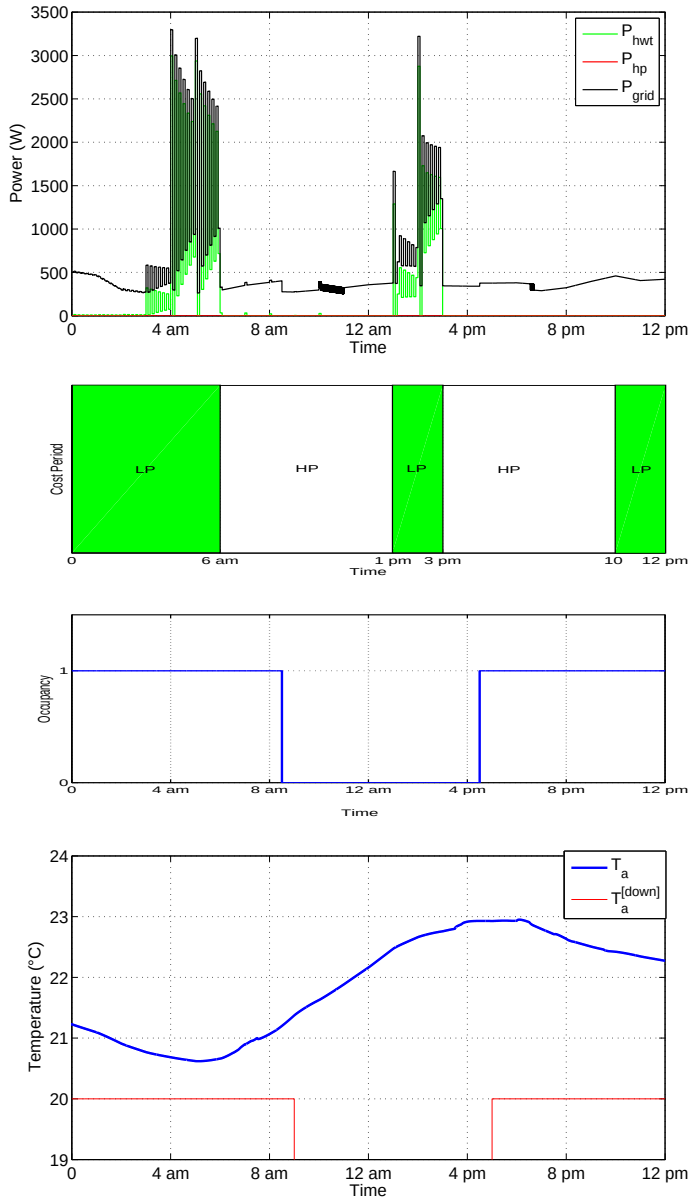

Figure 4.10: House A behavior in summer day

power.

We also note that globally the grid power is low. This is due to the low system capacities and the low house needs. This is especially shown in summer when the grid consumption is quasi equal to the fatal consumption. It is because there is free heat power provided by the sun on the air temperature and on the water temperature via the solar collector. In this case,

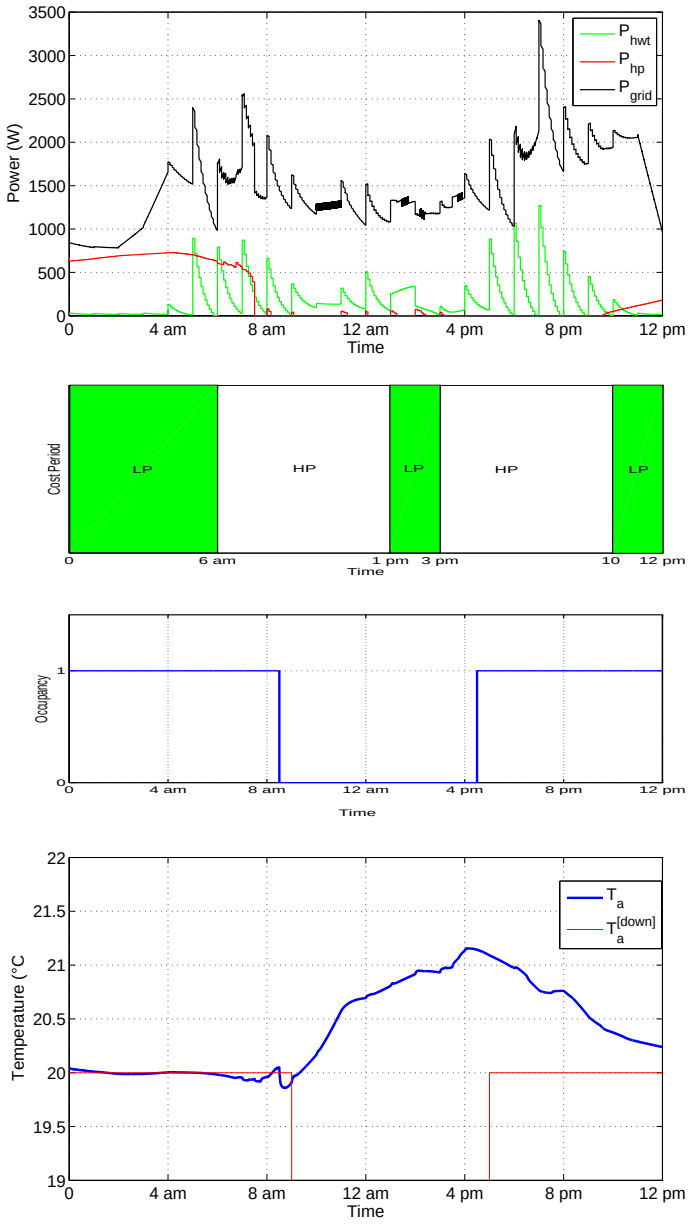

Figure 4.11: House A behavior in spring day

there is no real interest to optimize the energy cost function because it is a "near zero" energy house.

To sum up, due to the high insulated characteristics and its efficient renewable systems, we remark that the house A consumption behavior is not strongly impacted by the cost tariff profiles but it results in smooth

strategies with very low grid consumptions.

All-Electric house behavior.

The grid consumption and power distribution for a winter, a summer and a spring day are given in Figure 4.12 , 4.13 and 4.14 respectively.

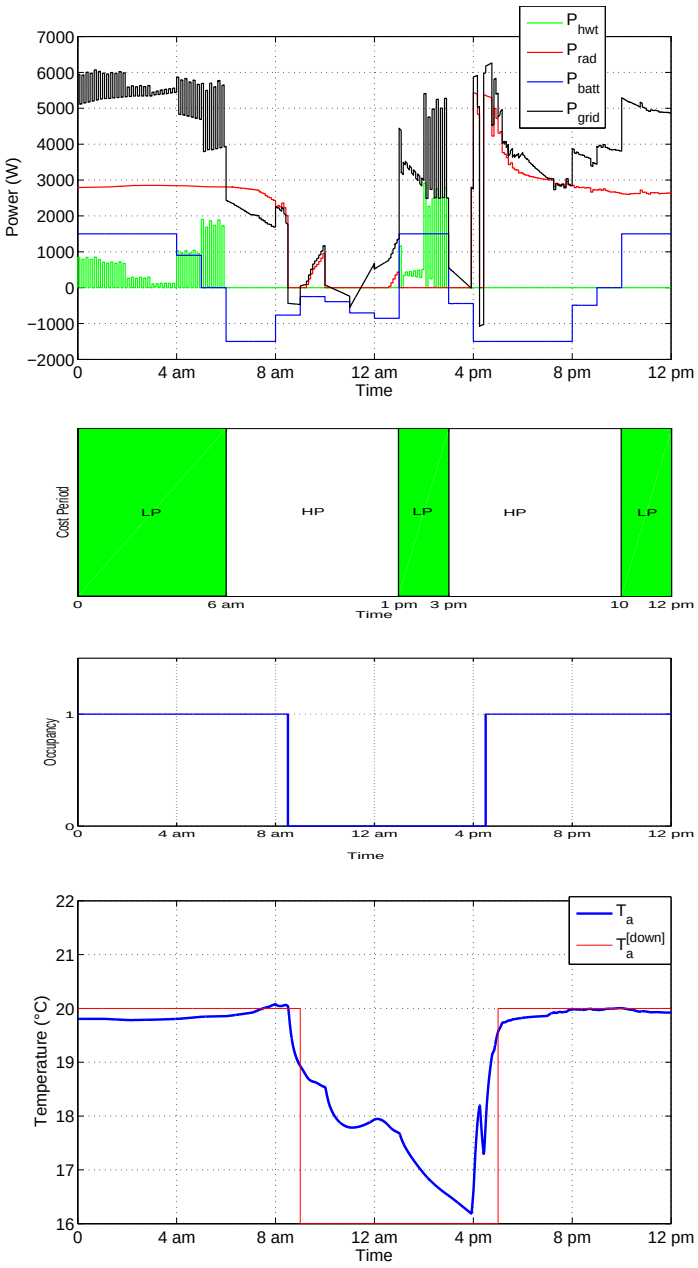

Figure 4.12: House B behavior in winter day

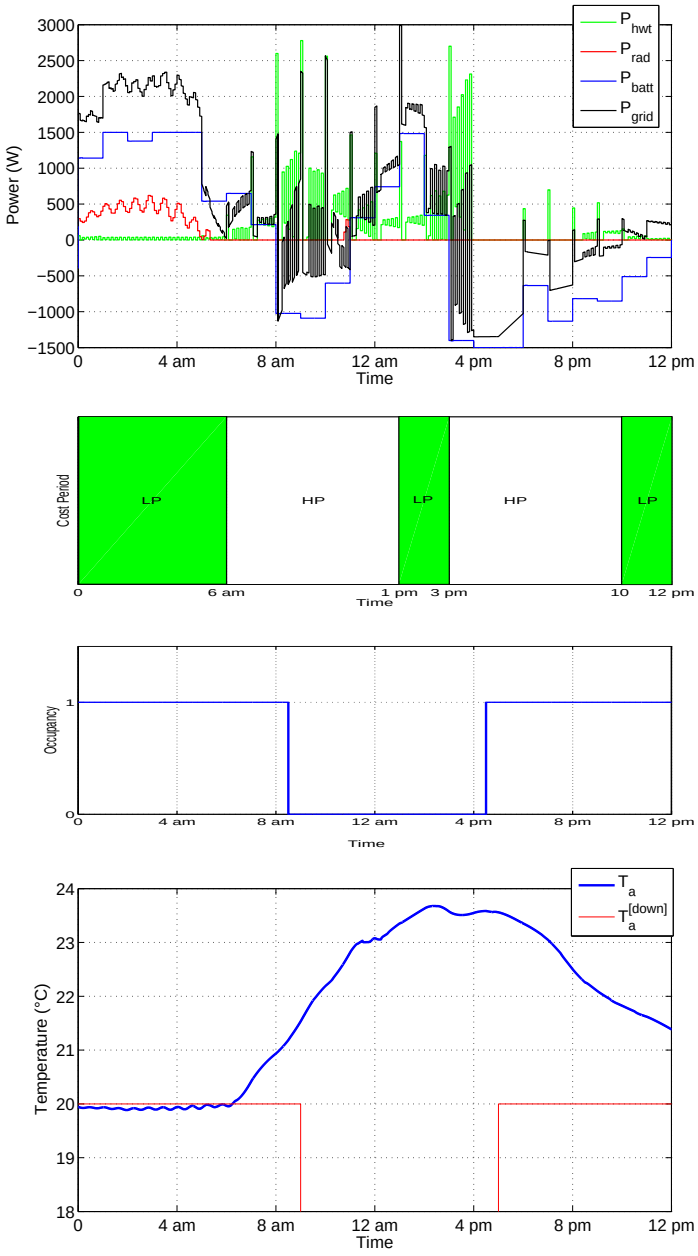

Figure 4.13: House B behavior in summer day

The first remark is, as there are more electrical consumption systems, there are bigger grid energy consumptions, and this especially during winter and spring. Moreover, we can see a large range of power variation due to the optimal BEMS strategy, which consists in storing energy during the LP period and minimizing the consumption during the HP period. Indeed, we

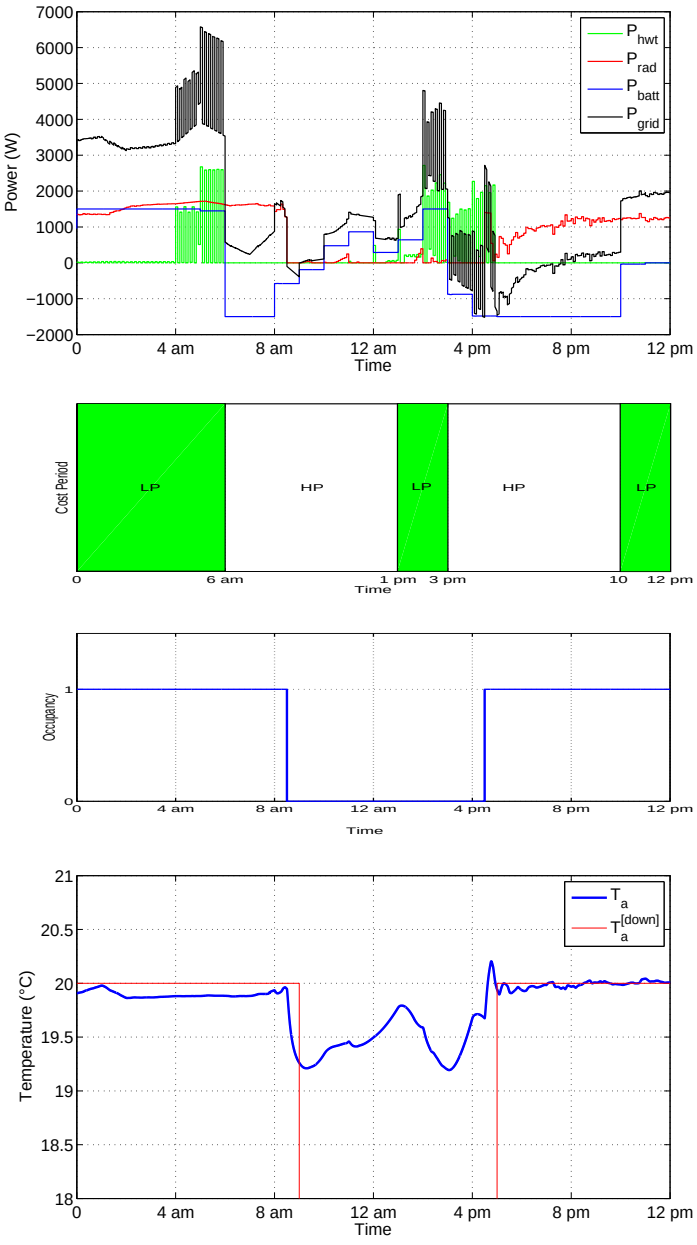

Figure 4.14: House B behavior in spring day

can see that the battery and the water tank are charged and heat at high level during the LP period.

Season strategies:

– In winter, contrary to the house A strategies where the BEMS heat

the temperature during the inoccupancy period, here the temperature is decreasing during the inocuppancy period. In contrast with the house A, it is explained by the bigger heating capacities and by the fact that building has lower thermal inertia. As a consequence, due to the thermal losses, heating building indoor air is not interesting during the inoccupancy period. It is better to proceed as an optimal start control and then, maximize the battery uses during the HP like electrical source for heating.

- In summer, similarly to the house A there is not much indoor temperature heating due to the external conditions. The house B is affected by the external high temperature and the important solar gain which leads to stop the radiator after 6 am. Similarly to the house A, we remark that the temperature increases up to 23 °C.
  About the other systems, we can see that due to the low fatal consumption, the battery is used to heat the hot water tank at the period of time when it is used (when there is hot water drawn). Moreover, power is fed into the grid during high price period corresponding to the higher sell price period too, especially between 4 and 6 pm.
- In spring, we note that the indoor temperature is heating up during all the occupancy periods while the hot water tank' heat and the battery' charge match with the LP period. Contrary to the winter week, there is no peak consumption at 4 pm because of the lower heat and fatal consumption load.

Regarding the control for smart grid, this building is much more interesting and important to control. It seems to be directly impacted by the price period, it implies more grid consumption and it results in dynamical BEMS loads strategies supported by several storage capacities with fast and slow completing dynamics.
In the part 4.3 we will test more tariff scenario in order to go further in our investigation. Before discussing this point and concluding on the BEMS pure performance, we will look at some errors impact on the performance to give some improvement guidelines.

Conclusion

Comparing the BEMS strategies for the two houses and for various weather conditions, we show that the BEMS takes into account the house types. It adapts to the energy plan in function of the houses devices and characteristics in order to optimize the energy consumption. It uses the different house storage capacities and takes advantages of the environment. It results in two different strategies depending on the house type, a smooth and a dynamic one as the indoor temperature' curves in Figure 4.15 shows.

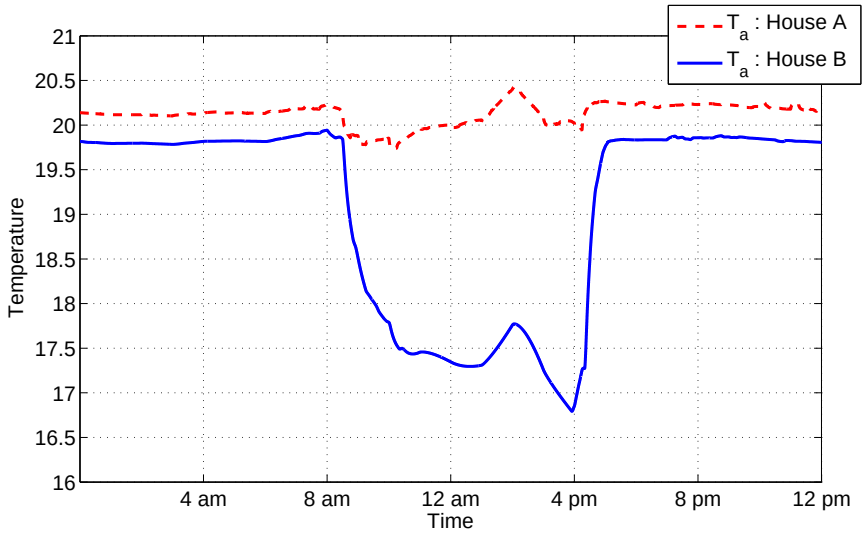

Figure 4.15: Internal temperature comparisons between the house A and B strategies for a winter day.

4.2.6 BEMS improvement

In this part, we will aim at giving some improvement guidelines for the BEMS. We will perform three simulations on the houses to show the impact of the thermal models, the external temperature predicted disturbance profile and the fatal consumption predicted disturbance profiles.

As said previously, in simulations cases, the BEMS controller uses bias predicted disturbances profiles and linear thermal building models. These choices were done in order to show the BEMS robustness considering that real disturbances profiles and accurate thermal building models are not available. Now, let's suppose that they are available and show the BEMS improvement.

We chose three configurations:
- configuration 1: In order to define the impact of thermal building model, we use a more accurate prediction model with a fit of 95%.
- configuration 2: We consider that the BEMS disposes of the real external temperature disturbance profile.
- configuration 3: We consider that the BEMS disposes of the real fatal disturbance profile.

The configuration 3 is especially important, because, according to the International Energy Agency (IEA) the appliances electricity consumption will grow by 25 % by 2020 [74]. The simulations are performed during the winter weeks for house A.

	House A			
Configurations	0	1	2	3
I_{cost} (€)	5.26	5.00	4.94	5.13
I_{dis}	0.24	0.27	0.18	0.31
$T_{I_{dis}}$ (min)	0.35	3.01	0.76	0.28
$E_{tot,grid}$ (kWh)	458	424	419	437

Table 4.11: Configurations results during a winter week on the house A

The results are displayed in the table 4.11. The configuration 0 corresponds to the normal simulations without improvement.

The configuration 1 results prove that the thermal model has an important effect on the BEMS performance. It enables to improve the operating cost while consuming less energy. However, it is not enough. We remark that the configuration 1 leads to a worse I_{dis} compared to configuration 0. In fact, as the configuration 2 results shown, an exact external temperature predicted disturbance profile enables even better performance (I_{cost} and I_{dis}). In this case, the external temperature impact the thermal building prediction and also the heat pump performance which can explain the good result.
For the configuration 3, in which we assume that we dispose of the real fatal disturbance profile, we show a reduction of the energy consumption and the operating cost. However, for this house and in these conditions the fatal consumption has less impact than the others tested.

To sum up, we can say that each of the three parameters tested seems important to improve the BEMS efficiency. In our study case with the *Low Energy* house, the external temperature seems to be the most important factor, then comes the thermal building model accuracy and the fatal consumption. These results depend on the house type and the condition scenario and so are subjective. To go further in this analysis and to enable us to draw a conclusion, a structured study on the BEMS sensibility has to be performed. This point is not addressed in this thesis but seems to be good investigations points.

4.2.7 Conclusion

In this part, we showed that the BEMS offers good performances compared to conventional rule-based controlled houses. The good performances were tested on two houses and with different weather conditions. The hierarchical and distributed BEMS structure correctly adapts to both buildings

which proves its modularity.

Then, we had assessed the BEMS behaviour in function of the building. It results that BEMS optimal control leads to different strategies. A near zero building energy leads to a smoothing strategy while, in a building with less inertia, the storage has been more used and the temperature range is bigger. Moreover, due to its bigger power capacities, the house B is more impacted by the cost periods and so seems the most interesting building actor for the grid.

However, despite the BEMS control robustness, we highlight that the BEMS performances depend clearly on the prediction model and disturbances profiles. We show that the fatal consumption has very important impact on the cost function while the thermal building model is important for the temperature regulation. However, a structured analysis has to be performed to assess correctly the BEMS sensibility.

4.3 Building Smart grid ready

To assess the integration of advanced buildings into the smart grid, we will perform simulation studies to show the impact of a Time-of-Use (TOU) strategy on building consumption behaviour. In this case, we consider a moving price period defined a day ahead by the grid aggregator. Then to offer more flexibility to the grid, we will consider dynamics tariff information and highlight the BEMS ability to react.
In the last part, we will investigate the H-Cmt mode in order to provide the grid with building load profile. First, the horizon impact on the performance considering a strict respect of the commitment profile sent is studied. Second, the commitment is relaxed and the H-Cmt mode possibilities are demonstrated.
In these simulations we will consider the approximated predicted disturbance profiles and simple models as in the first part. We perform simulations during the winter period with the house B which is the most consuming house.

4.3.1 Scenario

In this part, we suppose that the tariff is the same as the previous one to which a moving critical peak price (CPP) is added. The CPP period is one or two hours long corresponding to the global peak consumption period. This varying tariff profile is already used in different countries (Illinois, Ontario ...). The CPP is considered to be twice the price of the high price (HP) as seen in Figure 4.16.

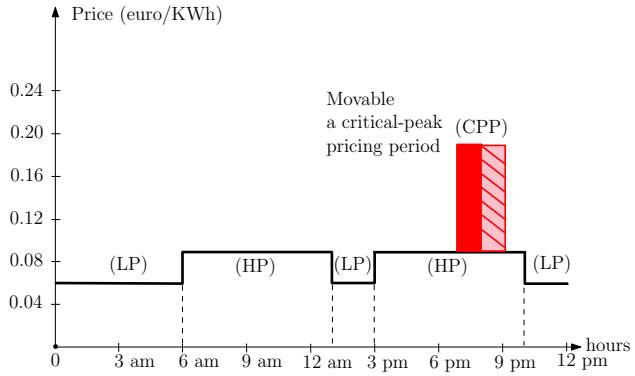

Figure 4.16: Hourly electricity tariff with low price (LP) period (6.14 c€.kWh^{-1}), high price (HP) (9.91 c€.kWh^{-1}) and critical-peak price (CPP) period (19.82 c€.kWh^{-1})

The weather conditions are those displayed in Figure 4.4 (a,b and c). The objective cost function and the air temperature limits are the same as in the previous part.

4.3.2 Indicator

In this part, we chose the same indicators as in the previous part, I_{dis}, I_{cost} and $E_{tot,grid}$ (see 4.2.2). In addition we define several energy consumption indicators to highlight the BEMS behaviors.

- The CPP energy consumption E_{CPP}. It is the building energy grid consumption during the CPP period such as:

$$E_{CPP} = \sum_{CPP_i} \int_{t_{start,CPP_i}}^{t_{end,CPP_i}} P_{grid}(\tau) d\tau \tag{4.23}$$

- The "no CPP" energy consumption noted E_{no-CPP} which corresponds to the potential building consumption during the CPP period when there is no tariff increase.
- The CPP fatal energy consumption note $E_{fatal,CPP}$. It corresponds to the fatal power consumption of the building during the CPP period defined such as:

$$E_{fatal-CPP} = \sum_{CPP_i} \int_{t_{start,CPP_i}}^{t_{end,CPP_i}} P_{fatal}(\tau) d\tau \tag{4.24}$$

4.3.3 Varying cost strategy

The objective is to assess the effect of the varying cost on the grid power consumption of building equipped with BEMS. Then we assess a dynamic

CPP period information in order to define building flexibility according to the horizon information.

Day ahead information

Here we suppose that the electricity tariff information is known at midnight for the entire day. We suppose six CPP periods summed up in the table 4.12.

One hour period (pm)	5 to 6	6 to 7	7 to 8
Two hours period (pm)	5 to 7	6 to 8	7 to 9

Table 4.12: CPP simulations' periods

The results are displayed in the tables 4.13 and 4.14 where we have: the energy consumption during the CPP period with a CPP tariff E_{CPP} and without CPP tariff E_{no-CPP}, the fatal energy consumption $E_{fatal,CPP}$ during the CPP period , the operating cost values I_{cost}, the global energy consumption E_{tot} and the dissatisfaction criterion I_{dis}.

It shows that longer CPP period does not leads to bigger E_{tot}. We see, in the columns of the tables, that week consumptions are the same whereas the CPP are different. This is due to the BEMS anticipation strategy. However, as it could be expected, longer CPP periods lead to higher operating costs I_{cost}. The tables show that the E_{CPP} are significantly reduced in comparison to the energy consumption without CPP tariff E_{no-CPP}. Moreover, the BEMS, thanks to the battery storage, ensures averaged 72 % of the fatal CPP energy consumption $E_{fatal,CPP}$ for a CPP period of one hour, and averaged 54 % for a CPP period of two hours.

Indicator CPP	5 to 6	6 to 7	7 to 8
E_{CPP} (kWh)	2.9	5.3	2.9
E_{no-CPP} (kWh)	28.1	26.8	23.6
$E_{fatal,CPP}$ (kWh)	12.2	14.7	12.9
I_{cost} (€)	6.62	6.70	6.71
E_{tot} (kWh)	582	578	580
$E_{tot,no-CPP}$ (kWh)	585	585	585
I_{dis}	0.27	0.27	0.34
$T_{I_{dis}}(min)$	3.7	3.7	2.9

Table 4.13: One hour CPP results

Looking at the CPP hourly energy consumption E_{CPP}, we can see in Figures 4.17, 4.18 and 4.19 that CPP period consumptions are shed. The

Indicator CPP	5 to 7	6 to 8	7 to 9
E_{CPP} (kWh)	10.1	14.1	11.7
E_{no-CPP} (kWh)	54.9	50.4	46
$E_{fatal,CPP}$ (kWh)	26.9	27.7	25.0
I_{cost} (€)	6.82	6.85	6.80
E_{tot} (kWh)	583	581	580
$E_{tot,no-CPP}$ (kWh)	585	585	585
I_{dis}	0.27	0.27	0.42
$T_{I_{dis}}(min)$	3.7	3.7	5.2

Table 4.14: Two hours CPP results

E_{CPP} are as much as possible reduced by the anticipation strategy while respecting the comfort.

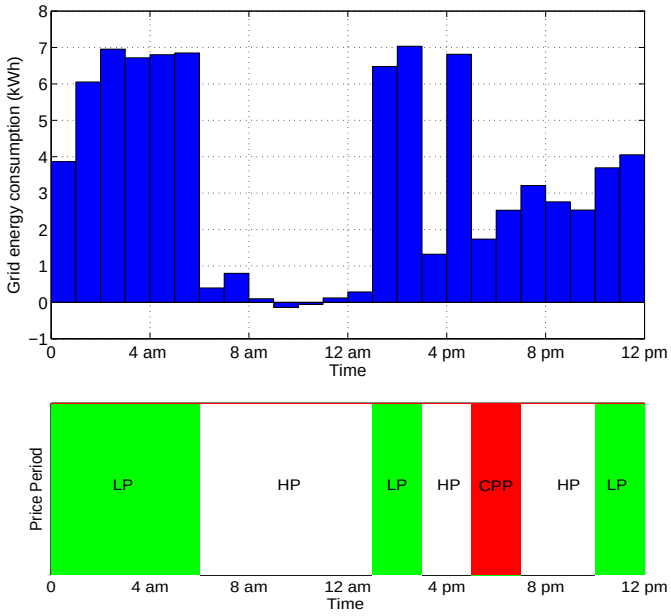

Figure 4.17: House B hourly energy consumption in a winter day. CPP between 5 to 7 pm.

From this case study, due to the complexity of the management, it is quite hard to draw many conclusions but it proves that the price acts on building consumption as a shifting demand. It results in a higher consumption some hours ahead the CPP period. We remark that there are bigger CPP energy consumptions when the CPP period is longer. It shows that it is more difficult to reduce the CPP consumption over a long period due to the limited storage systems capacities and the predictions approximations.

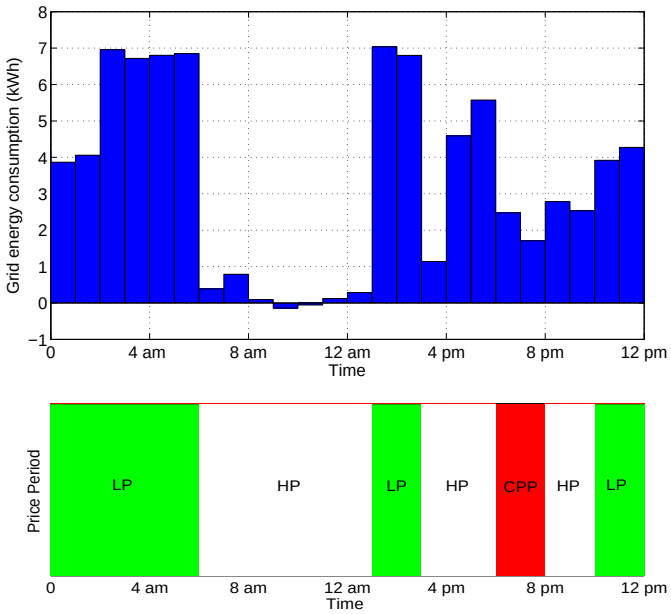

Figure 4.18: House B hourly energy consumption in a winter day. CPP between 6 to 8 pm.

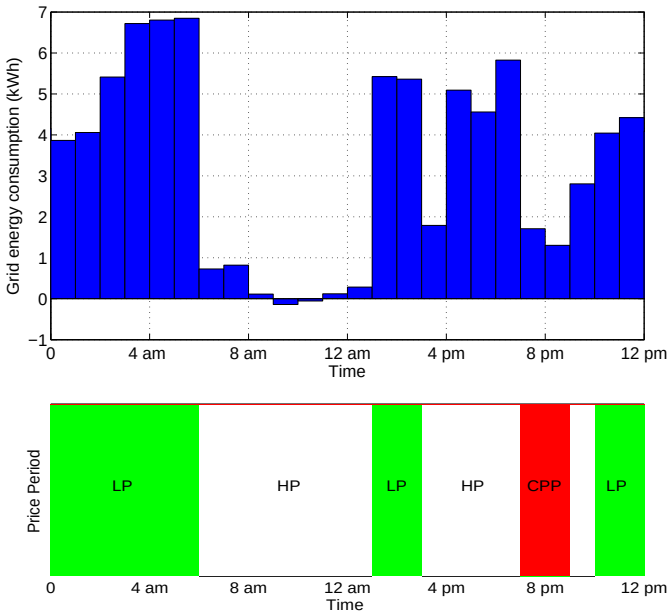

Figure 4.19: House B hourly energy consumption in a winter day. CPP between 7 to 9 pm.

Dynamic tariff information

In the previous part, it was considered that the day CPP period was known from the aggregator and sent to the BEMS at midnight each day. Indeed, CPP period could be difficult to plan 24 hours ahead for the grid aggregator. The CPP period is affected by the weather or the global consumer consumption or other effects during the day. That's why, in this part, it is considered that the CPP period is announced to building h_d hours in advance, e.g. if h_d=1 hour, the BEMS does not know that a CPP period could appear and receives the information 1 hour before it occurs.
The objective is to highlight building flexibility. In reducing the CPP information time while keeping the optimal building operating cost, we enable the grid to decide later the CPP period and as a consequence offer flexibility to the grid.
For this study the CPP period is set up between 7 to 9 pm, corresponding to the global peak consumption, and the information horizon h_d varies from 1 to 11 hours ahead. The simulations are performed on a winter week on the house B.

The results are summarized in Figure 4.20. The operating cost is displayed in function of the information horizon.

It shows that, to inform the BEMS, 4 hours ahead is sufficient to minimize its CPP period consumption. It is the time to shed the consumption during the HP period to go trough the CPP period.

We remark in Fig 4.20 (c) that the global energy consumption does not increase so much (about 500 Wh by day). This can be explained by the fact that as the CPP occurs during the HP period, the BEMS has already planned to minimize its consumption. We also note that the global energy consumption is for a horizon of 7 hours, which corresponds to the optimal operating cost. As seen in Figures 4.20 (d) and (e), the horizon of $h_d = 7$ hours corresponds to the times needed by the BEMS to optimize the distribution of its consumption.

Another solution to reduce the building consumption during the global peak consumption period should be to limit the grid power $P_{grid}^{[up]}$. However, to apply this solution without damaging the users' comfort, it is necessary to know on time all building load shift capacities. By the way, this strategy can be easily implemented in the BEMS.

Conclusion

To summarize, studies show the effect of the TOU on the advanced building consumption. It leads to a load shedding strategy with an important reduction of building CPP period consumption. In the second part, we

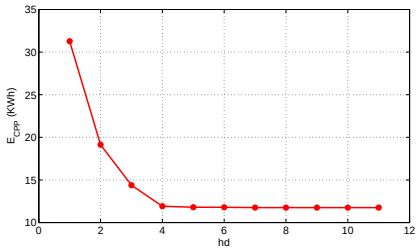

(a) CPP period consumption

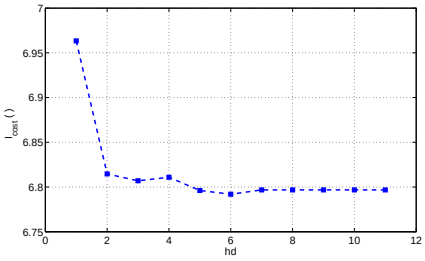

(b) Operating cost

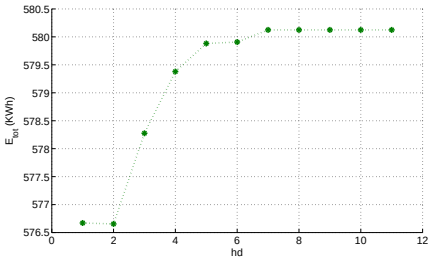

(c) Global energy consumption

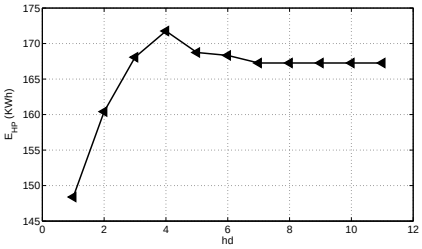

(d) HP period energy consumption

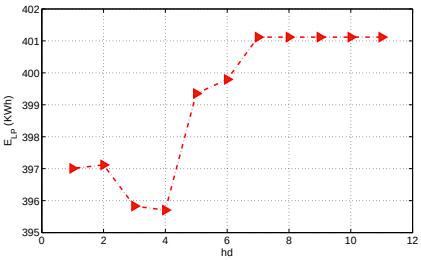

(e) LP period energy consumption

Figure 4.20: Effect of the information time h_d on the house B consumptions and operating cost

show that for advanced buildings, it exists different time horizons enabling to reduce the peak energy consumption. In our case, the optimal horizon to reduce the CPP period energy consumption is 4 hours, which gives more flexibility to the grid to inform the buildings.
To sum up, a TOU strategy dynamic leads to modify the building consumption behaviour which can create unpredicted global peak consumption on the grid. That is why, in the next part, we assess the H-Cmt BEMS mode

in order to inform the grid of the building energy consumption profile.

4.3.4 Building commitment

From a grid point of view, if we suppose that all buildings are equipped with an advanced BEMS control as the one developed, the grid aggregator will have to manage the TOU tool efficiently, otherwise, the peak load consumption period will only be shed or will still occur depending on buildings interest. However, it seems very complicated for the grid to deduce the load shedding amount of all houses relative to the TOU. As shown in the previous part, the amount of load shedding depends on building type, building capacities, building state, price, objective cost function, etc.
That is why in the H-Cmt mode, we consider that BEMS communicates with the grid aggregator to commit on a consumption profile. In our simulation cases, the energy stage profile corresponds to the grid electricity consumption, however for building provided by gas source or hot water source, the principle can also be applied.

In this part, we assess the H-Cmt mode of the BEMS developed. The principle, described in chapter 3, can be roughly explained in two steps. First the (S) scheduling control MPC layer plans the building consumption and system state trajectories over a given horizon in order to minimize the global building cost function (here the operating cost) while fulfilling the constraints. It results in an energy stage profile E_S which is sent to the grid and to the (P) piloting lower layer. The (P) layer has then to respect it while following the predicted state trajectories.

To assess the performance, we perform simulations with varying commitment horizon noted H_C on a winter day. We consider the house B and the CPP period is set between 7 and 9 pm. To match with the tariff period, we set the energy stage period to 1 hour.

In the following part, we will test the mode in simulations and assess the mode performance for a strict respect of the commitment profile and with a softer respect of the profile. The simulations are performed during a winter week on the house B.

Strict commitment

Here, we test a strict commitment of the energy stage profile which means that the BEMS must exactly comply with the energy consumption that it has predicted. To clarify, with a periodicity of H_C, the BEMS provides an energy consumption profile at the grid over the commitment horizon H_C. Then its aim is to respect it.

In Figures 4.21 (a), (b), (c) and (d) the BEMS performance are displayed for the horizon H_C. The associated indicators are detailed in table 4.15.

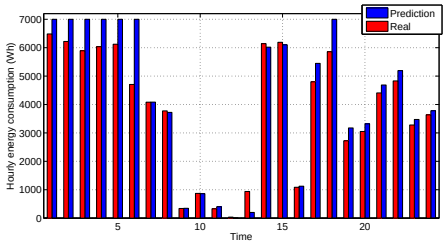

(a) $H_C = 2$ hours

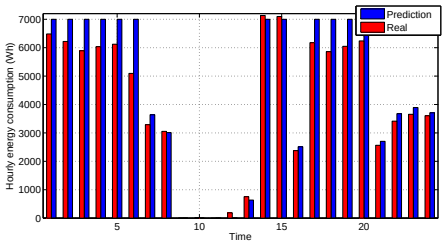

(b) $H_C = 4$ hours

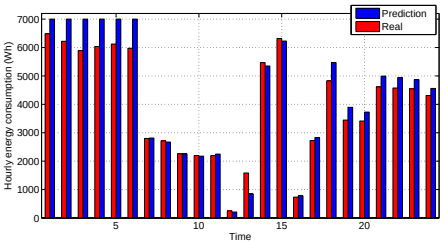

(c) $H_C = 6$ hours

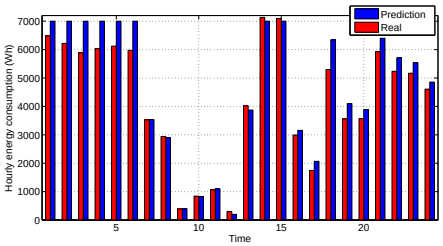

(d) $H_C = 8$ hours

Figure 4.21: Results of the commitment simulations over a day period

Indicator H_C	2 h	4 h	6 h	8 h
I_{cost} (€)	1.17	1.11	1.21	1.27
E_{tot} (kWh)	94	89	98	99
I_{dis}	0.93	1.04	0.84	1.17
$T_{I_{dis}}(min)$	4.63	4.55	3.7	1.2

Table 4.15: Simlulations results for the H-Cmt mode with a strict commitment

It shows that whatever H_C, the BEMS respects well its commitment energy stage profile. However, to respect the commitment profile, the BEMS damages the users' comfort. Another interesting point is that even with the energy stage constraint, it happens that the hourly energy constraint is exceeded. This effect is entirely due to the unpredicted fatal consumption which is the only uncontrollable consumption. We note that an smaller horizon H_C does not lead to better energy profile respect.

H_C (hours)	2	4	6	8
I_{cost}	1.00	0.98	1.00	0.99
E_{tot}	80	79	80	81
I_{dis}	0.91	0.98	0.98	0.98
$T_{I_{dis}}$	9.36	7.11	8	7.15

Table 4.16: Simulation result with a soften commitment energy consumption profile

The first study concludes that, in this case, the BEMS cannot respect exactly the predicted energy consumption profile. In the next study, we consider soft commitment constraint in order to show that with an admissible error the BEMS can ensure its commitment and the users' comfort.

Soft commitment

In this part we soften the constraint of the BEMS on the commitment energy stage profile. We consider the same conditions as previously and vary the commitment horizon H_C. We test a soft value equal to 10%. This means that the hourly energy stages have to be fulfilled with a margin error of 10 %. Thus the energy stage error becomes:

$$\begin{aligned} |\sigma_{E_{soft}}(t_K)| = \quad & |max(0,(1-0.1)E_S(t_K|\delta_j) - \textstyle\sum_{t_k=t_{K-1}}^{t_K} E_p(t_k|\rho_p))| \\ & +|min(0,(1+0.1)E_S(t_K|\delta_j) - \textstyle\sum_{t_k=t_{K-1}}^{t_K} E_p(t_k|\rho_p))| \end{aligned} \quad (4.25)$$

The results are displayed in the table 4.16. We show that the soft constraint enables to improve the user's comfort and reduce the global energy consumption as well as the operating cost. This result gives an idea about the commitment ability of the smart building. Knowing the high impact of the fatal consumption on the BEMS performance, it seems that the customer's load pattern changes have to be taken into account so as to improve the performance.

4.4 Conclusions

In a first part, we illustrated the proposed BEMS performances and compared them to a conventional rule-based control for three different weather conditions. The results showed that the BEMS have the potential to efficiently manage the houses energies reducing the operating cost and ensuring the users' comfort.
In addition, the modularity of the BEMS structure was established with its virtual implementations on two houses equipped with different systems. We showed that the BEMS adapt to houses devices and characteristics. It results in different strategies depending on the houses. A high insulated

house with low heating load and weak heating capacity leads to a smoothing strategy with no important grid consumption range. On the contrary, a less insulated house equipped with electrical appliances is very impacted by the price period and it leads to a complex strategy where the different storages play important roles.
Simulations were performed with great importance to be as close as possible to real conditions in order to highlight its real potential. However, because the BEMS behavior is based on predictions, a qualitative analysis showed the need to perform a structured sensibility analysis in order to identify the major impact factors.

In a second part, we concentrate on the smart grid integration. We perform simulations considering a varying tariff profile and show that it results in a load shedding grid consumption strategy from the BEMS. Then, we suppose a dynamic grid information. The study highlights the BEMS ability to react to the tariff profile. It shows that in the study case an information horizon of 4 hours is enough for the BEMS to shed its grid peak consumption.
To go further in the grid integration and ease the global energy management, we assess the BEMS commitment mode. We show that the BEMS enables to respect its energy profiles over a long horizon. However, because of the prediction errors, this leads to damage the users' comfort. To overcome this issue, a softened energy profile is considered. We show that with a hourly energy error of 10% the BEMS can ensure both.

Chapter 5

Conclusions and perspectives

The aim of this project was to develop a new Building Energy Management System (BEMS) for building issues. The investigated context has highlighted fourth main features:

- Creating an adaptable and modular control.
  Buildings are built for a long-term period of time and are continuously evolving. Systems are changing, uses are changing and buildings characteristics are changing as well. To face this evolution, the control structure has to be modular. Moreover, developing a building control for only one building is not viable. A BEMS has to be adaptable to be used on all kinds of buildings.
- Managing building efficiently requires a global control view.
  Nowadays, systems complement each other. To ensure their local objective, interactions are needed. Moreover, to ensure an optimal global control they cannot be managed independently anymore, a global control is required.
- Using advanced control method.
  Buildings behaviours and controls become more and more complex due to the increasing integration of advanced systems. The old controllers cannot take into account these new challenges and complexities. Other control methods, which are already used in different fields as in the industry, are more adapted.

- Adopting the smart grid development in the BEMS.
  Today, the world energy is in a transition phase and building issue has got one of the major places. It has to play an important role as a consuming actor thanks to the deployment of metering and communicating technologies.

In respond to the fourth features, we develop a predictive, hierarchical and distributed BEMS based on model predictive control (HD-MPC).

- the anticipation has for objective to minimize the energy bills while

satisfying the occupant's need.
- the hierarchical architecture enables to treat the high resolution problem complexity by working with two different time scales. Moreover, it offers a structuring control allowing to consider new smart grid demands.
- the distributed aspect ensures the control modularity bringing adaptability to the BEMS.

In addition, the control structure flexibility is ensured by a systemic view of the house appliances. This design method enables to modelize the system independently where couplings are ensured by an external input variable.
The development of this thesis is progressive. We first consider a monolayer control to define the best MPC configuration. As a result, a receding control combined with a varying sampling time was chosen. The receding optimization improves the robustness on account of the periodical states feedback. This enables to update the system states values and thus, to correct the predicted trajectories. The varying sampling time is used to reduce the computing time while affording to use a long optimization horizon with a fine sampling time.
Secondly, the hierarchical BEMS is presented. The high level receives the grid information and has to plan the energy flows over a long horizon. At low level, the piloting control receives the high level commands, works over a shorter horizon and has a finer sampling time. Its objective function is a multi-criterion which leads to develop two BEMS modes. The H-track mode is designed to optimize only the user's objective and so the piloting layer exclusively follows the state trajectories which are received. In H-Cmt mode, the piloting layer has to follow the state trajectories, however it has to respect the associated energy consumption profiles. This mode allows buildings to commit oneself on its consumption profile towards the grid.
The BEMS MPC configurations are summarized in the table 5.1.

The efficiency of the BEMS was assessed by simulations studies. We attach importance to reality aspect by using simple and generic models of the systems and bias on the predicted disturbance profiles. We compare the BEMS on two buildings to conventional controls and show their good performances. We note that buildings lead to two different strategies. Depending on buildings and systems characteristics and capacities, the BEMS manages the consumption either smoothly or more dynamically. Gain of the advanced BEMS developed is provided by the use of storage capacities (battery, hot water tank, internal air temperature) to shed the consumption.

In the last part, we focus on the BEMS behavior regarding the grid integration (see summarizes in table 5.2). We investigate the Time-Of-Use effect on building management. It results that a varying tariff profile leads to load shedding strategies. The storage capacities of the systems are used to anticipate the high price period. However, we highlight the limit of this

BEMS Configurations	Characteristics	Advantages	Drawbacks
Centralized MPC			
Open Loop	Long scheduling horizon	Only one optimization by day	Bad performance with unpredicted disturbances. High computing time burden.
Closed Loop (CL)	Long Receding scheduling horizon	Reject unpredicted disturbances thanks to feedback and receding optimization program	High computing time burden.
(CL) + Varying Sampling Time	Long Receding scheduling horizon with varying sampling time	Low computing time burden. Near optimal unpredicted disturbance rejection.	Fast receding scheduling not adapted with grid interface.
Hierarchical MPC	Multi-time scales approach with two receding MPC. Use varying sampling time for piloting	Offer grid interface possibility. Structuring control architecture.	
H-Track mode	Follows the scheduling trajectories.	Ensure user comfort	Operating cost depend on prediction accuracies
H-Cmt mode	Take into account the load energy stage predicted profile	Respect load consumption profile	Users' comfort satisfaction depends on prediction accuracies
Distributed resolution	Systemic view. Local independent system. Global coordinator agent.	Modular and adaptable structure. Optimal solution.	Need information exchange

Table 5.1: BEMS MPC studies summary.

Grid strategy	BEMS behaviour
Day ahead Tariff-Of-Use	Load shedding
Dynamics Tariff-Of-Use information	Load shedding reactivity
Strict grid load commitment	Users' dissatisfaction
Soft grid load commitment	Grid load profile respect and users comfort ensured

Table 5.2: BEMS application main results

dynamics tariff profile strategy. Late information doesn't ensure a significant reduction of the peak period consumption. To go further, communication between building and the grid is needed.
This possibility is investigated via the H-Cmt mode. To summarize, the BEMS could enable to transmit its energy consumption profile and respect it with conditions. A strict profile leads to users' discomforts and so has to be discussed with the occupants. A smoother profile under a certain horizon is conceivable without occupant's discomfort. We remark that good commitment performance is favoured by accurate disturbances information profiles and efficient storage systems. However, users' behaviours and their incomes have to be taken into account.

Coming back to the BEMS performance, the study highlights the weakness of the advanced structure which opens several work axis for the future BEMS improvement.
From a theoretical point:

1. Evaluating the sensitivity of the control to the model and profiles accuracies. A quick study highlights the impact of the thermal model and the fatal consumption predicted profile on the BEMS performance. A more structured and extensive study has to be done.
2. Expanding the control to hybrid and nonlinear models so as to enable to consider more complex installations. Even if linear models have proved their good performance in our building cases, they also constrain our cases. More complex systems with co-generation or flow exchanges need to be integrated.
3. Quantifying the optimality of the hierarchical control architecture. The choice of the low layer objective has not been the object of a study and better functions could be found.

From a practical point:

1. Adding more complex systems into the control (ventilation and blind system units ...).
2. Integrating the human's pattern.
3. Implementing the BEMS on real building.
4. Testing the advanced structure to a larger scale (district or office building) to increase the control gain.

Our work also shows the importance of the systems and their capacities on the BEMS performances. It proves that the residential houses have to integrate the new smartgrid demands and constraints during building period or during refurbishment in order to size the systems according to the needs. Some interesting results on house storage and producer systems size can be found in [75].

We believe that, through our work, we have contributed to the analysis of the residential building potential as an important actor of the smart grid, but we also managed to highlight the BEMS MPC-based potential in the energy context in order to manage and reduce the energy consumption.

Appendix A

This appendix gives the methods used to linearize the complementary constraints, relax constraints and transform inequality into equality constraints.

Linearization variables

For there demonstrations, considering a input variable u associated to the non linear specific constraint:

$$c = \begin{cases} c_1 & \text{if } u \geq 0 \\ -c_2 & \text{if } u < 0 \end{cases} \tag{5.1}$$

It is necessary that the parameters c_1 and c_2 associated to the variable respect:

$$c_1 > c_2 > 0 \tag{5.2}$$

Whatever the linearization is not possible. For our case, the variables concerned are the grid electricity power and the battery power and we have $\forall t$:

$$C_{buy} > C_{sell} > 0 \tag{5.3}$$

and

$$n_{ch,batt} > n_{dis,batt} > 0 \tag{5.4}$$

As result the linearization are valid.

Case 1: the input variable is included in the cost function

This case refer to the grid electricity power variable.

Suppose an input variable u, an uncontrollable variable w and the optimization problem follows:

$$\min_u \begin{cases} c_1.u & \text{if } u \geq 0 \\ -c_2.u & \text{if } u < 0 \end{cases} \tag{5.5}$$

s.t.

$$u - w = 0 \tag{5.6}$$

and such as:

$$u^{[up]} \geq u \geq u^{[down]} \tag{5.7}$$

It is supposed that the problem is always feasible $u^{[up]} \geq w$ and that:

$$c_1 > c_2 > 0 \tag{5.8}$$

To linearize the equation 5.5 we introduce two variables λ_1 and λ_2 such as the problem becomes:

$$\min_{u,\lambda_1,\lambda_2} = c_1.\lambda_1 - c_2.\lambda_2 \tag{5.9}$$

s.t.

$$u - w = 0 \tag{5.10}$$

and

$$u - \lambda_1 + \lambda_2 = 0 \tag{5.11}$$

such as:

$$u^{[up]} \geq u \geq u^{[down]} \tag{5.12}$$

$$u^{[up]} \geq \quad \lambda_1 \geq 0 \tag{5.13}$$

$$u^{[down]} \geq \quad \lambda_2 \geq 0 \tag{5.14}$$

This problem is linearized and equivalent the initial one.

Proof

Take the case $w \geq 0$: In this case, the equation (5.6) of the initial problem gives $u = w \geq 0$ and so the cost function is:

$$\min_{u} c_1.u \tag{5.15}$$

Take the linearized problem. In this case the equation (5.10) gives $u = w \geq 0$. As a result thanks to the equation (5.11) the objective function (5.9) becomes:

$$\min_{u,\lambda_1,\lambda_2} = c_1.u + (c_1 - c_2).\lambda_2 \tag{5.16}$$

As $c_1 > c_2$ so the term $(c_1 - c_2) > 0$. It results that the solution is $\lambda_2 = 0$ and the cost function is equivalent to the initial problem:

$$\min_{u,\lambda_1,\lambda_2} = c_1.u \tag{5.17}$$

For the case $w < 0$ the demonstration is similar.

Case 2: the input variable is only constrained

This case refer to the battery power variable.

Suppose an input variable u, an uncontrollable variable w such as:

$$\dot{T} = T + \begin{cases} c_1.u & \text{if } u \geq 0 \\ -c_2.u & \text{if } u < 0 \end{cases} \tag{5.18}$$

s.t.

$$u - w = 0 \tag{5.19}$$

and such as:

$$u^{[up]} \geq \quad u \geq u^{[down]} \tag{5.20}$$
$$T^{[up]} \geq \quad u \geq T^{[down]} \tag{5.21}$$

It is supposed that $u^{[up]} \geq w \geq u^{[down]}$ and that:

$$c_1 > c_2 > 0 \tag{5.22}$$

To linearize this problem similarly to the previous demonstration we introduce two linearization variables λ_1 and λ_2 such as the constraints becomes:

$$\dot{T} = T - c_1.\lambda_1 + c_2.\lambda_2 \tag{5.23}$$

s.t.

$$u - w = 0 \tag{5.24}$$

and

$$u - \lambda_1 + \lambda_2 = 0 \tag{5.25}$$

and such as:

$$u^{[up]} \geq \quad u \geq u^{[down]} \tag{5.26}$$
$$T^{[up]} \geq \quad u \geq T^{[down]} \tag{5.27}$$

$$u^{[up]} \geq \quad \lambda_1 \geq 0 \tag{5.28}$$
$$u^{[down]}| \geq \quad \lambda_2 \geq 0 \tag{5.29}$$

This problem is linearized and equivalent the initial one.

Proof

Take the case $w \geq 0$: In this case, the equation (5.19) of the initial problem gives $u = w \geq 0$. As result the equation (5.18) becomes:

$$\dot{T} = T - c_1.w \tag{5.30}$$

Take the linearized problem. In this case the equation (5.24) gives $u = w \geq 0$. This implied that, from the equation (5.25):

$$\lambda_1 = w + \lambda_2 \tag{5.31}$$

Introducing it in the equation (5.23), it becomes:

$$\dot{T} = T - c_1.w + (c_2 - c_1).\lambda_2 \tag{5.32}$$

As $c_1 > c_2 > 0$ so $(c_2 - c_1) < 0$. The resolution have no reason to take $\lambda_2 > 0$ otherwise the variable T will increase strongly and the equation 5.24 couldn't be respected at the future steps.
For the case $w < 0$ the demonstration is similar.

Slack relaxations variables

The slack relaxation variables are used to ensure the feasibility of the optimization. It enables to solve the optimization problem even if a constraint could not be respected.
Suppose a variable u define on $\mathbb{R}$, an linear objective cost function J:

$$J = \min_u c_1.u \tag{5.33}$$

and the constraint:

$$u^{[down]} \leq u \leq u^{[up]} \tag{5.34}$$

The relaxation consists in introducing two slack variables λ_1 and λ_2 such as the previous constraint is transform in:

$$u^{[down]} \leq u + \lambda_1 - \lambda_2 \leq u^{[up]} \tag{5.35}$$

with:

$$\lambda_1, \lambda_2 \geq 0 \tag{5.36}$$

The equivalence is ensured thanks to the addition of the term in the objective function J such as:

$$J^{'} = \min_{u,\lambda_1,\lambda_2} (J + c.\lambda_1 + c.\lambda_2) \tag{5.37}$$

with $c >> c_1$.

Transform inequality constraint

We consider a input variable u subject to:

$$u^{[down]} \leq u \leq u^{[up]} \tag{5.38}$$

with

$$u^{[down]}, u, u^{[up]} > 0 \tag{5.39}$$

To transform these constraints into equality constraints we introduce two slack variable $\lambda_1, 2$ such as:

$$u^{[down]} = u + \lambda_1 \tag{5.40}$$

$$u^{[up]} = u - \lambda_2 \tag{5.41}$$

with

$$u^{[down]}, u, u^{[up]}, \lambda_1, 2 > 0 \tag{5.42}$$

Bibliography

[1] D. Gyalistras and M. Gwerder. Use the wheather and occupancy forecasts for optimal building climate control (opticontrol): Two years progress report. Technical report, Terrestiral System Ecology ETH Zurich, 2010.

[2] M. Avci, M. Erkoc, A. Rahmani, and S. Asfour. Model predictive HVAC load control in buildings using real-time electricity pricing. *Energy and Buildings*, 60:199–209, 2013.

[3] Groupe de travail sur la maîtrise de la pointe électrique, http://www.developpement-durable.gouv.fr.

[4] Power smart pricing, `http://www.powersmartpricing.org/`.

[5] `http://openadr.lbl.gov/`.

[6] p.52 : `http://www.ibuilding.gr/handbook/index.html`.

[7] K. Yun, R. Luck, P.J. Mago, and H. Cho. Building hourly thermal load prediction using an indexed ARX model. *Energy and Buildings*, 54:225–233, 2012.

[8] H. Madsen and J.Holst. Estimation of continuous-time models for heat dynamics of a building. *Energy and Buildings*, 22:67–79, 1995.

[9] K. K. Andersen, H. Madsen, and L. H. Hansen. Modelling the heat dynamics of a building using stochastic differential equations. *Energy and Buildings*, 31:13–24, 2000.

[10] X. Xu and S. Wang. A simplified dynamic model for existing buildings using CTF and thermal network models. *International Journal of Thermal Sciences*, 47:1249–1262, 2008.

[11] J. Purdy and I. Beausoleil-Morrison. The significant factors in modelling residential buildings. In *Seventh International IBPSA Conference, RIo de Janeiro, Brazil, August 13-15*, 2001.

[12] F. Oldewurtel, D. Sturzenegger, and M. Morari. Importance of occupancy information for building climate control. *Applied Energy*, 101:521–532, 2013.

[13] Y. G. Yohanis, J. D. Mondol, A. Wright, and B. Norton. Real-life enerfy use in the UL : How occupancy and dwelling characteristics

affect domestic electricity use. *Energy and Buildings*, 40:1053–1059, 2008.

[14] T. Hong and Y. Jiang. Stochastic wheather model for building HVAC systems. *Building and Environment*, 30:521–532, 1995.

[15] R. Kramer, L. v. Schijndel, and H. Schellen. Simplified thermal and hygric building models: A literature review. *Fontriers of Architectural research*, 1:318–325, 2012.

[16] G. Fraisse, C. Viardot, O. Lafabrie, and G. Achard. Development of a simplified and accurate building model based on electrical analogy. *Energy and Buildings*, 34:1017–1031, 2002.

[17] T. R. Nielsen. Simple tool to evaluate energy demand and indoor environment in the early stages of building design. *Solar Energy*, 78:73–83, 2005.

[18] J. H. Kampf and D. Robinson. A simplified thermal model to support analysis of urban resource flows. *Energy and Buildings*, 39:445–453, 2007.

[19] A.I. Dounis, P. Tiropanis, A. Argiriou, and A.Diamantis. Intelligent control system for reconciliation of the energy savings with comfort in buildings using soft computing techniques. *Energy and Buildings*, 43:66–74, 2011.

[20] H. Zhang, A. Davigny, F. Colas, Y. Poste, and B. Robyns. Fuzzy logic based energy management strategy for commercial buildings integrating photovoltaic and storage systems. *Energy and Buildings*, 54:196–206, 2012.

[21] S. Soyguder, M. Karakose, and H. Alli. Design and simulation of a self-tuning PID-type fuzzy adaptative control for an expert HVAC system. *Expert Systems with Applications*, 36:4566–4573, 2009.

[22] B. Paris, J. Eynard, and S. Grieu. Hybrid PID-fuzzy control scheme for managing energy resources in buildings. *Applied Soft Computing*, 11:5068–5080, 2011.

[23] M. Pipattanasomporn, M. Kuzlu, and S. Rahman. An algorithm for intelligent home energy management and demand response analysis. In *IEEE Transaction on Smart Grid*, 2012.

[24] F. Oldewurtel, A. Parisio, C. N. Jones, D. Gyalistras, M. Gwerder, B. Lehmann V. Stauch, and M. Morari. Use of model predictive control and weather forecasts for energy efficient building climate control. *Energy and Buildings*, 45:15–27, 2012.

[25] L. M. Costa and G. Kariniotakis. A stochastic programming model for optimal use of local energy resources in a market environment. In *IEEE Power Tech, Lausanne page 449-454*, 2007.

[26] Y. Ma and F. Borrelli. Fast stochastic predictive control for building temperature regulation. In *2012 American Control Conference Fairmont Queen Elizabeth, Monréal, Canada June 27- June 29*, 2012.

[27] A.A. Argiriou, I. Bellas-Velidis, and C.A. Balaras. Development of a neural network heating controller for solar buildings. *Neural Networks*, 13:811–820, 2000.

[28] A. A. Argiriou, I. Bellas-Velidis, M. Kummert, and P. André. A neural network controller for hydronic heating systems of solar buildings. *Neural Networks*, 17:427–440, 2004.

[29] X. Guan, Z. Xua, and Q.-S. Jia. Energy-efficient buildings facilited by microgrid. *IEEE Transactions on Smart Grid*, 1:243–252, 2010.

[30] D. L. Ha, S. Ploix, M. Jacomino, and M. H. Le. Control of energy consumption in home automation by ressource constraint scheduling. In *15 International Conference on Control Systems and Computer Science*, 2005.

[31] S. Abras. *Systèmes Domotiques Multi-agents pour la gestion de l'énergie dans l'habitat*. PhD thesis, Mathématiques, Sciences et Technologies de l'Information, Informatique (MSTII) - Grenoble INP, 2009.

[32] G. De Oliveira. *Approche hybride d'optimisation pour la gestion d'énergie dans le bâtiment*. PhD thesis, Ecole Doctorale : Electronique, Electrotechnique, Automation & Traitement du Signal, 2013.

[33] M. Y. Lamoudi, M. Alamir, and P. Béguery. Unified NMPC for multivariable control in smart building. In *18th IFAC World Congress Milano (Italy) August 28 - Septembre 2*, 2011.

[34] J. Eynard, S. Grieu, and M. Polit. Predictive control and thermal energy storage for optimizing a multi-energy district boiler. *Jounral of Process Control*, 22:1246–1255, 2012.

[35] R. Yang and L. Wang. Multi-zone building energy management using intelligent control and optimization. *Sustainable cities and society*, 6:16–21, 2013.

[36] W. Huang and H.N. Lam. Using genetic algorithms to optimize controller parameters for HVAC systems. *Energy and Buildings*, 26:277–282, 1997.

[37] S. H. Kim. Building demand-side control using thermal energy storage under uncertainty: An adaptative multiple model-based predictive control (MMPC approach). *Building and Environment*, 67:111–128, 2013.

[38] I. Hazyuk, C. Ghiau, and D. Penhouet. Optimal temperature control of intermittently heated buildings using model predictive control: Part ii - control algorithm. *Building and Environment*, 51:388–394, 2012.

[39] J. Ma, J. Qin, T. Salsbury, and P. Xu. Demand reduction in building energy systems based on economic model prediction control. *Chemical Engineering Science*, 67:92–100, 2012.

[40] A. Di Giorgio and L. Pimpinella. An event driven smart home controller enabling consumer economic saving and automated demand side managment. *Applied Energy*, 96:92–103, 2012.

[41] H. Sane and M. Guay. Minmax dynamic optimization over a finite-time horizon for building demand control. In *American Control Conference*, 2008.

[42] G. J. Pappas T. Nghiem, M. Behl and R. Mangharam. Green scheduling: Scheduling of the control systems for peak power reduction. In *Green conputing conference and workshops (IGCC),*, 2011.

[43] Y. Zong, D. Kullmann, A. Thavlov, O. Gehrke, and W. Bindner. Active load managment in an intelligent building using model predictive control strategy. In *PowerThech, 2011 IEEE Conference Trondheim*, 2011.

[44] V. M. Zavala, J. Wang, and S. Leyffer. Proactive energy management for next-generation building systems. In *Fourth National Conference of IBPSA-USA, New York City, New York August 11 - 13*, 2010.

[45] C. Clastres, T.T. Ha Pham, F. Wurtz, and S. Bacha. Ancillary services and optimal household energy management with photovoltaic production. *Energy*, 35:55–64, 2010.

[46] V. R. Dehkordi, J. A. Candanedo, and M. Stylianou. Variable horizon MPC of a building system with thermal energy storage. In *Journal of Process Control*, 2013.

[47] G. Droge and M. Egertedt. Adaptive time horizon optimization in model predictive control. In *American Control Conference (ACC)*, 2011.

[48] R. Scattolini. Architectures for distributed and hierarchical model predictive control- a review. *Journal of Process Control*, 19:723–731, 2009.

[49] A. Tica, H. Gueguen, D. Dumur, D. Faille, and F.A. Davelaar. Hierarchical model predictive control approach for start-up optimization of a combined cycle power plant. In *Proceedings of the 8th IFAC Power Plant and Power Systems Control Symposium*, September 2012.

[50] M. H. Ramezani and N. Sadati. Hierarchical optimal control of large-scale nonlinear chemical process. *ISA Transactions*, 48:38–47, 2009.

[51] C. Hou, X. Hu, and D. Hui. Hierarchical control techniques applied in micro-grid. In *International Conference on Power System Technology*, 2010.

[52] F. Kennel, D. Gorges, and S. Liu. Energy management for smart grids with electric vehicles based on hierarchical MPC. In *IEEE Transaction on Industrial Informatics*, 2012.

[53] B. Picasso, D. De Vito, R. Scattolini, and P. Colaneri. A MPC approach to the design of two-layer hierarchical control systems. *Automatica*, 46:823–831, 2010.

[54] L. Magni and R. Scatolini. Stabilizing decentralized model predictive control of nonlinear systems. *Automatica*, 42:1231–1236, 2006.

[55] R. M. Hermans, M. Lazar, and A. Jokić. Almost decentralized Lyapunov-based nonlinear model predictive control. In *2010 American Conrol Conference Marriot Waterfont, Baltimore, MD, USA, June 30-July 02,*, 2010.

[56] D. L. Ha, S. Ploix, M. Jacomino, and M. H. Le. An optimal approach for electrical management problem in dwellings. *Energy and Buildings*, 45:1–14, 2012.

[57] A. Vahidi and W. Greenwell. A decentralized model predictive control approach to power management of a fuel cell-ultracapacitor hybrid. In *Predeedings of the 2007 American Control Conference Marriot Marquis Hotel at Times Square, New York City, USA, July 11-13*, 2007.

[58] E. Camponogara, D. Jia, B.H. Krogh, and S. Talukbar. Distributed model predictive control. *IEEE Control Systems*, 22:44–52, 2002.

[59] J. B. Rawlings and B. T. Stewart. Coordinating multiple optimization-based controllers: New opportunities and challenges. *Journal of Process Control*, 18:839–845, 2008.

[60] D. Moroşan, R. Bourdais, D. Dumur, and J. Buisson. Distributed model predictive control for building temperature regulation. In *ACC*, 2010.

[61] K. Edlund, J.D. Dendtsen, and J.B. Jorgensen. Hierarchical model-based predictive control of a power plant porfolio. *Control Engineering Practice*, 19:1126–1136, 2011.

[62] L. S. Lasdon. Duality and decomposition in mathematical programming. *IEEE Transactions on systems science and cybernetics*, 4:86–100, 1968.

[63] D. Moroşan. *Commande prédictive deistribuée, Approches appliquées à la régulation thermique des bâtiments.* PhD thesis, Supélec, 2011.

[64] A. Lefort, R. Bourdais, G. Ansanay-Alex, and H. Guéguen. Hierarchical control method aplied to energy management of a residential house. *Energy and Buildings*, 64:53–61, 2013.

[65] G. B. Dantzig and P. Wolfe. Decomposition principle for linear programs. *Operation Research*, 8:101–11, 1960.

[66] L. E. Sokoler. *Convex optimization Algorithms for Power Plant Operation.* PhD thesis, Technical University of Denmark, 2009.

[67] K. Edlund. *Dynamic Load Balancing of a Power System Portfolio.* PhD thesis, Aalborg University, 2010.

[68] A. Lefort, R. Bourdais, H. Guéguen, and G. Ansanay-Alex. Planification de la consommation énergétique d'un bâtiment par une méthode d'optimisation linéaire distribuée. In *Conférence Internationale Francophone d'Automatique, july 4*, 2012.

[69] A. Lefort, H. Guéguen, R. Bourdais, and G. Ansanay-Alex. A building energy management system based on distributed model predictive control. In *CISBAT International Conference Lausanne, 4-6 September*, 2013.

[70] R. Cheng, J. F. Forbes, and W. S.Yip. Dantzig-Wolfe decomposition and plant-wide MPC coordination. *Computers and Chemical Engineering*, 32:1507–1522, 2008.

[71] SIMBAD building and HVAC toolbox http://www.cstb.fr. Technical report, CSTB, 84 avenue Jean Jaurès - Champs-sur-Marne- B.P. 2 - F-77421 Marne La Vallée Cedex 2, -.

[72] M. E. Baster. *Modelling the performance of air source heat pump systems*. PhD thesis, Department of Mechanical Engineering, University of Strathclyde, 2011.

[73] M.S. Hossain, R. Saidur, and H. Fayaz eta. Review on solar water heater collector and thermal energy performance of circulating pipe. *Renewable and Sustainable Energy Rewiews*, 15:3801–3812, 2011.

[74] The power to choose : Demand response in liberalised electricity market. Technical report, International Energy Agency, 2003.

[75] A. Chabaudand, J. Eynard, and S. Grieu. Gestion multicritère des resources énergétiques à l'échelle d'un habitat individuel: interaction bâtiment / réseau électrique. In *JD-MACS*, 2013.